Understanding the contribution of tumour cells and stroma to changes in microRNA expression in malignant pleural mesothelioma

A thesis submitted in fulfilment of the requirements of the degree of Master of Science (MSc) (Research)

Submitted by

Kadir Harun Sarun

Faculty of Science, School of Life Sciences

University of Technology Sydney

June 2019

Certificate of original authorship

I, Kadir Harun Sarun, declare that this thesis is submitted in fulfilment of the requirements for the award of Master of Science (Research), in the Faculty of Science, School of Life Sciences at the University of Technology Sydney.

The thesis is wholly my own work unless otherwise referenced or acknowledged. In addition, I certify that all information sources and literature used are indicated in the thesis.

This document has not been submitted for qualifications at any other academic institution.

This research is supported by an Australian Government Research Training Program.

Signature:

Production Note:
Signature removed prior to publication.

Date: 13/6/2019

Acknowledgements

Fresh out of my UTS Bachelor's degree, at the end of 2014, I came to ADRI for a summer project to gain some laboratory experience. After the summer project, I was fortunate enough to be offered to work as a research assistant under the supervision of Associate Professor Glen Reid. During my employment as a research assistant Dr Najah Nassif and Dr Eileen McGowan persuaded me to study a rewarding Master of Science (Research) degree through UTS.

Firstly, I would like to thank my UTS supervisor's Dr Najah Nassif and Dr Eileen McGowan for their ongoing support and guidance during my Master of Science studies. Although, I was an external and part time student at ADRI they were always available and present. I would also like to express my deepest gratitude to my ADRI supervisor Associate Professor Glen Reid for his expert scientific advice and input towards my project. Without the combined effort of my supervisors throughout the years the work presented would not be possible.

I would especially like to thank Dr Yuen Yee Cheng for teaching me everything I have learnt over the years in the lab and pushing me to my limits. A special thank you to Dr Karin Schelch who taught me valuable lessons in research and motivated me by showing how fun and cool research can be. I want to thank past and present ADRI directors Professor Nico Van Zandwijk and Professor Ken Takahashi for allowing me to achieve my studies at an inspiring research institute.

I will always be grateful to my fellow ADRI colleagues and friends Thomas George Johnson, Patrick Winata and Hedi Kruse who were always there for mental support and keen for a coffee break. I am very fortunate to have met you all. A huge thanks to Tom for being my lab partner from day one at UTS and still six years later at ADRI, I wish you the best with your PhD.

I must thank my family for their unconditional love and always having faith in me. Without your encouragement I would not have made it through this thesis. Most importantly, I dedicate the completion of this thesis to my beloved wife Sena. Thank you for all your support, patience and taking care of me.

Achievements gained as part of my research work

Peer-reviewed journal publications

1. **Sarun KH**, Lee K, Williams M, Wright CM, Clarke CJ, Cheng NC, Takahashi K, Cheng YY. Genomic deletion of BAP1 and CDKN2A are useful markers for quality control of malignant pleural mesothelioma (MPM) primary cultures. Int J Mol Sci. 2018 Oct 7;19(10):3056. PMID: 30301262
2. Rath EM, Cheng YY, Pinese M, **Sarun KH,** Hudson AL, Weir C, Wang YD, Håkansson AP, Howell V, Liu GJ, Reid G, Knott RB, Duff AP, Church WB. BAMLET and BLAGLET kills chemotherapy-resistant mesothelioma cells, holding oleic acid in an activated cytotoxic state. PlosOne. 2018 Aug 29;13(8):e0203003. PMID: 30157247
3. Johnson TG, Schelch K, Cheng YY, Williams M, **Sarun KH,** Kirschner MB, Kao S, Linton A, Klebe S, McCaughan BC, Lin RCY, Pirker C, Berger W, Lasham A, van Zandwijk N, Reid G. Dysregulated expression of the microRNA miR-137 and its target YBX1 contribute to the invasive characteristics of malignant pleural mesothelioma. J Thorac Oncol. 2018 Feb;13(2):258-72. doi: 10.1016/j.jtho.2017.10.016. PMID: 29113949
4. Kao SC, Cheng YY, Williams M, Kirschner MB, Madore J, Lum T, **Sarun KH,** Linton A, McCaughan B, Klebe S, van Zandwijk N, Scolyer RA, Boyer MJ, Cooper WA, Reid G. Tumor suppressor microRNAs contribute to the regulation of PD-L1 expression in malignant pleural mesothelioma. J Thorac Oncol. 2017;12(9):1421-33. PMID: 28629895
5. Cheng YY, Wright CM, Kirschner MB, Williams M, **Sarun KH,** Sytnyk V, Leshchynska I, Edelman JJ, Vallely MP, McCaughan BC, Klebe S, van Zandwijk N, Lin RCY, Reid G. KCa1.1, a calcium-activated potassium channel subunit alpha 1, is targeted by miR-17-5p and modulates cell migration in malignant pleural mesothelioma. Mol Cancer. 2016 Jun 1;15(1):44. PMID: 27245839

Conference presentations

1. **Sarun KH**, Cheng YY, Kirschner M, van Zandwijk N, Lin R, Reid G. Expression of miR-223 in mesothelioma xenografts originates from stromal cells in the tumour microenvironment. J Thorac Oncol. 2017; 12(1):S248. IASLC 17th World Conference on Lung Cancer 2016, Vienna, 4 - 7 December 2016.
2. **Sarun KH**, Cheng YY, Kirschner MB, van Zandwijk N, Lin RC, Reid G. The expression of miR-223 in malignant pleural mesothelioma xenograft tumour samples originates from stromal cells. 6th Australian Lung Cancer Conference: 33, Melbourne, 18-20 August 2016.
3. **Sarun KH**, Cheng YY, Kirschner MB, Lin RCY, van Zandwijk N, Reid G. The expression of miR-143, miR-214 and miR-223 in malignant pleural mesothelioma xenograft tumours is primarily from stromal cells. Lorne Cancer Conference, Lorne, 8-10 February 2018.

Travel Awards

1. **Sarun KH.** Awarded the Young Investigator Award by the International Association for the Study of Lung Cancer (IASLC) and the Local Organising Committee of the 17th IASLC World Conference on Lung Cancer for the abstract "Expression of miR-223 in mesothelioma xenografts originates from stromal cells in the tumour microenvironment". The award was presented at the IASLC Business Meeting Vienna 6th December 2016.

2. **Sarun KH.** Concord Repatriation General Hospital Research Travel Scholarship. IASLC 17th World Conference on Lung Cancer 4-7 December 2016 Vienna, Austria.

Abbreviations

3'UTR	Three prime untranslated region
Ago	Argonaute
ALL	Acute lymphoblastic leukaemia
AML	Acute myeloid leukaemia
ATCC	American Type Culture Collection
AUC	Area under the curve
BCL2	B-cell lymphoma 2
BCL6	B-cell lymphoma 6
CAF	Cancer associated fibroblast
CCND1	Cyclin-D1
CD4	Cluster of differentiation 4
CD14	Cluster of differentiation 14
CD31	Cluster of differentiation 31
CD45	Cluster of differentiation 45
CD68	Cluster of differentiation 68
cDNA	Complementary DNA
CEA	Carcinoembryonic antigen
CK5/6	Cytokeratin 5/6
CK19	Cytokeratin 19
CK20	Cytokeratin 20
CO_2	Carbon dioxide
CT	Computed tomography
CTLA-4	Cytotoxic T-lymphocyte-associated protein 4
CuSO4	Copper sulphate
D2-40	Podoplanin
DAB	3,3’-Diaminobenzidine
DB	Diagnostic biopsy
ddPCR	Digital droplet polymerase chain reaction
DEPC	Diethylpyrocarbonate
DGCR8	DiGeorge syndrome critical region 8
DMSO	Dimethyl Sulfoxide

DNA	Deoxyribonucleic acid
DNMT1	DNA methyltransferase 1
DNMT3A	DNA methyltransferase 3A
DPBS	Dulbecco's phosphate-buffered saline
EDTA	Ethylenediaminetetraacetic acid
EDV	EnGeneIC dream vector
EFEMP1	EGF-containing fibulin-like extracellular matrix protein 1
EGFR	Endothelial growth factor receptor
ELISA	Enzyme-linked immunosorbent assay
EMA	Epithelial membrane antigen
EORTYC	European Organisation for Research and Treatment of Cancer
EPB41L3	Erythrocyte membrane protein band 4.1 like 3
EPP	Extrapleural pneumectomy
FACS	Fluorescence-activated cell sorting
FBLN3	Fibulin-3
FBS	Fetal bovine serum
FFPE	Formalin-fixed paraffin-embedded
FGF	Fibroblast growth factor
FGF-2	Fibroblast growth factor 2
HCL	Hydrogen chloride
HRP	Horseradish peroxidase
IGF1R	Insulin-like growth factor-1 receptor
IHC	Immunohistochemistry
IL-13	Interleukin 13
IMRT	Intensity modulated radiotherapy
IRS1	Insulin receptor substrate 1
ISH	*In situ* hybridisation
LNA	Locked nucleic acid
M-MLV	Moloney murine leukemia virus
MEF2C	Myocyte-specific enhancer factor 2c
miRNA (or miR)	MicroRNA
MPF	Megakaryocyte potentiating factor

MPM	Malignant pleural mesothelioma
MRI	Magnetic resonance imaging
mtDNA	Mitochondrial DNA
NK	Natural killer
NNP	Non-neoplastic pleura
NSCLC	Non-small cell lung cancer
NTC	No-template control
OCT4	Octamer-binding transcription factor 4
P/D	Pleurectomy/decortication
PACT	Protein activator
PBS	Phosphate-buffered saline
PCR	Polymerase chain reaction
PD-1	Programmed cell death protein 1
PDL-1	Programmed death ligand 1
PET	Positron emission tomography
PFA	Paraformaldehyde
PPP6C	Protein phosphatase 6 catalytic subunit
pre-miRNA	Precursor microRNA
pri-miRNA	Primary microRNA
qPCR	Quantitative polymerase chain reaction
RISC	RNA-induced silencing complex
RNA	Ribonucleic acid
RNU6B	U6 small-nuclear ribonucleoprotein
ROC	Receiver operator characteristic
RPMI	Roswell Park Memorial Institute
RT	Reverse transcription
SCC	Saline-sodium citrate
SMC	Smooth muscle cell
SMRP	Soluble mesothelin-related protein
SOCS	Suppressor of cytokine signaling
STMN1	Stathmin 1
SV40	Simian virus 40

TAM	Tumour-associated macrophage
TLR	Toll like receptor
TRBP	Thyroid hormone receptor-binding protein
TTF-1	Thyroid transcription factor-1
VEGF	Vascular endothelial growth factor
WHO	World health organisation
WT-1	Wilms tumour antigen-1
XPO5	Exportin-5

Table of contents

List of figures

List of tables

Abstract

Malignant pleural mesothelioma (MPM), a relatively rare cancer arising from the mesothelial lining of the pleura, is a highly aggressive cancer with a very poor prognosis, and an urgent need for more effective treatments. MicroRNAs (miRNAs) are short, non-coding RNA sequences that negatively regulate gene expression and their abundance is frequently dysregulated in cancers. Dysregulation of miRNA expression plays an important role in the biology of MPM and candidate miRNAs have been investigated as diagnostic and prognostic biomarkers, or as potential treatment targets for MPM.

Dysregulation of miRNA expression is determined through comparisons of miRNA expression profiles of tumour and corresponding normal tissues. Tumours, however, consist of non-tumour stromal cell types that also play important roles in tumour development. The contribution of stromal cell miRNA expression can influence the selection of dysregulated miRNAs, and their gene targets for analysis. Since in tumour miRNA profiling studies, the source of miRNAs may be from tumour cells, stromal cells or a combination of both, this thesis aims to better understand the contribution of tumour cells and stroma to changes in miRNA expression in MPM.

This project investigated the relative contribution of miRNAs from tumour and stromal cells in MSTO and H226 cell line-derived xenograft tumours compared to their corresponding cultured tumour cells. RT-qPCR quantification detected high expression of miR-143-3p, miR-214-3p and miR-223-3p in xenograft tumours and confirmed their stromal origin. Additionally, digital droplet PCR (ddPCR) quantification of the species-specific pri-miRNA transcripts of these three miRNAs further confirmed predominant expression by mouse stromal cells.

Although there is strong evidence supporting the expression miR-143-3p, miR-214-3p and miR-223-3p predominantly in stromal cells, these miRNAs have all been reported to be downregulated in MPM. This study therefore also explored the functional consequences of overexpressing these miRNAs in MPM cell lines to test their reported tumour suppressor effects but found an absence of such effects.

In conclusion, identifying miRNA dysregulation in MPM by comparing tumour and normal tissue expression profiles is ineffective due to the presence of stromal cells that can contribute to the miRNA expression pool at varying levels, hence influencing downstream gene targets. It is therefore of absolute importance to understand the cell source of miRNAs prior to carrying out functional studies to gain a better understanding of the contribution of miRNAs to the roles of tumour and stromal cells in MPM.

Chapter 1 - Introduction

1.1 Malignant pleural mesothelioma

Malignant pleural mesothelioma (MPM) is a relatively rare cancer arising from the mesothelial lining of the pleura. It is a highly aggressive cancer with a very poor prognosis, in which median survival is less than 12 months [1-3] and with few effective treatments. At least 80% of MPM cases are linked to asbestos fibre exposure with other potential carcinogenic factors including exposure to simian virus 40 (SV40), radiation and erionite [4]. The incidence of MPM has risen in industrialised nations due to past widespread exposure to asbestos and is predicted to increase in developing countries where the use of asbestos has yet to be banned [2].

1.1.1 Mesothelioma

Malignant mesothelioma is a tumour derived from mesothelial cells. Mesothelial tissue is a thin membrane covering the surfaces of the pleura, peritoneum, pericardium and tunica vaginalis testis [5]. Malignant pleural mesothelioma (MPM) is the most common form, accounting for approximately 80% of all cases, and occurs in the pleural lining surrounding the lungs (Figure 1.1).

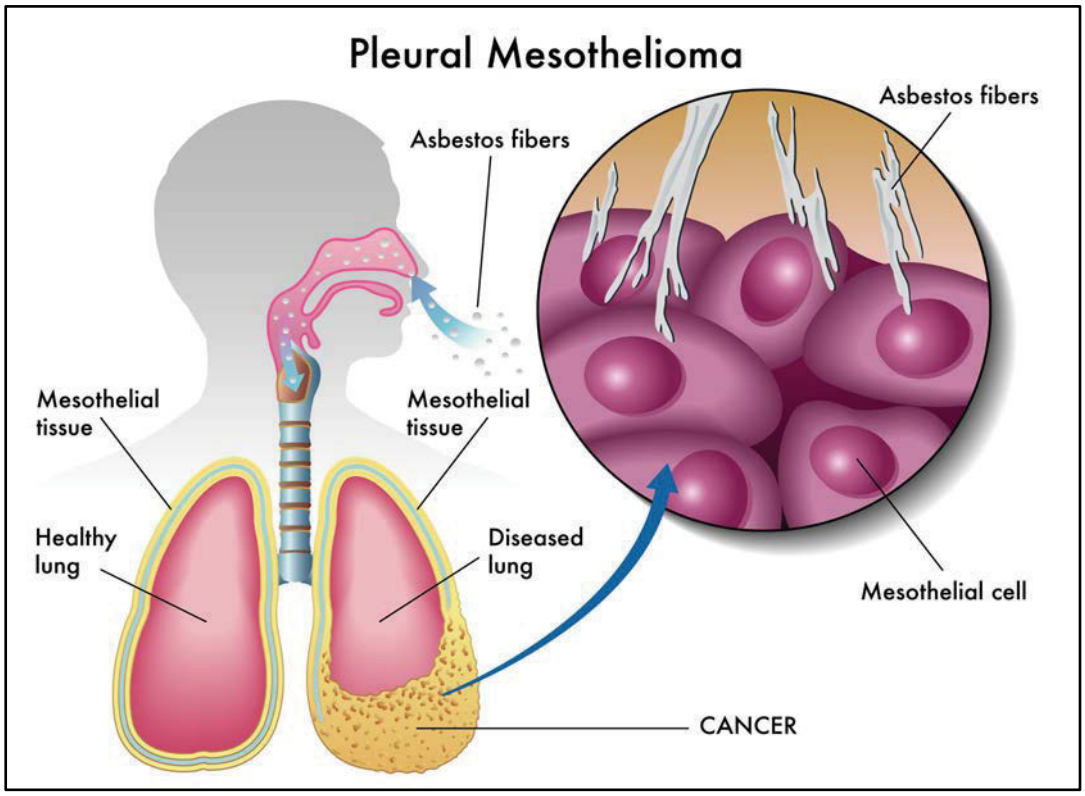

Figure 1.1: Malignant pleural mesothelioma is caused by asbestos exposure. Schematic depiction of inhaled asbestos fibres making their way to pleural mesothelial cells and inducing malignancy resulting in tumour growth around the diseased lung (Accessed 12/10/2017)[6].

MPM consists of three main histological subtypes, epithelioid, sarcomatoid, and biphasic, based on the morphological appearance of the tumour cells and tumour composition (Figure 1.2) [5]. The most common subtype, epithelioid (50-70%), is characterised by its well differentiated cobblestone-like structure. The least common sarcomatoid subtype (7-20%) consists of more spindle shaped, elongated cells in a diffusive pattern set in variable amounts of stroma. The biphasic subtype (20-35%) is a mixture consisting of at least 10% of the epithelioid and sarcomatoid types [5, 7]. Of these subtypes, patients with an epithelioid diagnosis tend to have a better prognosis and median survival compared to patients diagnosed with the sarcomatoid and biphasic types [2, 8].

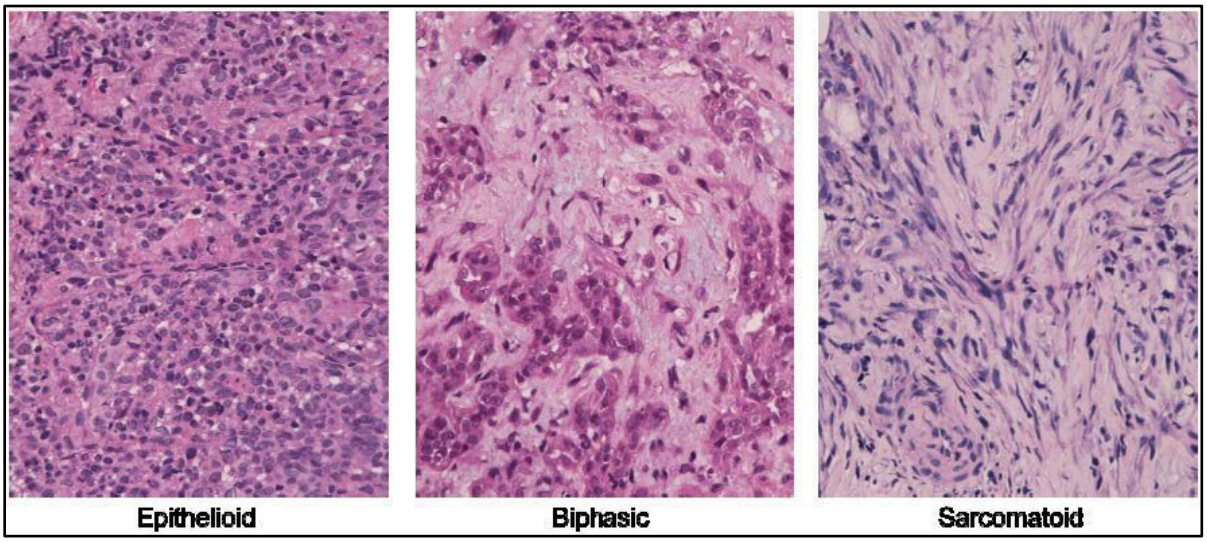

Figure 1.2: MPM histological subtypes. Microscopic images of hematoxylin and eosin-stained, formalin-fixed and paraffin embedded tumour specimens representing epithelioid, biphasic and sarcomatoid subtypes of MPM (provided by Dr Karin Schelch, Medical University of Vienna, Austria).

1.1.2 Understanding asbestos

Asbestos is a naturally occurring fibrous silicate mineral mined for its properties of thermal resistance, tensile strength and insulation. It is divided into two main groups: 1) serpentine, consisting of only chrysotile (white asbestos); and 2) amphibole, consisting of amosite (brown asbestos), crocidolite (blue asbestos), tremolite, anthrophyllite, and actinolite [9]. Epidemiological studies suggest that exposure to the commercially important amphibole variants, amosite and crocidolite, carries a much higher risk of developing mesothelioma compared to chrysotile. The exposure-specific risk of mesothelioma, studied in an occupational cohort, was found to be 1:100:500 for chrysotile, amosite and crocidolite respectively [10]. However, there is ongoing controversy towards correlating the risk of developing mesothelioma with fibre type [11]. Nevertheless, all forms of asbestos exposure can result in MPM as reported by the World Health Organization (WHO) [9, 12]. Asbestos fibres are easily

airborne when disturbed, where they can be inhaled into the lungs and, over time, their bio-persistence can induce MPM.

1.1.3 Epidemiological impact of asbestos exposure

Although MPM is a relatively rare cancer, global incident rates are continuing to rise. The WHO recorded 92,253 mesothelioma deaths reported by 83 countries between 1994 and 2008 [13]. Analysis found more than 75% of these deaths were reported after the year 2000. Corresponding age-adjusted mortality rates were 4.0 per million during 1994 to 2000 and 5.3 per million during 2001 to 2008 [13]. Despite many developed countries banning asbestos use, the long latency period of 30-50 years between asbestos exposure and MPM diagnosis means increasing MPM incidence rates have either peaked, or are yet to peak, depending on when bans were introduced [14-16]. Unfortunately, asbestos is still being mined, exported and used by several countries including Russia, China, Kazakhstan, India and Brazil [5]. The mesothelioma epidemic, which is currently being experienced by developed countries that have already banned asbestos, is yet to impact those countries still handling asbestos.

Australia has a long history of asbestos mining and had the world's highest use per capita in the 1950s [17]. Thus, there is no surprise that Australia held one of the highest age-adjusted annual incidence of mesothelioma at 29 per million reported in 2008 [18] and is currently still at 29 per million reported in 2017 [19]. Since 1980, Australia has maintained a national malignant mesothelioma register [17]. In the last three decades, incidence rates have increased substantially and are currently fairly stable between 700-800 new cases annually (Figure 1.3) [19].

Although occupational exposure mesothelioma cases will decrease over the next 20 to 30 years, there are growing concerns about an increase in mesothelioma cases caused by environmental exposure [20]. These cases include people with short-term and/or low level exposure to asbestos at home, mainly during home maintenance and renovation involving asbestos-containing building products, or in asbestos-contaminated workplaces [20]. There is still insufficient data to determine when, and at what level, these cases may peak. Therefore, raising awareness towards the widespread presence of asbestos products in homes and other buildings across Australia is an important preventative measure.

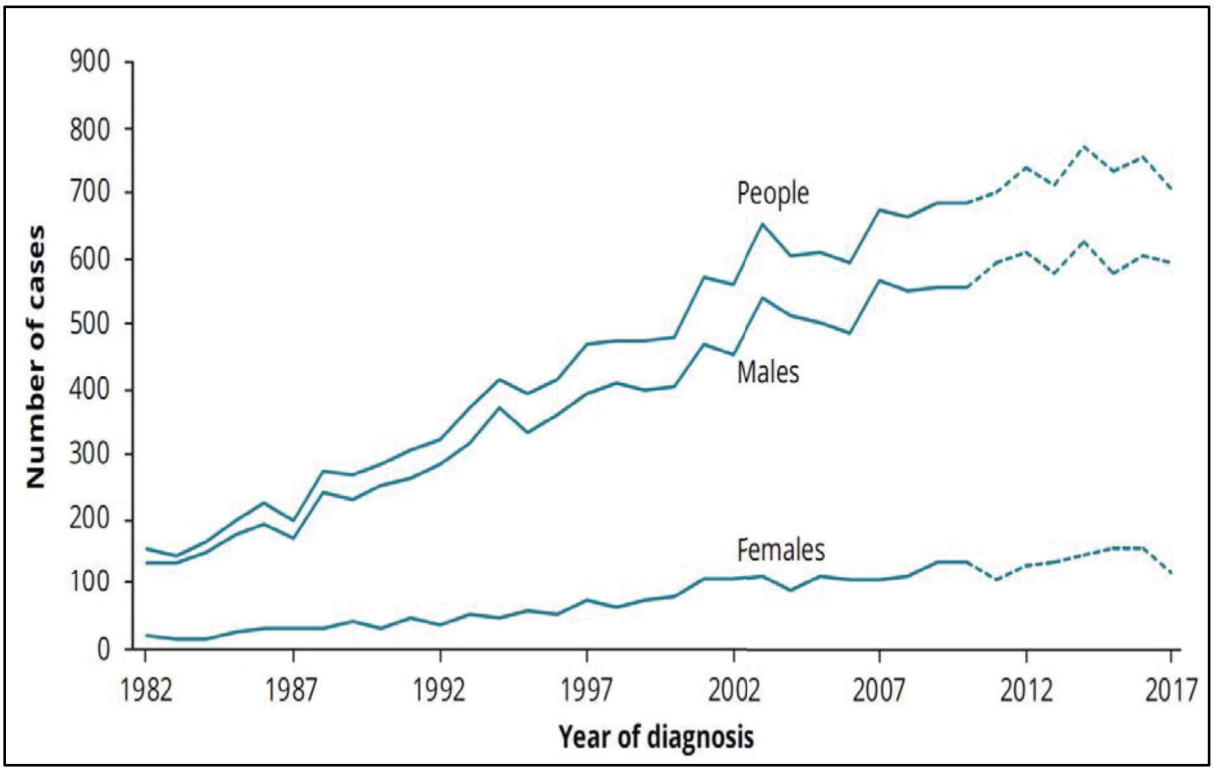

Figure 1.3: New cases of mesothelioma in Australia (1982-2017) by year and sex. The solid graphed line (1982-2010) indicates sourced data and the dotted graphed line (2011-2017) indicates Australian Institute of Health and Wellbeing data (Accessed 01/06/2019) [19].

1.1.4 MPM patient diagnosis

The diagnosis of MPM is particularly difficult as symptoms are similar to benign pleural disease, primary lung adenocarcinoma or the metastasis of other cancers to the pleura [21, 22]. Some of the most common symptoms include difficulty breathing, fatigue, coughing, weight loss and chest wall pain [23]. In addition to these symptoms, patients presenting a history of asbestos exposure usually supports a clinical suspicion of MPM.

Computed tomography (CT) scanning can be used to help discriminate between MPM and benign pleural disease by depicting circumferential pleural thickening, parietal thickening (>1cm), nodular pleural thickening and mediastinal pleural involvement. However, these findings are not definitive for diagnosis and cannot differentiate MPM from pleural metastases [24]. Therefore, once MPM is suspected based on clinical and CT data, thoracoscopy is performed to obtain a biopsy sample to confirm MPM diagnosis through immunohistochemistry (IHC) staining, except in the case of pre-operative contraindication or pleurodesis [22]. More recent research claims that in experienced hands

MPM can be diagnosed on pleural fluid cytology alone, providing a less invasive diagnostic technique which may possibly lead to earlier confirmation of diagnosis [25].

Current standards recommend a panel of IHC markers to diagnose and differentiate epithelioid MPM from adenocarcinoma. Guidelines published by the European Respiratory Society and European Society of Thoracic Surgeons suggest a minimum of two positive mesothelioma markers (selected from calretinin, Wilms tumour antigen-1 (WT-1), epithelial membrane antigen (EMA) (membrane staining), cytokeratin (CK5/6), Podoplanin (D2-40)) and two negative markers (selected from Ber-EP4, thyroid transcription factor-1 (TTF-1), carcinoembryonic antigen (CEA), B72-3, MOC-31, oestrogen/progesterone, EMA (cytoplasmic staining)) to confirm an MPM diagnosis [22]. Reaching a definitive diagnosis based on IHC requires an invasively acquired biopsy sample that must be of sufficient quantity and quality to allow for IHC characterisation. As patients usually present in the later stages of MPM, this is not always possible. Thus, less invasive diagnostic techniques and feasible screening programs are needed for earlier diagnosis.

1.1.5 Screening for MPM

A screening program can only be medically justified if earlier detection of the disease improves patient prognosis and the benefits outweigh the risks. The two most common methods explored for MPM screening include thoracic imaging and biological (blood-based) markers but despite extensive research there is, to date, no established screening program for MPM [22]. Nevertheless, as MPM incidence continues to increase, the search for a useful screening method remains an important area of research. In particular, biomarkers present in the blood have the potential to serve as both an aid to diagnosis as well as being suitable for use as screening tools.

Although CT scans have been proven to be an important tool for detecting suspected MPM, unfortunately not a single case of MPM was detected in a screen of 1045 asbestos exposed workers [26]. Other thoracic imaging techniques, including positron emission tomography (PET) and magnetic resonance imaging (MRI), are useful in the clinical management of MPM and in the differentiation of MPM from benign pleural disease, but are not available and/or applicable for screening purposes [22].

The three main blood-based biomarkers that have been evaluated for MPM diagnosis are: osteopontin, soluble mesothelin and fibulin-3, however these three markers are not MPM specific. Osteopontin is a glycol-phosphoprotein that is expressed and secreted by numerous human cancers [27]. Osteopontin is also reported to be regulated by proteins in cell-signalling pathways that are associated with asbestos-induced carcinogenesis. Furthermore, high levels of osteopontin have been correlated with tumour invasion, progression, and metastases [28]. An *in vivo* study observed up-regulated osteopontin levels in asbestos-induced tumours in a rat model and in cells exposed to

asbestos *in vitro* [29]. A population study comparing serum osteopontin levels found elevated osteopontin in MPM patients compared to healthy asbestos exposed patients, with an area under the curve (AUC) of 0.888. For the purpose of screening, a high level of sensitivity (95%-99%) is most appropriate and with a cut-off value of 10.9 ng of osteopontin per millilitre, a sensitivity of 96.1% was achieved. However, at this sensitivity, a low specificity level of 23.2% was recorded, meaning there would be many false positives amongst already known asbestos-exposed, but otherwise healthy, individuals [28].

Mesothelin is a differentiation marker of mesothelial cells. Differential post transcriptional and translational processing of the mesothelin gene produces four different protein products: megakaryocyte potentiating factor (MPF), mesothelin variant 1, mesothelin variant 2, and soluble mesothelin-related protein (SMRP) [30]. MPF is a soluble protein with cytokine activity [31]. Mesothelin is a glycosylated protein that is predominantly anchored to the cell surface of normal mesothelial cells, but also found in a soluble form [32]. Mesothelin variant 1 is the predominant form of the protein and differs from variant 2 by only 8 amino acids [30]. SMRP is a soluble protein with an identical N-terminal sequence to mesothelin but with a unique C-terminus [33]. A study using an enzyme-linked immunosorbent assay (ELISA), which detects both mesothelin variant 1 and SMRP, demonstrated increased levels of this biomarker in the serum of patients with mesothelioma. When increased levels of mesothelin were compared against healthy controls and patients with benign asbestos-related disease, an AUC of 0.915 was reported. In regards to screening potential, a high specificity threshold set at 85% still maintained a modest 81% sensitivity [30].

Fibulin-3 (FBLN3) is encoded by the *EGF-containing fibulin-like extracellular matrix protein 1 (EFEMP1)* gene and is a member of the fibulin family of secreted extracellular glycoproteins [34]. Increased levels of FBLN3 protein were found in the plasma and pleural effusion of MPM patients and was initially identified as a very promising diagnostic and prognostic MPM biomarker [35]. Early studies reported plasma FBLN3 levels to have an AUC of 0.87, when comparing patients with MPM and asbestos exposed controls, with a specificity of 100% and a sensitivity of 33% [35]. However, a subsequent study reported a much lower AUC value of 0.67 when distinguishing plasma FBLN3 levels amongst MPM patients from other patients [36]. Similarly, a further study analysing plasma FBLN3 levels in two separate cohorts from Sydney and Vienna reported AUC values of 0.63 and 0.56 respectively [37].

Together, these data suggest that mesothelin remains the most useful biomarker. Most recently, SMRP has become the only clinically validated blood-based biomarker for MPM. The SMRP serum levels have been reported to correlate with pleural thickness (measure by CT). Providing clinicians with a convenient tool to monitor tumour progression and treatment response of MPM.

Another growing area of biomarker research in MPM focuses on changes in circulating microRNA levels. Many studies have described characteristic changes in microRNA expression in MPM tumours, and changes are also evident in the levels of microRNAs present in the blood.

1.1.6 Current MPM treatments

Despite extensive research into MPM treatment, cytotoxic chemotherapy remains one of the only therapeutic options with a proven survival benefit in patients with MPM. The majority of MPM patients pursue palliative treatment with cytotoxic chemotherapy over the more radical surgical approach [38]. This is mostly due to the late diagnosis of MPM in patients who are often elderly and unfit for invasive surgery. A pivotal phase III trial, in 2003, set the current standard of treatment by demonstrating that cisplatin in combination with pemetrexed, compared to cisplatin alone, improved median survival from 9.3 months to 12.1 months [39]. Ongoing research over the past decade has been investigating strategies to improve the current chemotherapy standard of care. Research into tumour angiogenesis has influenced another phase III trial which evaluated bevacizumab treatment alongside the standard pemetrexed and cisplatin followed by maintenance bevacizumab until progression versus pemetrexed and cisplatin alone. The median overall survival with bevacizumab was 18.8 months compared to 16.1 months without and the 2.7 month survival benefit was statistically significant ($P = 0.0167$) amongst the 448 patients [40].

A more aggressive treatment approach involves surgery for eligible MPM patients and is usually performed with a palliative intent by debulking the tumour burden and controlling symptoms. The two main surgical procedures performed are pleurectomy/decortication (P/D) and extrapleural pneumonectomy (EPP). A P/D is a less aggressive surgery that removes the affected pleural lining of the lung and decorticates any remaining tumour on the cavity or lung whereas an EPP is a much more aggressive surgical approach that attempts to remove all macroscopic evidence of tumour and involves the resection of pleura, lung, pericardium, diaphragm and regional lymph nodes [21]. Analysis of large surgical datasets have favoured results of P/D over EPP, both in terms of median overall survival (16 months and 12 months, respectively) and surgical mortality and morbidity [41].

Radiotherapy has also been widely used for MPM patients for the palliation of symptoms [42]. Unfortunately, systematic reviews have not shown evidence that radiotherapy prolongs survival amongst MPM patients, which is expected given its palliative purpose [43]. Adjuvant hemithoracic radiotherapy treatment can be given after EPP to clear remaining tumour cells, but it is challenging to target viable disease while avoiding vital thoracic structures. Initial experiences with high dose radiotherapy were not favourable as they were highly toxic to patients [44]. However, improvements in radiotherapy technology have now been introduced, including the introduction of intensity

modulated radiotherapy (IMRT), which is a more accurate technique. A large study of 63 patients treated with IMRT after EPP recorded a median overall survival of 14.2 months and 3 year survival rate of 20% [45].

Multi-modality therapy, combining chemotherapy, surgery and radiotherapy is another method of treatment for MPM patients where applicable. A phase II trial by the European Organisation for Research and Treatment of Cancer (EORTC) investigated the feasibility of trimodality therapy consisting of induction cisplatin/pemetrexed combination chemotherapy followed by EPP and post-operative radiotherapy. The median overall survival time was 18.4 months and median progression-free survival was 13.9 months [46]. Although this multi-modality therapy has some success, it is intensive and limited to selected patients with a completion rate of 64.9% [46].

Recently, immunotherapy approaches involving the targeting of immune checkpoints such as cytotoxic T-lymphocyte-associated protein 4 (CTLA-4) and programmed cell death 1 (PD-1) have generated impressive results in several cancers including melanoma, renal cell cancer, and lung cancer [47]. Based on this evidence, immune checkpoint inhibitors are being evaluated as a therapeutic option for patients with unresectable MPM seeking second- and third-line treatment. The anti-CTLA-4 monoclonal antibody tremelimumab was tested on chemotherapy-resistant MPM patients in two small phase II trials with promising results of median overall survival of 10.7 months [48] and 11 months [49]. However, a subsequent phase II-III trial with the primary objective of improving overall survival amongst unresectable mesothelioma patients having second- and third-line treatment with tremelimumab, compared to placebo, failed to achieve the primary end point [50].

PD-1 is a transmembrane inhibitory immunoreceptor, expressed by activated T cells, that negatively regulates immune responses by interacting with its ligand PD-L1. Blockade of PD-1 or PD-L1 inhibits the repression of T-cell activation, hence unleashing an immune response towards the tumour [47]. In a phase IB study of PD-L1 positive tumour patients, treatment with pembrolizumab, an anti-PD-1 antibody, showed promising toxicity results and a modest median overall survival of 18 months [51]. Another phase IB study of unresectable pleural and peritoneal mesothelioma patients treated with avelumab, an anti-PD-L1 antibody, reported an overall disease control rate of 60% and showed an acceptable safety profile [52]. Recently, in a phase II clinical trial, DREAM, the PD-L1 inhibitor durvalumab, was administered in combination with first-line therapy of cisplatin and pemetrexed to MPM patients. Preliminary results from this study indicate the addition of durvalumab resulted in higher rates of progression-free survival at 6 months (71%) and objective response rates (61%) than expected for chemotherapy alone [53]. Overall, immune checkpoint inhibition seems to be a promising therapeutic strategy in MPM but results are still preliminary and trials are ongoing.

Although CTLA-4 inhibitor treatment failed to improve patient overall survival, there are trials in other cancers such as melanoma and lung cancer exploring the additive or synergistic effects of targeting both PD-1/PD-L1 and CTLA-4 [54, 55]. Also, phase II trials of PD-1 and PD-L1 inhibitors in mesothelioma patients are ongoing with early promising results [56].

As outlined above, there is still a lack of effective treatments for MPM patients and despite the initial promising results from immunotherapy trials, further research is desperately needed to develop more effective treatments. Another approach involves molecular characterisation of MPM tumours relative to matched normal tissue to identify changes in the tumour genome. A comprehensive next generation sequencing study of the mesothelioma genome discovered many tumour-specific rearrangements and point mutations. These findings helped identify a panel of disrupted genes, that were differentially expressed in tumours, as potential therapeutic targets [57]. Similar to differential gene expression, identifying differentially expressed microRNAs in MPM has also been important in the search for more effective MPM treatment.

1.2 MicroRNA definition and role in cancer

MicroRNAs (miRNA) are short non-coding RNAs, approximately 20 nucleotides in length, that are derived from endogenous hairpin transcripts [58]. They negatively regulate gene expression by partially pairing to complementary mRNA sequences usually within the three prime untranslated region (3'UTR). This binding leads to either translational repression, exonucleolytic mRNA decay, or endonucleolytic cleavage for highly complementary targets. A number of studies indicate that a single miRNA may target, on average, over 100 mRNAs, making them powerful gene regulators [59]. Hence the recent boom of miRNA studies in translational cancer research.

1.2.1 MicroRNA biogenesis

The biogenesis of miRNAs is a multi-step process starting in the nucleus and ending in the cytoplasm (Figure 1.4) [60]. Firstly, miRNA genes are transcribed into primary capped and polyadenylated precursors (pri-miRNAs) by RNA Polymerase II [61]. These pri-miRNAs are several kilobases long and harbour the mature miRNA sequence within the 5' or 3' arm of their characteristic stem loop structure. In the nucleus, the pri-miRNA is then cropped at the stem by a Drosha/DGCR8 heterodimer to produce a hairpin structured pre-miRNA of 60-100 nucleotides [62]. The approximately 2 nucleotide 3' overhangs of pre-miRNA are recognised by Exportin-5 (XPO5) and Ran-GTP, enabling their nuclear export [63]. The pre-miRNAs are then cleaved at the loop by RNase III enzyme Dicer and related proteins (TRBP and PACT), releasing a miRNA duplex of ~22 nucleotides in length [64-66]. These miRNA duplexes then associate with Argonaute (Ago) proteins and form an RNA-induced silencing complex (RISC). One strand of the duplex remains in Ago as the mature miRNA while the other strand is

degraded [67]. MicroRNAs then direct Ago proteins to target mRNAs by imperfect complementary binding [68].

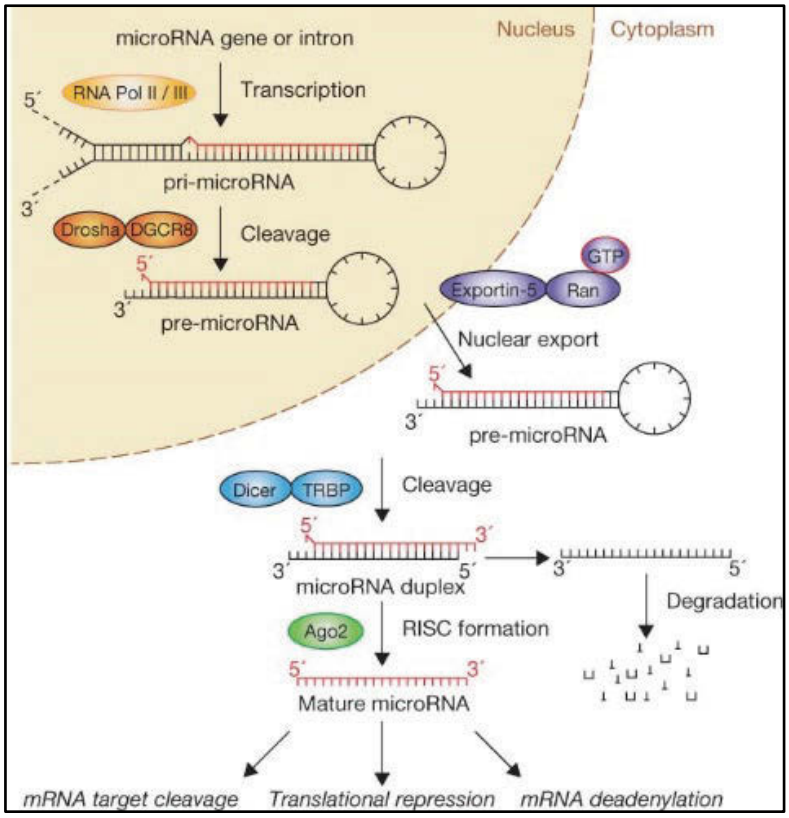

Figure 1.4: miRNA biogenesis: from nuclear origins to cytoplasmic maturation and downstream effects. This flow diagram demonstrates pri-microRNA transcription and its cleavage to a pre-miRNA in the nucleus before being exported to the cytoplasm. In the cytoplasm further cleavage and processing degrades one of the strands and leaves the mature strand in a RISC complex for downstream mRNA targeting. *Image acquired from [69]*.

1.2.2 MicroRNAs in cancer

MicroRNA expression is frequently dysregulated in cancer. Despite the expression of some miRNAs being upregulated or unchanged, most are downregulated in tumours compared to normal tissue [70]. MicroRNAs have been strongly associated with tumourigenesis, functioning either as tumour suppressors or oncogenes. Usually miRNAs downregulated in tumours are shown to have a tumour suppressor role while upregulated miRNAs are conveyed as oncogenic miRNAs promoting tumour development. For example, a few miRNAs deemed to have a wide tumour suppressor role are the miR-15/16, miR-34 and miR-200 clusters whereas some miRNAs described as oncogenes include the miR-17/92, miR-222/221, miR-21 and miR-155 clusters [59, 71].

MicroRNA expression profiling of tumours and corresponding normal tissue across a range of cancers has identified dysregulation of miRNA expression [59, 71]. These differences are further explored to correlate altered miRNA expression with changes in tumour biology, hence identifying potential therapeutic targets. Interestingly, miRNA profiles have been found to correlate with clinical and biological characteristics of tumours such as tissue origin, subgroup and patient prognosis [70, 71]. An example of tissue development origin is the difference in miRNA profiles between tumours of epithelial origin and hematopoietic malignancies [70]. Also, comparing miRNA profiles of acute lymphoblastic leukaemia (ALL) allowed subgrouping into three major groups [70]. MicroRNA profiling has even shown the potential to be used as a prognostic tool in lung cancer where high expression of miR-155 correlated with poor patient prognosis [72].

Overall, there is compelling evidence supporting the important role miRNAs play in regulating pathways involved in cancer. There are also promising results suggesting that miRNA profiles can be used to diagnose and subtype tumours and even reflect patient prognosis.

1.2.3 MicroRNA expression is altered in MPM

In common with other cancer types, MPM shows characteristic changes in miRNA expression. These changes agree with previously reported miRNA dysregulation in other solid tumours as well as present some new miRNA candidates that may reveal specific biological roles in MPM [73]. Research in miRNA expression dysregulation in MPM aims to discover functional consequences (Table 1), as well as identify miRNAs as potential biomarkers and/or therapeutic targets in MPM [74].

Studies investigating the dysregulation of miRNAs in MPM have associated biological functions with the altered miRNA expression observed. Initial studies of miRNA expression in MPM identified miR-29c as a frequently downregulated miRNA in MPM cell lines compared to normal mesothelial cells. Overexpression of miR-29c in MPM cell lines was subsequently shown to inhibit cell proliferation and invasion *in vitro* by targeting DNA methyltransferases 1 (DNMT1) and 3A (DNMT3A) [75]. Another study identified reduced miR-31 expression in MPM cell lines and subsequent re-expression of miR-31 decreased cell proliferation through cell cycle arrest, and inhibited cell migration and invasion. Restoration of miR-31 expression also reduced the expression of protein phosphatase 6 catalytic subunit (PPP6C), a phosphatase linked to chemotherapy resistance, which is expressed at high levels in MPM tumour samples [76].

Additionally, downregulated expression of the well-known tumour suppressor miR-34 and miR-15 miRNA families, has also been described in MPM cell lines and tumours. The co-expressed miR-34b and miR-34c (miR-34b/c) have been shown to be silenced by methylation in 100% of MPM cell lines tested and in the majority (85.1%) of MPM tumours [77]. The transfection of MPM cells with

physiological miR-34b/c expression resulted in decreased colony-forming ability with G1 cell cycle arrest and inhibition of cell motility, migration and invasion. Forced overexpression of miR-34b/c in MPM cells inhibited cell growth by inducing apoptosis [77]. Further research investigated the cellular effect of inhibiting miR-34b/c expression in normal mesothelial cells and reported a significant increase in cell proliferation and invasion. This strongly suggests that miR-34b/c play an important role in the carcinogenic transformation of mesothelial cells to MPM [78].

The miR-15 family of miRNAs are known to act as tumour suppressors with expression of these miRNAs inhibiting cell proliferation and promoting apoptosis of cancer cells [79]. The detectable members of the miR-15 family, including miR-15a, miR-15b, miR-16 and miR-195 have all been found to be downregulated in both MPM cell lines and tumours [80]. Transfection of MPM cell lines with miR-15a, miR-15b and miR-16a leads to an inhibition of cell proliferation and induction of cell cycle arrest and apoptosis, through targeting of the B-cell lymphoma 2 (BCL2) and cyclin-D1 (CCND1) genes. Also the re-expression of miR-16 sensitised MPM cells to the chemotherapy drugs pemetrexed and gemcitabine [80].

Another miRNA significantly downregulated in malignant mesothelial tissues and MPM cell lines is miR-145. Expression of this miRNA was shown to be suppressed by promoter hypermethylation in both tumours and MPM cell lines [81]. The transfection of MPM cell lines with miR-145 negatively affected cell proliferation, clonogenicity, cell migration and tumour growth *in vitro*. The over-expression of miR-145 also decreased the levels of the target octamer-binding transcription factor 4 (OCT4), a gene known to correlate with increased resistance of mesothelioma cells to pemetrexed *in vitro* [82]. This suggests that the miR-145 and OCT4 interaction plays an important role in the survival and drug resistance of MPM cells.

Changes in microRNA expression influence the metabolism and behaviour of malignant cells, and changes in miR-126 expression levels, observed in MPM and mesothelial cells, have been found to be caused by stress [83]. These stresses included oxidative stress, aberrant mitochondrial function, mitochondrial DNA (mtDNA) depletion, and hypoxia. With the exception of oxidative stress, the remaining stimuli all suppressed the expression of miR-126 in MPM cells. MPM cells stably transfected with miR-126 showed impaired respiration, a glycolytic shift, and failed to form tumours *in vivo*. These results were partly due to the downregulation of target insulin receptor substrate 1 (IRS1), which subsequently suppressed the activation of Akt signalling [83]. An ensuing study also reported the overexpression of miR-126 in MPM cells to induce autophagic flux and suppress tumour formation [84]. Overall, miR-126 supressed MPM by targeting IRS1, interfering with mitochondrial function and inducing autophagy.

MPM patient specimens also show reduced levels of miR-223 compared to normal tissue [85] and this was consistent in both human and mouse MPM cell lines, with both showing downregulation compared to normal mesothelial cells. A target of miR-223, Stathmin (STMN1), is a microtubule regulator associated with MPM [86]. Levels of STMN1 expression were found to be higher in human and mouse MPM cell lines compared to normal primary mesothelial cells. The overexpression of miR-223 in MPM cell lines reduced STMN1 levels, inhibited cell motility and induced tubulin acetylation [85], reflecting the important role miR-223 plays in MPM cell motility.

In summary, the reduced expression of the described miRNAs appears to play an important role in MPM biology. These downregulated miRNAs all appear to have tumour suppressor functions when re-expressed in MPM cell lines by regulating cell proliferation through cell cycle arrest, inducing apoptosis and impairing pro-tumorigenic metabolism, as well as inhibiting cell movement and inducing sensitivity to chemotherapeutic drugs. It is the importance of miRNAs in the abovementioned biological roles that promote the use of miRNAs as potential therapeutic targets in MPM (Table 1.1).

Table 1.1: Expression level and biological functions of miRNAs in MPM

MicroRNA	Expression in MPM vs normal tissue	Experimentally validated function(s)	Reference(s)
miR-29c	Downregulated	Inhibits cell proliferation and invasion; targets DMNT1/3A	[75]
miR-31	Downregulated	Inhibits cell proliferation, migration and invasion; targets PPP6C	[76]
miR-34b/c	Downregulated	Inhibit cell growth, motility, migration and invasion	[77]
miR15/16	Downregulated	Inhibit cell proliferation; sensitises to pemetrexed and gemcitabine; targets BCL2 and CCND1	[79, 80]
miR-145	Downregulated	Inhibits cell proliferation and migration; targets OCT4; sensitises to pemetrexed	[81, 82]
miR-126	Downregulated	Inhibits cell growth; suppresses tumour growth; targets IRS1	[83, 84]
miR-223	Downregulated	Inhibits cell motility; induces tubulin acetylation; targets STMN1	[85, 86]

1.2.4 MicroRNAs as biomarkers in MPM

Similar to other cancers, dysregulated miRNA expression in MPM has been investigated for the identification of potential diagnostic and prognostic biomarkers. The following studies investigate the discriminating power of miRNA expression levels in tumour samples or less invasive blood samples.

Initial tumour diagnostic studies aimed at differentiating between malignant adenocarcinoma found in the pleura from MPM by comparing miRNA levels [87, 88]. Using the ROC curve analysis, the first

study identified that the expression of the miR-200 family could be used to distinguish between malignant adenocarcinoma and MPM samples. The lower expression levels of the miR-200 family in MPM was able to distinguish between samples with an accuracy greater than 0.9 [87]. The second study identified a miRNA signature involving higher miR-192, miR-200c and lower miR-193a-3p expression levels in MPM samples compared to malignant adenocarcinoma. This signature was able to correctly identify MPM in blinded samples with an accuracy of 95% [88].

A more recent study, aimed at distinguishing MPM from benign pleural samples, initially compared matched diagnostic biopsies of MPM and non-neoplastic pleura (NNP) from five patients. These researchers found miR-126, miR-143, miR-145 and miR-652 to be significantly downregulated in MPM and diagnostic biopsies compared with NNP. This miRNA expression pattern was validated in a larger cohort of 40 patients before reaching a combined 4 miRNA signature that could differentiate between MPM and NNP with an accuracy of 0.96 [89].

MicroRNA expression in tumours has also been investigated to assist in predicting prognosis of patients after diagnosis. A large scale study of MPM tumours involving a training set of 37 tumours and a validation set of 92, identified miR-29c-5p as an independent prognostic indicator. Amongst epithelioid tumours, miR-29c expression was found to be significantly higher and associated with a longer period to progression and a greater overall survival [75]. Another tumour expressed miRNA linked to a prognostic value is miR-31 [75]. The expression of this miRNA was found to be significantly reduced in MPM compared to reactive mesothelial proliferation. Four out of the five cases deemed to have upregulated miR-31 expression were of biphasic or sarcomatoid histology, which are known to be the more aggressive compared to the epithelioid type. The mean overall survival rates of the patients with upregulated miR-31 (5.3 months) were significantly lower than the normal and those cases with downregulated miR-31 expression (30.1 and 27.3 months respectively) [90]. This reflects the promising prognostic potential of tumour expressed microRNAs, miR-29c and miR-31, in predicting overall patient survival.

As MPM patients are usually elderly, the option of surgery for tumour samples is not always available. Thus, the development of a blood-based biomarker would be a less invasive and desired approach. As a result, there are few reports that have investigated circulating miRNA levels in serum, plasma and whole blood of MPM patients for both diagnostic and prognostic value.

An initial small scale study analysed the whole blood of MPM patients, asbestos exposed and unexposed healthy controls. MPM patients had lower levels of miR-103 compared to both control groups and was able to discriminate between asbestos exposed controls (AUC =0.757) and unexposed healthy controls (AUC =0.871) [91]. Another larger study found low levels of miR-126 in MPM tumours,

compared to healthy mesothelial controls, to correlate with miR-126 levels in the serum. The low levels of miR-126 in the serum of MPM patients were significantly lower than those in the asbestos-exposed and healthy control groups [92]. A follow up study of miR-126 also added that the expression levels amongst MPM patients was significantly lower compared to non-small cell lung cancer (NSCLC) patients and controls. This study also identified that MPM patients with the lowest expression of miR-126 had significantly shorter survival rates [93]. A third study identified circulating miR-625-3p at significantly higher levels in the plasma and serum of MPM patients. Plasma miR-625-3p levels identified MPM patients against normal controls (AUC =0.824), while serum miR-625-3p levels distinguished MPM from asbestosis patients (AUC =0.793). These higher levels were also seen in MPM tumour samples suggesting that they may be originating from the tumour [94]. All of these examples emphasise the potential for circulating miRNAs in the blood to be potential diagnostic and prognostic biomarkers for MPM.

1.2.5 MicroRNAs as therapeutic targets in MPM

From the abovementioned studies, it is apparent that a global downregulation of miRNAs is observed in MPM. Additionally, various studies have shown that the restored expression of some of these downregulated miRNAs can bring about MPM tumour suppression. In particular, the miR-15/16 family of microRNA was consistently found to be downregulated in MPM tumour samples and cell lines. Using synthetic mimics to restore miR-15/16 expression led to growth inhibition in MPM cell lines. Following *in vitro* experiments, mesothelioma xenograft-bearing mice systemically received intravenous administration of tumour supressing miR-16 mimics packaged in minicells. These bacterial derived minicells, known as EDV™ nanocells (EDVs), were targeted with epidermal growth factor receptor (EGFR) specific antibodies which ensured targeted delivery as MPM is known to highly express EGFR [95]. The results of this study showed that miR-16 mimic loaded EDVs were able to control tumour growth in a dose and time dependent manner with the highest dose almost completely inhibiting tumours [80]. Subsequently, the first-in-man, phase I trial was conducted using miR-16-based mimic loaded minicells called TargomiRs. The aim of the study was to assess the safety, optimal dosing, and activity of TargomiRs in patients with recurrent MPM. The maximum tolerable dose was determined to be 5×10^9 TargomiRs once weekly. Of the 22 patients who were assessed for response by computed tomography (CT), one (5%) had a partial response, 15 (68%) had stable disease, and six (27%) had progressive disease. Although only one patient achieved an objective response, the median overall survival was 200 days [96]. Overall, the trial achieved an acceptable safety profile and early signs of clinical activity of the TargomiRs, and supports additional future studies exploring the restoration of downregulated miRNAs as a therapeutic approach in MPM.

1.2.6 MicroRNAs in the tumour microenvironment

Tumour samples also include cells from the tumour microenvironment, referred to as stromal cells. Stromal cells consist of tumour supporting cells such as fibroblasts, endothelial cells, and immune cells [97]. These cells play an important role in tumour development by supporting tumour cell growth, invasion and angiogenesis [98]. Due to their presence within tumours, stromal cells also contribute to the miRNA expression of tumour samples, hence contributing to the dysregulated miRNA expression observed in tumours. This was shown in a small, pancreatic periampullary adenocarcinoma study that generated miRNA profiles of matched tumour and stromal tissue as well as normal healthy tissue [99]. MicroRNA profiling found a large number of differentially expressed miRNAs between the stroma and tumour (43 miRNAs), between stroma and normal tissue (287 miRNAs), and tumour and stromal tissues (331 miRNAs) ($P < 0.05$). While a large proportion ($n = 228$) of differentially expressed miRNAs were common amongst stromal and tumour tissue as compared to normal tissue, 43 miRNAs were differentially expressed ($P < 0.05$) between stromal and tumour tissue. Of these miRNAs 26 were upregulated and 17 downregulated in the stroma. This reflects the influence stromal cells can have on dysregulation of miRNA expression in whole tumour samples.

MicroRNAs expressed by stromal cells are also likely to have functional consequences impacting tumorigenesis. More specifically, an ovarian cancer study compared microRNA expression levels between cancer-associated fibroblasts (CAFs) with normal or tumour-adjacent fibroblasts [100]. Results showed that CAFs had significant miR-31 and miR-214 downregulation and miR-155 upregulation ($P < 0.05$) compared to normal fibroblasts. This was also seen in induced CAFs, made by the co-culture of normal fibroblasts with ovarian cancer cells for 7 days. It was also possible to program normal fibroblasts into CAFs and vice versa by altering miR-31, miR-214 and miR-155 expression levels accordingly through a triple transfection. MicroRNA programmed CAFs were then co-cultured with ovarian cancer cells (HeyA8 and SKOV3ip1), enhancing fibroblast migration as well as cancer cell invasion and colony formation. The functional effects of each miRNA was also assessed separately with miR-214 being active in regulating fibroblast migration and cancer cell invasiveness, miR-155 predominantly affecting cancer cell invasiveness, and miR-31 affecting colony formation of the cancer cells.

Endothelial cells are another type of stromal cell that influence tumour development through promotion of angiogenesis, which is the branching of endothelial cells from existing blood vessels to form new vessels. This is necessary for tumours to meet their high metabolic and nutritional demands during tumour growth. MicroRNAs have been shown to regulate tumour angiogenesis. For example, in a lung cancer study, miR-126 was shown to regulate endothelial cell recruitment by targeting

vascular endothelial growth factor (VEGF) in lung cancer [101] and, interestingly, the expression of miR-126 is silenced in many human cancers [102]. The lung cancer study showed that transduction with a miR-126 expressing lentivirus led to downregulation VEGF-A expression in the A549, Y-90, and SPC-A1 cell lines, and also inhibited cell proliferation and induced cell cycle arrest at G1 *in vitro*. An *in vivo* xenograft tumour model, transducing A549 cells with the lentiviral miR-126 vector significantly inhibited tumour development, as shown by a 22.4% reduction in tumour weight.

Inflammation is a potent contributor to tumour progression and many cancers arise from sites of infection, chronic irritation and inflammation [103]. Immune cells, including tumour-associated macrophages (TAMs), neutrophils, dendritic cells, natural killer (NK) cells and B and T cells, have been shown to play both pro- and anti-tumorigenic roles [104]. Many of these cells are derived from the bone marrow, particularly the myeloid lineage, and are recruited by tumour cells to enhance their survival, growth, invasion and dissemination [105]. One of the main immune cell types present in the tumour microenvironment are the TAMs, which have been linked to differing tumorigenic roles depending on whether they are the classical M1 or alternate M2 activated type [106]. Several miRNAs have been associated with modulating macrophage activation and functions. For example, in response to Toll-like receptors (TLR), NFkB signalling promotes expression of miR-155 [107]. This expression enhances the classic pro-inflammatory response by targeting suppressor of cytokine signalling (SOCS) 1, B-cell lymphoma-6 protein (BCL6) and the interleukin 13 (IL-13) receptor, which promote alternative activation [108, 109]. Interestingly TAMs also produce miRNA-containing microvesicles that can fuse with tumour cells. An *in vitro* study has demonstrated that the invasive properties of breast cancer cells can be modulated by microvesicle-mediated transfer of miR-223, which downregulates myocyte-specific enhancer factor 2C (MEF2C) expression in cancer cells, leading to increased cell invasion [110].

This handful of examples reflects the functional impact miRNAs can have on stromal cells in the tumour microenvironment, demonstrating another avenue for miRNAs in regards to regulating tumorigenesis. However, with the exception of the release of microvesicles containing miR-223, by TAMs in breast cancer, these examples do not identify the cell type of origin of the specific miRNAs.

1.3 Contribution of tumour and stromal cells to tumour microRNA expression

Although miRNA studies associated with cancer have exploded in the last decade, there remains a lack of understanding concerning how different cell types contribute to the expression levels of particular miRNAs in normal tissue and to tumour miRNA expression profiles. Studies investigating miRNA profiles between tumour and normal tissue biopsies often fail to consider the cellular composition of the studied samples. MicroRNAs are expressed in cells, not tissues, therefore miRNA expression

variation between tissue samples, such as tumour tissue compared to normal tissue, is in fact a combined result of differing cell type composition and cell specific expression [111].

When interpreting miRNA profile studies for the selection of candidate miRNAs in diseases, including cancer, it is important to consider the expression of cell-specific miRNAs. This would then allow miRNA functional studies to be performed in the appropriate cell types and hence experimental findings would hold biological relevance. The issue is commonly overlooked in studies aiming to identify dysregulated miRNA expression, as these are often based solely on the comparison of miRNA profiles between normal and tumour tissues. MiRNAs with altered expression between normal and tumour tissues are usually further investigated in pure tumour cell populations grown in tissue culture *in vitro*. Prominent examples of non-epithelial microRNAs studied for their potential roles in tumour cell biology include miR-126 [83], miR-145 [81] and miR-223 [85].

1.3.1 The importance of the miR-143/145 cluster in cancer

The importance of understanding the cell type expression patterns of miRNAs is shown in the example of the expression of the miR-143/145 cluster. These two co-expressed miRNAs have been shown to be downregulated in a range of epithelial cell malignancies and linked to various tumour promoting targets, hence labelling them as tumour suppressors [112, 113]. Colorectal cancer is the most abundantly studied cancer describing the tumour suppressive role of miR-143/145. It is widely accepted that the expression of these miRNAs, especially miR-143, is abundant in normal colonic tissue and that the loss of its expression is commonly believed to be due to the transformation of normal epithelial cells to a malignant state [111]. However, careful research has demonstrated that miR-143/145 is not expressed by intestinal epithelial cells. Instead, *in situ* hybridisation studies have demonstrated miR-143/145 to be exclusively expressed in mesenchymal cells and quantitative RT-qPCR confirmed this with almost undetectable levels in epithelial preparations [114]. In an independent evaluation, small RNA RNA-seq was performed on flow-sorted $EPCAM^{+}$ epithelial cells, isolated red blood cells and cultured endothelial, fibroblast and smooth muscle cells (SMCs). Results of this study showed that miR-143-3p was expressed at a level that was at least 33-fold higher in fibroblasts and SMCs compared to other cell types. The low levels detected in other cell types were hypothesised to be due to either mesenchymal contamination or a leaky promoter. miR-145 was also expressed in both mesenchymal cell types with much lower and negligible expression in other cell types [111]. A sample of colonic adenocarcinoma would predominantly contain more malignant epithelial cells with less fibroblasts and no SMCs compared to a normal colon sample. Therefore, the loss of miR-143/145 expression is explained by the major change in cellular composition between normal and malignant colorectal tissue rather than a loss of expression in epithelial cells [114].

Another study exploring the tumour suppressive role of the miR-143/145 cluster was in an autochthonous mouse model of lung adenocarcinoma [115]. Initial findings demonstrated that the loss of the miR-143/145 cluster did not promote tumour development. Also, the forced expression of miR-143 and miR-145 through lentiviral infection in mice did not show any significant difference in tumour burden compared to controls and hence did not support the tumour suppressive role of miR-143 and miR-145 in previously studied tumour cell lines [112, 113]. However, histological analysis of mice with organism wide deletion of the miR-143/145 cluster revealed dramatically reduced tumour burden with a 3-fold decrease in tumour area, indicating that systemic miR-143/145 expression may play a role in promoting tumour development [115]. This data suggests that miR-143/145 expression in the tumour stroma may actually be promoting lung tumorigenesis. In order to determine the miR-143/145 expressing cells, fluorescence-activated cell sorting was used to evaluate miRNA levels in endothelial cells ($CD31^+$), immune cells ($CD45^+$), epithelial cells ($EpCAM^+$) and in the triple-negative fraction thought to include SMCs, fibroblasts, pericytes, and activated neutrophils. Results indicated epithelial cells to be lacking miR-143/145 expression and endothelial cells to be rich in miR-143/145 expression. Further investigation of the loss of the miR-143/145 expression found endothelial cell proliferation to be reduced by preventing mitotic entry hence inhibiting neoangiogenesis. These findings demonstrate that miR-143/145 expression in the stroma stimulates neoangiogenesis and supports tumour development [115].

Overall, the above examples force us to consider the cell source of miR-143 and miR-145 when investigating their functional roles in tumorigenesis, as well as reconsider the biological relevance of past functional studies undertaken in epithelial tumour cells. The loss of miR-143/145 expression was determined to be due to a lack of mesenchymal cells, which exclusively express miR-143/145, in the cellular composition of colorectal tumour tissue compared to normal colon tissue, suggesting that miR-143/145 could have a biologically relevant role in tumourigenesis through mesenchymal cell expression [114]. Also, the demonstration of stromal miR-143/145 in promoting tumourigenesis by stimulating neoangiogenesis in mouse lung adenocarcinoma models provides caution against the use of these miRNAs as cancer therapeutic agents.

In regards to the miR-143/145 cluster, these miRNAs have also been studied in MPM. An example is a study aiming to identify specific diagnostic markers for MPM [89]. In this study, qPCR screening and validation of miRNA expression in patient-matched diagnostic pleural biopsy samples (DB), surgical MPM samples, and corresponding non-neoplastic pleura (NNP) was performed. The validated results found the expression of miR-126 ($P < 0.05$), miR-143 ($P < 0.05$), miR-145 ($P < 0.001$), and miR-652 ($P < 0.01$) to be significantly downregulated in matched MPM ($n = 14$) and NNP samples [89]. Although these miRNAs have promising diagnostic value, caution should be taken to not assume loss of miR-

143 and miR-145 in mesothelioma as they may originate from stromal cells. The transfection of MPM cell lines with miR-145 was also shown to negatively affect cell proliferation, clonogenicity, cell migration and tumour growth *in vitro*. Over expression of miR-145 targeted OCT4, a gene known to correlate with increased resistance of mesothelioma cells to pemetrexed [81]. As these experiments were carried out *in vitro,* it would be of interest to see whether they would have the same functional consequences in an *in vivo* setting where stromal cells known to express miR-145 may have a more significant role in tumorigenesis.

1.3.2 miR-126 regulation in cancer

Endothelial cells are abundant in nearly all tissues including tumours. Deep-sequencing reveals that miR-126 is the second most highly expressed miRNA in endothelial cells [116]. Studies have shown endothelial cell-restricted miR-126 expression to mediate angiogenesis. Endothelial cells obtained from miR-126 null mice showed dramatically impaired proliferation compared to wild type derived endothelial cells when grown in *ex vivo* culture. An *in vivo* matrigel plug endothelial cell invasion assay containing proangiogenic fibroblast growth factor 2 (FGF-2) or PBS as control was used to study endothelial cell invasion between miR-126 deficient and expressing cells. Endothelial cells derived from miR-126 null mice showed significantly lower ($P < 0.001$) angiogenic response to FGF-2 compared to controls. The study also demonstrates miR-126 to target Spred-1, an intracellular inhibitor of the Ras/MAP kinase pathway that represses angiogenic signalling. Hence, the overexpression of miR-126 relieves the repressive influence of Spred-1 on the signalling pathways activated by VEGF and FGF, favouring angiogenesis [117].

The expression of miR-126 has been studied across various cancer types with most of the studies showing downregulation [102]. Although miR-126 is described as promoting angiogenesis, suggesting a supporting role in tumour development, miR-126 overexpression has been shown to inhibit endothelial cell recruitment and suppress metastasis in breast cancer cells [118]. To determine the role of miR-126 in metastatic progression, stable miR-126 expressing and miR-126 knockdown control cells were generated and injected into immunodeficient mice. The silencing of miR-126 in MDA-231 breast cancer cells significantly increased lung metastatic colonisation and systemic metastatic colonisation to other multiple organs. Consistent with these findings, restoring miR-126 in metastatic LM2 cells after extravasation in the lung significantly reduced metastatic colonisation. These results show miR-126 expression to be a suppressor of metastatic initiation and colonisation. The study also investigated miR-126 ability to recruit endothelial cells to metastatic cells. When the miR-126 silent and metastatic LM2 cells were placed in the bottom of a Boyden chamber they strongly recruited human umbilical cord endothelial cells through a porous trans-well insert. The recruitment of

endothelial cells was significantly more compared to their less metastatic parental line. Hence endothelial cell recruitment was found to be strongly inhibited by miR-126 overexpression [118].

Undoubtedly miR-126 expression is strongly associated with endothelial cells, considering their recruitment and functional role in tumorigenesis. However, the global downregulation of miR-126 in many cancer studies has resulted in the investigation of functional roles within malignant epithelial cells. The following are a few examples that have investigated the functional consequences of forced expression of miR-126 in cancer cell lines shown to have downregulated miR-126. The re-expression of miR-126 in colon cancer cells supresses their viability and inhibits migration and invasion by targeting chemokine receptor type 4 [119]. Also, introducing miR-126 expression reduced gastric cancer cell proliferation, by inducing cell cycle arrest in G0/G1 phase, and also inhibited migration and invasion *in vitro* [120]. The overexpression of miR-126 in prostate cancer cells was shown to reduce cell migration [121]. Another example is the forced overexpression of miR-126 in renal cancer cells which inhibited cell growth by supressing cell cycle progression from G0/G1 to S phase. This study also confirmed that miR-126 targets IRS1, resulting in reduced growth of transfected cells [122].

In line with studies in other tumour types, stable miR-126 expression in MPM cell lines was shown to act as a tumour suppressor by targeting IRS1 as well as interfering with mitochondrial function [83]. Unfortunately, this MPM study among other epithelial cell malignancies mentioned have neglected to investigate the functional role miR-126 plays in endothelial cells. Instead they have investigated the functional consequences of miR-126 expression in epithelial cells which may not be as biologically relevant. Also, studies aiming to identify diagnostic and prognostic biomarkers in MPM that have identified miR-126 as a biomarker need to consider endothelial cell contribution to expression levels. MPM expression levels of miR-126 derived from tumour samples [89, 92] and circulating serum [93] both may be an indication of endothelial cell activity, hence tumour promoting neoangiogenesis suggested by the correlation between increased miR-126 expression and worse MPM patient prognosis.

1.3.3 miR-223 in differentiation and cancer

miR-223 is specifically expressed in the myeloid cell lineage [123, 124]. The first important role of miR-223 was discovered in the field of haematology as it was shown to modulate the differentiation of haematopoietic lineages. In the bone marrow, miR-223 is primarily expressed in myeloid cells and is induced during the lineage differentiation of myeloid progenitor cells [124]. Expression of miR-223 is also known to fine-tune the differentiation of myeloid progenitor cells as miR-223 expression is repressed during monocyte differentiation and highly expressed during granulocyte differentiation [125].

A comprehensive study investigating the distinct role of miR-223 during granulocyte differentiation generated miR-223 mutant mice. Interestingly, the absence of miR-223 expression in these mice did not inhibit the production of granulocytes but, instead, granulocyte numbers increased. This was associated with an increase in MEF2C, a transcription factor, and target of miR-223, that drives granulocyte-monocyte progenitor proliferation. Another effect seen in the miR-223 mutant mice was the production of hyperactive neutrophils and the presence of spontaneous lung inflammation suggesting that miR-223 plays a role in the homeostasis of mature neutrophils. Although miR-223 is upregulated during granulocyte differentiation, it is not strictly essential for granulocyte production [126].

Given the role of miR-223 in differentiating myeloid progenitor cells, it is no surprise that it is found to be downregulated in leukaemia and lymphomas. The most common fusion protein, AML1/ETO, in acute myeloid leukaemia (AML), reduces miR-223 expression through chromatin remodelling. Ectopic re-expression of miR-223, targeting AML1/ETO, or demethylating treatments, have been shown to restore cell differentiation of myeloid cancer cells by enhancing miR-223 levels [127]. These observations provide a potential therapeutic option for AML patients.

The expression of miR-223 has also been investigated in solid tumours, where expression is usually downregulated, and miR-223 is described to play a tumour suppressor role. Lentiviral transfected HeLa cells overexpressing miR-223 show significant suppression of proliferation, growth rate and colony formation *in vitro* and *in vivo*. The functional target of miR-223 in HeLa cells was identified as the insulin-like growth factor-1 receptor (IGF1R), which was also seen in leukaemia and hepatoma cells [128]. Another example is the re-expression of miR-223 in hepatocellular carcinoma cells which revealed a consistent inhibitory effect on cell viability by targeting microtubule regulatory protein (STMN1) [86]. As previously described, the overexpression of miR-223 in MPM cell lines also targeted STMN1 and led to inhibition of cell motility and induced tubulin acetylation [85].

In addition to the above examples, the functional role of miR-223 has been investigated in many epithelial cancer cell lines. The question is whether these roles are biologically relevant in cancer cells given that miR-223 expression is specific to the myeloid cell lineage. An interesting perspective described in recent studies is the delivery of miRNAs between cells in microvesicles [129]. Macrophage derived microvesicles have been shown to transport miRNAs to a range of cells including monocytes, endothelial cells, epithelial cells, and fibroblasts. The same study found transported miR-223 to be functionally active in target cells and also that microvesicles induce the differentiation of macrophages [130]. Further functional studies of these microvesicles have shown them to play a role in promoting invasion in cancer cell lines. An important example is the exosomes of tumour associated

macrophages which have been shown to deliver miR-223 to co-cultured breast cancer cells SKBR3 and MDA-MB-231 without direct contact. Further to this, functional studies have revealed that the increase in miR-223 expression promotes invasion of these breast cancer cells by targeting the MEF2C-β-catenin pathway [110]. Finally, a study of the rapid delivery of miR-223 by platelet-derived microvesicles to the lung cancer cell line A549 demonstrated that platelet-secreted miR-223 promotes lung cancer cell invasion by targeting tumour suppressor erythrocyte membrane protein band 4.1 like 3 (EPB41L3) [131]. Thus, miR-223 functional roles in cancer cells may be relevant considering its delivery by microvesicles. This also suggests that miR-223 possibly acts as a signal in the crosstalk between tumour and immune cells in the tumour microenvironment.

1.4 Preliminary data and rationale

In order to investigate the relative contribution of miRNAs from tumour and stromal cells in MPM tumours, the miRNA expression of xenograft tumours was compared to corresponding cultured tumour cells. As subcutaneously injected human mesothelioma cells develop into a xenograft tumour, mouse stromal cells will be recruited. The harvested tumour will therefore be a mixture of human tumour cells and mouse stromal cells. In parallel to this, the corresponding cultured cells will only consist of human tumour cells. Ultimately, the isolated RNA will consist of a mixture of RNAs from tumour and stromal cells from the xenograft tumour and only tumour cells from cell culture (Figure 1.5).

Previous work in the laboratory generated miRNA expression profiles from RNA isolated from MSTO and H226 cell-line-derived xenografts and their corresponding cultured cells. Based on this preliminary data, there is clearly a significant increase in the expression of particular miRNAs in both MSTO and H226 xenografts compared to the corresponding cultured cells (Table 1.2). Such an increase in miRNA expression observed in both xenograft models strongly suggests stromal cell contribution to the expression of these miRNAs.

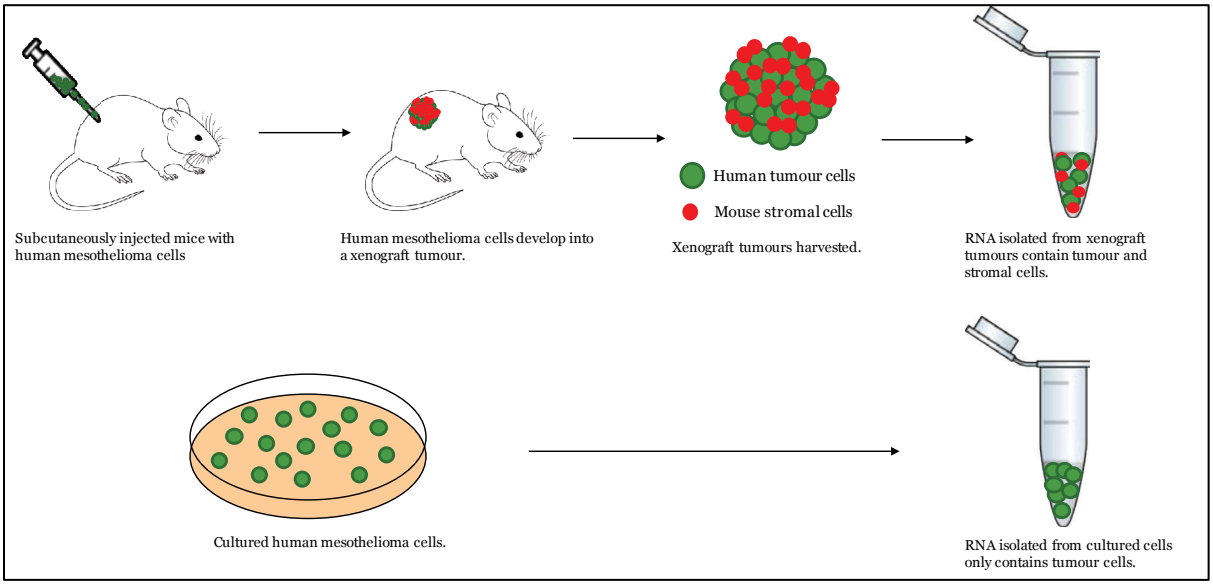

Figure 1.5: Workflow representation of RNA isolation and cell composition between xenograft tumours and cultured cells. Human MPM cells injected into mice develop into xenograft tumours. These human xenografts, with adjacent mouse stromal cells, were harvested and RNA isolated. MPM cells were cultured *in vitro* and RNA isolated.

Table 1.2: Most relevant fold changes in miRNA expression of MSTO and H226 xenografts compared against corresponding cultured cells

MicroRNAs	Fold Change (against cultured cells)	
	MSTO Xenograft	H226 Xenograft
hsa-miR-126-3p	19	17
hsa-miR-143-3p	6230	6140
hsa-miR-145-5p	1189	5264
hsa-miR-206-3p	9071	131
hsa-miR-214-3p	34302	2618
hsa-miR-223-3p	23074	11911
hsa-miR-872-5p	155	340
hsa-miR-451-5p	292	34
*hsa-miR-15a-5p	2	2

***included to show ubiquitous expression**

1.5 Project hypothesis and aims

1.5.1 Hypothesis

Both tumour cells and stromal cells contribute to the characteristic changes in miRNA expression observed in MPM.

1.5.2 Project aims

1) Investigate the relative contribution of miRNAs from tumour and stromal cells in MPM xenograft tumours.

2) Determine the tumour and stromal cell source of miRNAs in MPM xenograft tumours.

3) Identify which specific stromal cells in the tumour microenvironment are expressing these miRNAs.

4) Explore the functional consequences of the dysregulated expression of these miRNAs in MPM cell lines.

Chapter 2 – Materials and Methods

2.1 Materials and reagents

2.1.1 Mesothelioma cell lines

The mesothelioma cell lines used in this study were available at the Asbestos Diseases Research Institute (ADRI) and are presented in Table 2.1.

Table 2.1: List of mesothelioma cell lines used

Cell line	Type	Subtype	Source
MSTO-211H	Mesothelioma	Biphasic	American Type Culture Collection (ATCC)
NCI-H226	Mesothelioma	Epithelioid	American Type Culture Collection (ATCC)
NCI-H28	Mesothelioma	Epithelioid	American Type Culture Collection (ATCC)
VMC23	Mesothelioma	Epithelioid	Medical University of Vienna
MeT-5A	Immortalised Mesothelioma	N/A	American Type Culture Collection (ATCC)
AB1	Murine Mesothelioma	Epithelioid	School of Medicine and Pharmacology, University of Western Australia

2.1.2 Reagents for tissue culture

All reagents for cell and tissue culture are listed in Table 2.2.

Table 2.2: List of tissue culture reagents

Reagents	Catalogue ID	Supplier
Roswell Park Memorial Institute (RPMI) 1640 Medium, Glutamax Supplement, HEPES	72400047	Gibco by Life Technologies Australia Pty Ltd
Fetal Bovine Serum (FBS), qualified, USDA-approved regions	10437028	Gibco by Life Technologies Australia Pty Ltd
Trypsin-EDTA (0.05 %), phenol red	25300054	Gibco by Life Technologies Australia Pty Ltd
Dulbecco's Phosphate-buffered saline (DPBS), no calcium, no magnesium	14190144	Gibco by Life Technologies Australia Pty Ltd
Dimethyl Sulfoxide (DMSO)	PHR1309	Sigma-Aldrich by Merck

Table 2.3: List of reagents used in total RNA isolation

Reagents	Catalogue ID	Supplier
TRIzol Reagent – Phenol, Thiocyanic acid compound with guanide (1:1), Ammonium thiocyanate	15596018	Invitrogen by Life Technologies Australia Pty Ltd
Chloroform – contains 100-200 ppm amylenes as stabilizer, ≥99.5 %	C2432	Sigma-Aldrich by Merck
Isopropanol (2-Propanol) – BioReagent, for molecular biology, ≥99.5 %	I9516	Sigma-Aldrich by Merck
Absolute Ethanol (diluted to 75 % with Milli-Q water)	JJOOABS10P	Fronine by Thermofisher
UltraPure™ DNase/RNase-Free Distilled Water	10977023	Invitrogen by Life Technologies Australia Pty Ltd
3 M Sodium Acetate solution – BioUltra for molecular biology	71196	Sigma-Aldrich by Merck

Table 2.4: List of reagents and consumables for microRNA RT-qPCR arrays

Reagents	Catalogue ID	Supplier
Megaplex RT Primers, Human Pool Set v3.0	4444745	Applied Biosystems by Life Technologies Australia Pty Ltd
TaqMan Human MicroRNA Array Card v3.0:		Applied Biosystems by Life Technologies Australia Pty Ltd
- Card A	4398977	
- Card B	4428123	

Table 2.5: List of microRNA reverse transcription (RT) reagents

Reagents	Catalogue ID	Supplier
TaqMan MicroRNA Reverse Transcription Kit: - 100 mM dNTPs (with dTTP) - Multiscribe Reverse Transcriptase, 50 U/μL - 10X Reverse Transcription Buffer - RNase Inhibitor, 20 U/μL	4366596	Applied Biosystems by Life Technologies Australia Pty Ltd
UltraPure DNase/RNase-Free Distilled Water	10977023	Invitrogen by Life Technologies Australia Pty Ltd

TaqMan 5X RT primers: - hsa-miR-223 (002295) - hsa-miR-214 (002293) - hsa-miR-143 (002249) - RNU6B (001093)	4427975	Applied Biosystems by Life Technologies Australia Pty Ltd

Table 2.6: List of microRNA qPCR reagents and consumables

Reagents and consumables	Catalogue ID	Supplier
KAPA PROBE FAST Universal qPCR kit: - KAPA PROBE FAST qPCR Master Mix (2X) Universal - KAPA PROBE FAST Rox Low (50X)	KK4701	KAPA Biosystems by Merck
TaqMan 20X TM primers: - hsa-miR-223 (002295) - hsa-miR-214 (002293) - hsa-miR-143 (002249) - RNU6B (001093)	4427975	Applied Biosystems by Life Technologies Australia Pty Ltd
MicroAmp Fast Optical 96-Well Fast Reaction Plate, 0.1 mL	4346907	Applied Biosystems by Life Technologies Australia Pty Ltd

Table 2.7: List of pri-miRNA reverse transcription reagents

Reagents	Catalogue ID	Supplier
Moloney Murine Leukemia Virus (M-MLV) Reverse Transcriptase kit: - M-MLV Reverse Transcriptase - M-MLV RT 5X Buffer	M1705	Promega Corporation
dNTP Mix 10 mM (diluted to 2.5 mM with UltraPure water)	U1515	Promega Corporation
Oligo(dT) 50 μM (mix of 18T and 15T primers 1:1 from 100 μM stocks)	Custom order	Integrated DNA technologies
Random Hexamer (NNNNNN) 10 μM	51-01-18-01	Integrated DNA technologies
Recombinant RNasin Ribonuclease Inhibitor	N2511	Promega Corporation

Table 2.8: List of pri-miRNA ddPCR reagents and consumables

Reagents and consumables	Catalogue ID	Supplier
2X ddPCR Supermix for Probes (No dUTP)	186-3024	Bio-Rad Laboratories, Inc
TaqMan Pri-miRNA Assays: - hsa-miR-223 (Hs03303017_pri) - mmu-miR-223 (Mm03307156_pri) - hsa-miR-214 (Hs03302971_pri) - mmu-miR-214 (Mm033307122_pri) - hsa-miR-143 (Hs03303166_pri) - mmu-miR-143 (Mm03306564_pri) - hsa-miR-15a (Hs03302582_pri) - mmu-miR-15a (Mm03306795_pri)	4427012	Applied Biosystems by Life Technologies Australia Pty Ltd
DG8 Cartridge (for QX200 Droplet Generator)	1864008	Bio-Rad Laboratories, Inc
Droplet Generation Oil for Probes	1863005	Bio-Rad Laboratories, Inc
Droplet Generator DG8 Gasket	1863009	Bio-Rad Laboratories, Inc
ddPCR 96-Well Plates	12001925	Bio-Rad Laboratories, Inc
Pierceable Foil Heat Seal	1814040	Bio-Rad Laboratories, Inc

Table 2.9: List of *in situ* hybridisation reagents

Reagents and consumables	Catalogue ID	Supplier
Menzel-Glaser Superfrost Plus microscope slide	4951PLUS4	Thermo Scientific
Paraformaldehyde (diluted to 4 % with DPBS)	C007	ProSciTech Pty Ltd
Diethyl pyrocarbonate - ≥97 % (NMR)	D5758	Sigma-Aldrich by Merck
Xylene – ACS reagent, ≥98.5% xylenes + ethylbenzene basis (ethylbenzene ≤25 %)	676748	Sigma-Aldrich by Merck
Absolute Ethanol (also diluted to 90, 80, and 70 % with DEPC treated water)	JJOOABS10P	Fronine by Thermofisher
Dulbecco's Phosphate – buffered saline (DPBS), no calcium, no magnesium	14190144	Gibco by Life Technologies Australia Pty Ltd
Proteinase-K buffer (5 mM Tris-HCL pH7.4, 1 mM EDTA, 1 mM NaCl)	N/A	Made at ADRI

microRNA ISH Buffer Set (FFPE) Hybridization Buffer:	90000	Exiqon by Qiagen
- microRNA ISH Buffer 2X		
- Proteinase K		
miRCURY LNA miRNA Detection probes:		Exiqon by Qiagen
- hsa-miR-223-3p (biotin labelled)	YD00619871	
- U6, hsa/mmu/rno (biotin labelled)	YD00699002	
- Scramble miR (biotin labelled)	YD00699004	
LifterSlip coverglass, 18 x 18 mm, 7.55 µL	G481	ProSciTech Pty Ltd
UltraPure 20X SCC Buffer (diluted to 5X, 1X, and 0.2X using DEPC treated water)	15557-044	Invitrogen by Life Technologies Australia Pty Ltd
Blocking buffer (5 % FBS and 0.3 % Triton X-100 made in DPBS)	N/A	Made at ADRI
Streptavidin-HRP Conjugate antibody mix:		
- Streptavidin-HRP Conjugate (1:250)	19534050	Invitrogen by Life Technologies Australia
- Triton X-100 (0.3 %)	T9284	Sigma-Aldrich by Merck
- Bovine Serum Albumin (1 %)	A9647	Sigma-Aldrich by Merck
made in DPBS		
DAB Peroxidase Substrate Kit:	SK-4100	Vector Laboratories, Inc
- Buffer pH7.5 Stock Solution		
- Hydrogen Peroxidase Solution		
- DAB Stock Solution		
1 % Copper sulfate made in distilled water:		
- Copper(II) sulfate - ReagentPlus, ≥ 99%	C1297	Sigma-Aldrich by Merck
Water for Irrigation (used as distilled water)	AHF7113	Baxter Healthcare Pty Ltd
Eosin (1 %) staining solution, made with:		
- Eosin Y disodium salt (1 %)	E5382-25G	Sigma-Aldrich by Merck
- Absolute Ethanol (diluted to 95 % with MilliQ water) (~80 %)	JJOOABS10P	Fronine by Thermofisher
- Glacial acetic acid (0.5 %)	A9967-2.5KG	Sigma-Aldrich by Merck
- Distilled tap water (20 %)		

Hematoxylin Solution, Harris Modified	HHS32	Sigma-Aldrich by Merck
0.3 % Acid Alcohol, made with:		
- Absolute Ethanol (diluted to 70 % with MilliQ water)	JJOOABS10P	Fronine by Thermofisher
- Hydrochloric acid (37 %)	320331	Sigma-Aldrich by Merck
Scotts Water, in 1 L of Milli-Q filtered water add:		
1 g Sodium bicarbonate	S5761	Sigma-Aldrich by Merck
5 g Magnesium sulfate	208094	Sigma-Aldrich by Merck
Entellan New Mounting Medium	IM0225	ProSciTech
Coverslip glass (No.1, 18 x 18 mm)	G409	ProSciTech

Table 2.10: List of miRNA mimic transfection reagents in addition to tissue culture reagents

Reagents	Catalogue ID	Supplier
Lipofectamine RNAiMAX Transfection Reagent	13778150	Invitrogen by Life Technologies Australia Pty Ltd
Synthetic RNA and microRNA mimics (antisense sequence):	Custom order	Shanghai GenePharma Co.,Ltd
- hsa-miR-16-5p (UAGCAGCACGUAAAUAUUGGCG)		
- hsa-miR-143-3p (UGAGAUGAAGCACUGUAGCUC)		
- hsa-miR-214-3p (ACAGCAGGCACAGACAGGCAGU)		
- hsa-miR-223-3p (UGUCAGUUUGUCAAAUACCCCA)		
- RRM1-3 (positive control) (UAGAAGUGCAUACUAGUGAGUUUGC)		
- C81 (negative control) (AAGCAACUUGGUAAGACUCGUGUGG)		

Table 2.11: List of SYBR green growth assay reagents

Reagents	Catalogue ID	Supplier

SYBR Green I Nucleic Acid Gel Stain, 10,000X concentrate in DMSO	S7585	Invitrogen by Life Technologies Australia Pty Ltd
20X SYBR Green Lysis Buffer (Tris HCl, pH8, 200 mM, EDTA 50 mM, Triton X-100 2 % v/v)	N/A	Made at ADRI
Millipore Milli-Q water	N/A	Milli-Q filter at ADRI

Table 2.12: List of Colony Formation assay reagents

Reagents	Catalogue ID	Supplier
Crystal Violet – Dye content ≥90 %	C3886	Sigma-Aldrich by Merck
Millipore Milli-Q water	N/A	Milli-Q system at ADRI
Absolute Ethanol	JJOOABS10P	Fronine by Thermofisher

Note: Life Technologies Australia is now a subsidiary of Thermo Fisher Scientific.

2.2 Methods

2.2.1 Tissue culture

Mesothelioma cell lines (Table 2.1) were cultured in T75 culture flasks with 10 mL of Roswell Park Memorial Institute (RPMI) medium supplemented with 10 % fetal bovine serum (FBS) and grown in a cell culture CO_2 incubator set at 37 °C with 5 % CO_2. When cells reached approximately 80 % confluence, they were passaged accordingly (usually split 1:10). In order to achieve a 1:10 split of cells, the old medium was removed by aspiration and cells gently washed with 5 mL of DPBS to remove any residual FBS from the original medium. The cells were then detached from the surface of the flask by adding 1 mL of trypsin and incubating in the CO_2 incubator for 2-3 minutes at 37 °C. Once cells were detached, 4 mL of FBS supplemented RPMI was added to deactivate the trypsin activity. After mixing well, 0.5 mL of the cell suspension was transferred to a new secondary T75 flask and topped up with 9.5 mL of fresh FBS supplemented RPMI medium.

2.2.2 Reviving frozen cells

Mesothelioma cell lines (Table 2.1) stored in liquid nitrogen were defrosted from frozen stocks as required. Cells were originally frozen in RPMI/FBS medium supplemented with 10 % DMSO. To revive cells, they were partially defrosted just enough to dislodge the frozen sample and then tipped into 5 mL of RPMI/FBS. The solution was centrifuged to pellet the cells and the DMSO-containing supernatant was aspirated. The cell pellet was resuspended in fresh RPMI/FBS and transferred into an appropriate tissue culture flask.

2.2.3 Freezing cells for cryostorage

When mesothelioma cell lines (Table 2.1) reached 80-90 % confluence in a T75 culture flask, the medium was aspirated and the cells washed with DPBS and incubated with trypsin under routine tissue culture conditions. The detached cells were then resuspended in RPMI/FBS to a total of 9 mL and transferred to a sterile centrifuge tube. Then 1 mL of DMSO was added and mixed to suspend cells in RPMI/FBS supplemented with 10% DMSO. This was then aliquoted to 10 cryovial tubes at 1 mL volumes each before slow freezing in an isopropanol freezing buoy at least overnight at -80 °C. Frozen cells were then transferred to liquid nitrogen for long term storage.

2.2.4 Mouse xenograft and syngraft tumour samples

Control mouse xenograft tumour samples consisted of tumours derived from engraftment of established human mesothelioma cells MSTO and H226 in the flank of BALB/c nude mice, previously carried out at ADRI (ethics approval; Sydney Local Health District Animal Welfare Committee approval 2011-003). The process involved the subcutaneous injection of 2.5 x 10^6 MSTO or H226 cells into immunodeficient nude mice resulting in the development of corresponding xenograft tumours. As the tumours developed they recruited mouse stromal cells to support tumourigenesis. The harvested xenograft tumour then consisted of a mixture of human mesothelioma and mouse stromal cells. These samples were snap frozen in -80 °C and formalin-fixed paraffin-embedded (FFPE) for future downstream use in this project. Control syngraft tumour samples were also included from samples from the engrafting of murine mesothelioma cells AB1 in immunocompetent BALB/c mice (ethics approval; Sydney Local Health District Animal Welfare Committee approval 2017-017).

2.2.5 Total RNA isolation

Total RNA isolation was performed using TRIzol reagent following the manufacturer's instructions with slight modifications. All centrifugations for RNA isolation were performed at 13,000 rpm at 4 °C using the Heraeus Fresco 17 refrigerated centrifuge. To isolate total RNA from cultured cells, the medium was first aspirated before adding 1 mL of TRIzol reagent to homogenize the sample. The cells were

then vigorously scraped off and pipetted into a 1.5 mL microcentrifuge tube. For frozen xenograft tumours the sample was first homogenized using a disposable grinder pestle in a 1.5 mL microcentrifuge tube. Then 1 mL of TRIzol was added and mixed by pipetting up and down.

The homogenized samples were allowed to incubate for 5 min at room temperature. Then 0.2 mL of chloroform was added to the TRIzol and cell suspension, the lid capped securely and shaken vigorously for 15 s. The mixture was allowed to incubate for 2-3 min at room temperature before centrifuging for 15 min. The RNA containing aqueous phase was then pipetted out whilst avoiding any draw up of the interphase or lower organic phase. The aqueous phase was then placed into a new 1.5 mL microcentrifuge tube and 0.5 mL 100 % isopropanol was added. The mixture was then incubated by freezing overnight at -80 °C to precipitate RNA.

After RNA precipitation, samples were centrifuged for 30 min. The supernatant was removed and 1 mL of 75 % ethanol (previously chilled at -20 °C) was added to the RNA pellet. The pellet was then washed in the ethanol by briefly shaking until the pellet was dislodged. The sample was then centrifuged for 10 min to reobtain an RNA pellet and supernatant discarded. This ethanol wash process was repeated once more and the pellet was left to air dry for about 10 min whilst avoiding complete drying. The remaining RNA pellet was then resuspended in UltraPure water depending on pellet size (usually 20-50 μL) by pipetting up and down gently several times. The resuspension was then heated on a heat block at 60 °C for 10 min to completely dissociate the RNA pellet before placing on ice for RNA concentration reading on an Implen NanoPhotmeter.

The instrument was first blanked with 3 μL of UltraPure water before 3 μL of each sample was analysed to obtain RNA concentration. Sample quality was also assessed by recording the 260:280 and 260:230 ratios indicating protein and TRIzol contamination respectively. If the samples were of good quality (both ratios ≥1.8) then proceed downstream or freeze at -80 °C. For samples of insufficient quality, a 1:10 volume of 3M sodium acetate was added to the RNA suspension and a further 1 mL of chilled 75 % ethanol was added on top. The solution was then mixed well by inverting several times and then frozen overnight at -80 °C before proceeding to RNA precipitation step again.

2.2.6 TaqMan miRNA stem-loop primer based RT

A miRNA specific, reverse transcription (RT) of RNA samples (table 2.13) was performed to generate complementary DNA (cDNA) for subsequent qPCR. The TaqMan MicroRNA Reverse Transcription Kit was implemented according to manufacturer's protocol with slight modifications. Initially, a multiplex of 5X miRNA RT primers was prepared with specific miRNA and reference RNU6B in a ratio of 1:2 (Table 2.14). Then the required RT mix was prepared based on a total downscaled reaction of 5 μL for

each RNA sample which was previously adjusted and aliquoted to a concentration of 50 ng/μL (Table 2.15). The resulting RT mix was then mixed and briefly centrifuged before placing in a MultiGene thermal cycler under the manufacturer's recommended conditions (Table 2.16).

Table 2.13: List of RNA samples used for validation

Cultured mesothelioma cell line (Reference)	Mouse xenograft tumour
MSTO	MSTO Xenograft 1
	MSTO Xenograft 2
	MSTO Xenograft 3
	MSTO Xenograft 4
	MSTO Xenograft 5
	MSTO Xenograft 6
H226	H226 Xenograft 1
	H226 Xenograft 2
	H226 Xenograft 3
	H226 Xenograft 4
	H226 Xenograft 5
	H226 Xenograft 6
	Mouse syngraft tumour
AB1	AB1 Syngraft 1
	AB1 Syngraft 2
	AB1 Syngraft 3
	AB1 Syngraft 4

Table 2.14: Multiplex of 5X miRNA RT primers prepared with specific miRNA and reference RNU6B in a ratio of 1:2

TaqMan™ 5X RT Primer	Volume (μL)
hsa-miR-143-3p	4.5
hsa-miR-214-3p	4.5
hsa-miR-223-3p	4.5
RNU6B	9

Table 2.15: Reaction proportions for a 5 μL multiplex RT mix

Reagent and sample	Volume (μL)
100 mM dNTPs (with dTTP)	0.05
Multiscribe Reverse Transcriptase, 50 U/μL	0.33
10X Reverse Transcription Buffer	0.5
RNase Inhibitor, 20 U/μL	0.06
TaqMan 5X RT Primer mix	1
UltraPure water (DNase/RNase free)	2.06
RNA (50 ng/μL)	1

Table 2.16: Thermal cycler reaction conditions for miRNA RT

Temperature (°C)	Time (minutes)
16	30
42	30
85	5
4	∞

2.2.7 TaqMan miRNA probe based qPCR

Following miRNA specific RT, the now cDNA synthesised miRNAs and RNU6B control were diluted by adding 28.9 μL of UltraPure water. This dilution was necessary to achieve the correct cDNA concentration for downstream qPCR. For qPCR, the KAPA PROBE FAST Universal qPCR kit was used in conjunction with the TaqMan 20X TM primers according to the manufacturer's recommendations with slight modifications. The qPCR reactions were prepared separately for each TaqMan 20X TM primer with all corresponding cDNA in a downscaled total reaction of 10 μL and was plated in a 0.1 mL MicroAmp Fast Optical 96-Well Fast Reaction Plate in duplicates including non-template control (NTC) (Table 2.17). The plates were then sealed, shaken to mix, then briefly spun down and checked to ensure there were no bubbles that would interfere with fluorescent detection. The plated samples were then run on an Applied Biosystems ViiA 7 qPCR system under the manufacturer's recommended conditions (Table 2.18).

The Ct values were determined by setting the threshold above the background fluorescence and within the linear phase of amplification. The raw Ct value data was then exported and analysed in Microsoft Excel 2016. The Ct value was averaged for each sample and the fold change was calculated using the Delta-delta method equation $2^{-\Delta\Delta Ct}$ [132] compared to the reference RNU6B and corresponding cultured cells. The fold change results were visualised with GraphPad software, Prism 7.

Table 2.17: Reaction components for a 10 μL qPCR mix

Reagent	Volume (μL)
KAPA PROBE FAST qPCR Master Mix (2X) Universal	5
KAPA PROBE FAST Rox Low (50X)	0.2
TaqMan™ 20X TM primer mix	0.25
UltraPure™ water (DNase/RNase free)	2.3
Corresponding cDNA	2.25

Table 2.18: qPCR reaction conditions performed on the Applied Biosystems ViiA 7 qPCR system

Temperature (°C)	Time (seconds)	Step
95	20	Hold
95	1	X 40
60	20	

2.2.8 Moloney-Murine Leukemia Virus (M-MLV) reverse transcription

For the non-specific RT of pri-miRNA transcripts, fresh RNA from remaining samples (Table 2.19) were reverse transcribed using the M-MLV RT kit. This RT kit consists of a two-step reaction RT and was used following the manufacturer's recommendation with slight modifications. The first reaction mix was prepared for each RNA sample which was previously adjusted and aliquoted to a concentration of 500 ng/μL (Table 2.20). The resulting first mix was then mixed and briefly centrifuged before placing in a MultiGene thermal cycler under the manufacturer's recommended first-step conditions (Table 2.21). Once the first reaction was complete and cooled to 4 °C the mix was briefly centrifuged and the second-step reaction components were added to each mix (Table 2.22). The samples were again

mixed and briefly centrifuged before placing back into the MultiGene thermal cycler under the manufacturer's recommended second-step conditions (Table 2.23).

Table 2.19: List of RNA samples used for the M-MLV RT and subsequent ddPCR of species specific pri-miRNA transcripts

Cultured mesothelioma cell line (Reference)	Mouse xenograft tumour
MSTO	MSTO Xenograft 2
	MSTO Xenograft 3
	MSTO Xenograft 5
	MSTO Xenograft 6
H226	H226 Xenograft 2
	H226 Xenograft 3
	H226 Xenograft 4
	H226 Xenograft 5
	H226 Xenograft 6

Table 2.20: First-step reaction components of M-MLV RT

Reagent	Volume (μL)
dNTP Mix 2.5 mM	4
Oligo(dT) 50 μM (mix of 18T and 15T)	2
Random Hexamer (NNNNNN) 10 μM	1
UltraPure water	7
RNA (500 ng/μl)	2

Table 2.21: Thermal cycler reaction conditions for the first-step of M-MLV RT

Temperature (°C)	Time (minutes)
72	5
4	∞

Table 2.22: Second-step reaction components of M-MLV RT

Reagent	Volume (μL)
M-MLV Reverse Transcriptase	0.5
UltraPure water	0.5
M-MLV RT 5X Buffer	4

Table 2.23: Thermal cycler reaction conditions for the second-step of M-MLV RT

Temperature (°C)	Time (minutes)
42	60
94	10
4	∞

2.2.9 TaqMan pri-miRNA probe based Digital Droplet PCR (ddPCR)

The non-specific cDNA synthesised by M-MLV-RT was then diluted by adding 24 μL of UltraPure water to obtain a concentration of 22.22 ng/μL for the following ddPCR. The ddPCR Supermix for Probes (No dUTP) was used in conjunction with the TaqMan Pri-miRNA Assays according to the manufacturer's recommendations with slight modifications. The ddPCR reactions were prepared separately for each TaqMan Pri-miRNA Assay for all cDNA samples including an NTC with a total reaction volume of 25 μL (Table 2.24). The samples were then mixed well and briefly centrifuged before slowly pipetting 20 μL into the sample wells of a DG8 Cartridge without creating any bubbles. Then 70 μL of the Droplet Generation Oil for Probes was also carefully added to designated oil wells of the DG8 Cartridge while avoiding bubble formation. Once the samples and appropriate oil was added, the DG8 Cartridge was then sealed with a DG8 Gasket and carefully placed into the QX200 Droplet generator. Within minutes the QX200 Droplet generator partitioned each PCR mix into about twenty thousand droplets. These droplets were then carefully and slowly pipetted out of the cartridge to avoid droplet shearing and pipetted gently into a ddPCR 96 –Well plate. The plate was then sealed with a Pierceable Foil Heat Seal in a preheated PX1 PCR Plate Sealer. The sealed plate with samples was then placed in a C1000 Touch Thermal Cycler under the recommended conditions (Table 2.25). Once the ddPCR reaction was complete, the plate with samples was placed in the QX200 Droplet Reader which absolutely quantified pri-miRNA transcripts to copies per 20 μL. The data was then exported to Prism 7, GraphPad Software

for plotting and statistical analysis. In parallel, the same data was also exported to Microsoft Excel 2016 and normalised to pri-miR-15a tumour and stromal cell expressions separately. As pri-miR-15a was so abundantly expressed only 10 % of the total copies per 20 μL was used to normalise the expression of the remaining pri-miRNAs. The normalised data was also exported to Prism 7, GraphPad Software for plotting and statistical analysis. All statistical analysis of both data sets was generated using a two-tailed, unpaired *t*-test with a confidence interval of 95 %.

Table 2.24: Reaction components of a pri-miRNA ddPCR mix

Reagent	Volume (μL)
2X ddPCR Supermix for Probes (No dUTP)	12.5
TaqMan Pri-miRNA primer mix	1.25
UltraPure water	7.25
cDNA (22.22 ng/μL)	4

Table 2.25: ddPCR reaction conditions performed on the C1000 Touch Thermal Cycler

Temperature (°C)	Time (minutes)	Step
95	10	Hold
94	0.5	X 40
60	1	
98	10	Hold
4	∞	Hold

2.2.10 Localising miR-223-3p with *in situ* hybridisation

To identify the specific stromal cells in the xenograft tumour microenvironment expressing the most abundant miRNA, miR-223-3p, *in situ* hybridisation (ISH) was performed on xenograft tumour sections using biotin labelled miRCURY LNA miRNA Detection probes specific for hsa-miR-223-3p along with positive control U6 and negative control Scramble miR. The manufacturer's, miRCURY LNA microRNA ISH Optimization Kit, instruction manual recommendations were followed with slight modifications to optimise the experiment. Formalin fixed paraffin embedded (FFPE) xenograft tumour samples were sectioned using a Leica Biosystems RM2245 Microtome. Sections were initially cut at 4 μm but later optimised to 5 μm after testing at different thicknesses. A tissue floating bath filled with DEPC treated

water was previously warmed to 45 °C. This bath was used after sectioning to spread any creases in the FFPE sectioned samples. Once spread well, the tissue sections were carefully mounted onto Menzel-Glaser Superfrost Plus microscope slides and left to dry overnight.

The next day sections were melted at 60 °C for 30 min and briefly left to cool to room temperature. The slides were then deparaffinised in xylene and rehydrated gradually in a series of ethanol concentrations until submerged in DPBS (Table 2.26). Sections were then post fixed in fresh 4 % paraformaldehyde (PFA) at room temperature for 15 min to help preserve RNA but this step was later excluded as it was found to interfere with final staining results. Immediately before use, Proteinase-K (2 mg/mL) stock was diluted in Proteinase K buffer to the suppliers recommended working concentration (10 μg/mL) which was later modified to optimise treatment conditions. The slides were removed from DPBS and briefly dried by tapping before adding enough Proteinase-K to cover the sectioned sample. The slides were then placed in an oven at 37 °C and left to incubate for an optimised duration of 30 min. The Proteinase-K treated slides were then washed in DPBS twice.

As required, frozen 10 μM aliquots of the biotin labelled miR-223-3p, U6 and Scramble miR LNA probes were thawed, denatured at 90 °C for 4 min and then briefly centrifuged. The 2X microRNA ISH Buffer was diluted to 1X using UltraPure water. The 1X buffer was then used to dilute miR-223-3p, U6 and Scramble miR probes to the recommended concentrations which was also optimised as needed. The slides were removed from DPBS and again dried briefly by tapping. Excess 1X ISH buffer was used to pre-treat sectioned tissues and also removed by briefly tapping. Then 20 μL of ISH buffer/LNA probe mix was pipetted onto each corresponding slide and a LifterSlip coverglass placed on top gently without generating bubbles. These slides were then placed in the hybridisation oven at the recommended 53 °C for 90 min to hybridise. The 5X, 1X and 0.2X SSC buffers were also placed in the hybridisation oven at 53 °C for preheating and to be used next. Once hybridisation was completed the slides were immersed in room temperature 5X SSC buffer to remove the coverglass and then washed and incubated in a series of concentrated to dilute SSC buffers (Table 2.27).

The slides were then placed in Blocking buffer for 15 min at room temperature while the biotin binding Streptavidin-HRP Conjugate antibody mix was prepared fresh. The samples were then dried again briefly by tapping and 20 μL of Streptavidin-HRP mix was added onto each section. A LifterSlip coverglass was placed on top gently without generating bubbles and incubated at room temperature for 60 min. After incubation, the slides were again placed into DPBS to detach the coverglass and further washed in DPBS 3 times for 3 min each. To develop a colorimetric stain, the DAB Peroxidase Substrate was prepared according to manufacturer's recommendations where for every 2.5 mL of distilled water 1 drop of Buffer pH7.5 stock solution, 2 drops of Hydrogen peroxide solution and 1

drop of DAB stock solution was added from specially designed drip bottles. Before adding the DAB peroxidase substrate, the slides were dried again briefly by tapping and the substrate was added on top enough to cover the section and left to incubate in the dark for 5-10 min until the section developed brown staining. To improve the intensity of DAB staining treatment with 1 % copper sulfate solution was added to the protocol. The samples were dried briefly by tapping and copper sulfate solution was added enough to cover the sections and left to incubate for about 10 min at room temperature to enhance DAB staining.

After DAB staining and enhancement, the slides were washed in running distilled tap water for 2 min before counterstaining. Initially, slides were counterstained with Eosin but was then replaced by Hematoxylin as it proved to be a better counterstain. Eosin counterstaining involved dipping the slides briefly (~10 dips) in 95 % ethanol before staining in Eosin for 5 minutes and then moving onto the dehydrating steps (Table 2.28). Whereas, for hematoxylin counterstaining the slides were stained in hematoxylin for 10 min then rinsed in running distilled tap water for 5 min until the excess hematoxylin washes away. The slides were then briefly dipped in 0.3 % acid alcohol for about 3 s and then rinsed in running distilled tap water for 1 min. The slides were then placed in Scott's tap water for 2 min for blueing and rinsed again with water for 1 min.

After counterstaining, the slides were placed in a fume hood and gradually dehydrated in increasing concentrations of ethanol and finally xylene treated (Table 2.28). Following xylene, the slides were briefly dried again by tapping and a drop of Entellan New Mounting Medium was placed on each section. Coverslip glasses were used to seal the stained sections by firmly and carefully pressing down on the section to thin out the mounting medium as much as possible and massaging out any air bubbles. Slides were left to dry in the fume hood overnight and bright field images were captured at a later date using the Zeiss Axio Imager 2.

Table 2.26: Deparaffinising and rehydration of xenograft tumour slides for ISH

Step	Solvent	Duration (minutes)
1	Xylene	5
2	Xylene	5
3	Xylene	5
4	100 % Ethanol	3
5	100 % Ethanol	3
6	100 % Ethanol	3
7	90 % Ethanol	5

8	80 % Ethanol	5
9	70 % Ethanol	5
10	DPBS	2-5

Table 2.27: Series of concentrated to diluted SCC buffers used to wash hybridised sections

Step	Solvent	Duration (minutes)	Temperature (°C)
1	5X SSC Buffer	5	53 °C
2	1X SSC Buffer	5	53 °C
3	1X SSC Buffer	5	53 °C
4	0.2X SSC Buffer	5	53 °C
5	0.2X SSC Buffer	5	53 °C
6	0.2X SSC Buffer	5	Room temperature
7	DPBS	5	Room temperature

Table 2.28: Dehydration steps of stained sections before mounting

Step	Solvent	Duration (minutes)
1	95 % ethanol	5
2	100 % ethanol	5
3	100 % ethanol	5
4	Xylene	5
5	Xylene	5

2.2.11 Transfecting mesothelioma and mesothelial cell lines

Mesothelioma cell lines MSTO, H28, VMC23 and immortalised mesothelial cell line MeT-5A were transfected with miRNA mimics to explore functional roles. The cells were transfected with mimics using Lipofectamine RNAiMAX reagent to overexpress miRNAs miR-143-3p, miR-214-3p and miR-223-3p including positive control mimic miR-16-5p and siRNA controls C81 and RRM1-3 as negative and positive controls respectively. The mimics were prepared in a 1 in 3 serial dilution in RPMI medium (FBS free) to give a final concentration of 10, 3.3 or 1.1 nM. The negative control siRNA (C81) and the positive control siRNA (RRM1-3) were also prepared in RPMI medium (FBS free) to give a final

concentration of 5 nM and 1 nM respectively. The transfection reagent, Lipofectamine RNAiMAX, was also prepared in RPMI medium (FBS free) to give a final concentration of 0.083 % and left to incubate for 5 min at room temperature. The prepared mimic and siRNA solutions were then incubated with the transfection reagent solution at a 1:1 volume ratio and incubated for 20 min at room temperature. The Lipofectamine RNAiMAX complexed mimics and siRNAs were then plated in 96 well tissue culture treated plates as required at 20 μL volume per well (Figure 2.1).

The cell to be transfected were harvested by routine tissue culture method and counted using a Bright-Line hemocytometer by applying 10 μL of the cell suspension between the chamber and cover slip. The live cells were counted in 4 outlined regions and the average result was the cell concentration at 10^4 cells/mL. The cells were then prepared in RPMI/FBS at a concentration of $2x10^4$ cells/mL and 100 μL was pipetted to seed 2000 cells into each corresponding transection well including empty untreated (UT) wells. The remaining wells were then filled with 120 μL of DPBS to minimise evaporation and plates were placed into the CO_2 incubator set at 37 °C with 5 % CO_2.

	miR-16 10nM	miR-16 3.3nM	miR-16 1.1nM	miR-214 10nM	miR-214 3.3nM	miR-214 1.1nM	C81 5nM	RRM1-3 1nM			
	miR-16 10nM	miR-16 3.3nM	miR-16 1.1nM	miR-214 10nM	miR-214 3.3nM	miR-214 1.1nM	C81 5nM	RRM1-3 1nM			
	miR-16 10nM	miR-16 3.3nM	miR-16 1.1nM	miR-214 10nM	miR-214 3.3nM	miR-214 1.1nM	C81 5nM	RRM1-3 1nM			
	miR-223 10nM	miR-223 3.3nM	miR-223 1.1nM	miR-143 10nM	miR-143 3.3nM	miR-143 1.1nM	UT				
	miR-223 10nM	miR-223 3.3nM	miR-223 1.1nM	miR-143 10nM	miR-143 3.3nM	miR-143 1.1nM	UT				
	miR-223 10nM	miR-223 3.3nM	miR-223 1.1nM	miR-143 10nM	miR-143 3.3nM	miR-143 1.1nM	UT				

Figure 2.1: Transfection layout of mimics and siRNAs in a 96 well tissue culture plate. Cells were seeded at 2000 cells in 100 μL medium. Empty wells were filled with DPBS to reduce evaporation.

2.2.12 SYBR green based cell proliferation assay

A SYBR green based cell proliferation assay was performed to measure any growth inhibitory effects of overexpressing miRNA mimics; miR-143-3p, miR-214-3p and miR-223-3p. Transfected cells were harvested at 48, 72 and 96 h after transfection. Time point designated 96 well plates were decanted of their transfection medium and gently tapped dry. The plates were then sealed and frozen at -80 °C at least overnight. Once all the time points were harvested and frozen they were left to thaw at room temperature for 1 h. The DNA binding SYBR green solution was prepared by diluting 20X SYBR Green lysis buffer to 1X in Millipore Milli-Q water and adding SYBR Green I Nucleic Acid Gel Stain at a 1:8000 volume ratio. Then 200 μL of SYBR green solution was pipetted to each transfected well and left to incubate in the dark at room temperature for an hour. The fluorescence intensity of the plates was read on a FLUOstar Omega (BMG Labtech) by exciting DNA bound SYBR green with blue light (485 nm) and measuring emitted green light (520 nm). The data was then exported to Microsoft excel 2016 and analysed on prism 7, GraphPad software. All statistical analysis was generated using a two-way ANOVA test of repeated measures, corrected for multiple comparisons using the Dunnett's method with a confidence interval of 95 %. Statistical significance was determined by multiplicity adjusted P values <0.05. Each cell line was repeated 3 times at different passages to generate 3 biological repeats.

2.2.13 Crystal violet stained colony formation assay

A crystal violet staining colony formation assay was performed to explore the effects on colony formation after overexpressing miRNA mimics; miR-143-3p, miR-214-3p and miR-223-3p in mesothelioma and mesothelial cell lines. The medium was aspirated from the wells of the culture plates, the transfected cells washed with 100 μL of DPBS before incubating with 50 μL of Trypsin for 5 min at 37 °C. The detached cells were quickly transferred from their triplicate 96 wells to a corresponding single 6 well pre-filled with 2 mL of RPMI/FBS. These low density cells were then incubated in a CO_2 incubator set at 37 °C with 5 % CO_2 and left to form colonies for about 2 weeks. Once there was sufficient colony formation, the medium was decanted and cells were fixed by adding 2 mL of 75 % ethanol to each well and incubating for 30 min at room temperature. Crystal violet staining solution was made with 0.1 % crystal violet dye and 10 % ethanol in Millipore Milli-Q water. After fixing, the 75 % ethanol was removed and 2 mL of the crystal violet staining solution was added to each well and stained for 15 min at room temperature. The crystal violet staining solution was also decanted and the plates were gently rinsed with distilled tap water to remove excess staining solution and left to dry overnight. Pictures were taken of each well using a Zeiss Stemi 508 stereo microscope and exported to Microsoft Powerpoint 2016 for layout editing. Experiments were repeated 3 times with each cell line at different passages to generate 3 biological repeats.

Chapter 3 – Results

3.1 Investigating the relative contribution of miRNAs from tumour and stromal cells in MPM xenograft tumours.

Previous work performed by others in our laboratory generated miRNA expression profiles of the RNA isolated from MSTO and H226 cell line derived xenografts and their corresponding cultured cells. RNA samples were initially reverse transcribed using Megaplex RT Primers for Human Pool A and Pool B and complementary DNA was analysed by qPCR using the TaqMan Array Human MicroRNA A+B Cards Set v3.0 following the manufacturer's protocol. This generated an expression profile of 754 human miRNAs for each RNA sample. The normalised Ct values were exported and the fold changes were calculated using the $2^{-\Delta\Delta Ct}$ method [132] for each xenograft tumour miRNA compared against corresponding cultured cells.

Based on preliminary data, the miRNAs miR-143-3p, miR-214-3p and miR-223-3p were expressed several thousand-fold higher in both MSTO and H226 cell line derived xenograft tumours (n =1, each) compared to corresponding cultured cells suggesting strong stromal cell miRNA contribution. In order to validate these preliminary findings TaqMan miRNA probe based RT and qPCR was conducted on a larger sample of MSTO and H226 xenograft tumours (n =6, each). MSTO xenograft samples expressed markedly high mean fold change values for miR-143-3p (2728$\pm$757), miR-214-3p (8769$\pm$4494) and miR-223-3p (186062$\pm$37823) (Figure 3.1A). Also, H226 xenograft samples expressed high mean fold change values for miR-143-3p (2192$\pm$814), miR-214-3p (2038$\pm$362) and miR-223-3p (2512$\pm$572) (Figure 3.1B). Both MSTO and H226 xenograft tumours consistently expressed high fold change values for these miRNAs, validating the initial preliminary data while also increasing the sample size to increase reliability.

An interesting addition to the investigation was the inclusion of the AB1 syngraft tumour samples to allow comparison of miR-143-3p, miR-214-3p and miR-223-3p expression against the cultured murine mesothelioma cell line AB1. The AB1 syngraft tumour is composed of established AB1 murine mesothelioma cells developing into a tumour within the species of origin whilst also recruiting stromal cells. Thus, this model was included with the hypothesis that the candidate miRNAs would still hold notably higher expression levels. However, the AB1 syngraft samples (n =4) only expressed a high fold-change value for miR-223-3p (12397$\pm$1813) and minimal fold changes for miR-143-3p (0.320$\pm$0.079) and miR-214-3p (2.438$\pm$0.602) (Figure 3.1C).

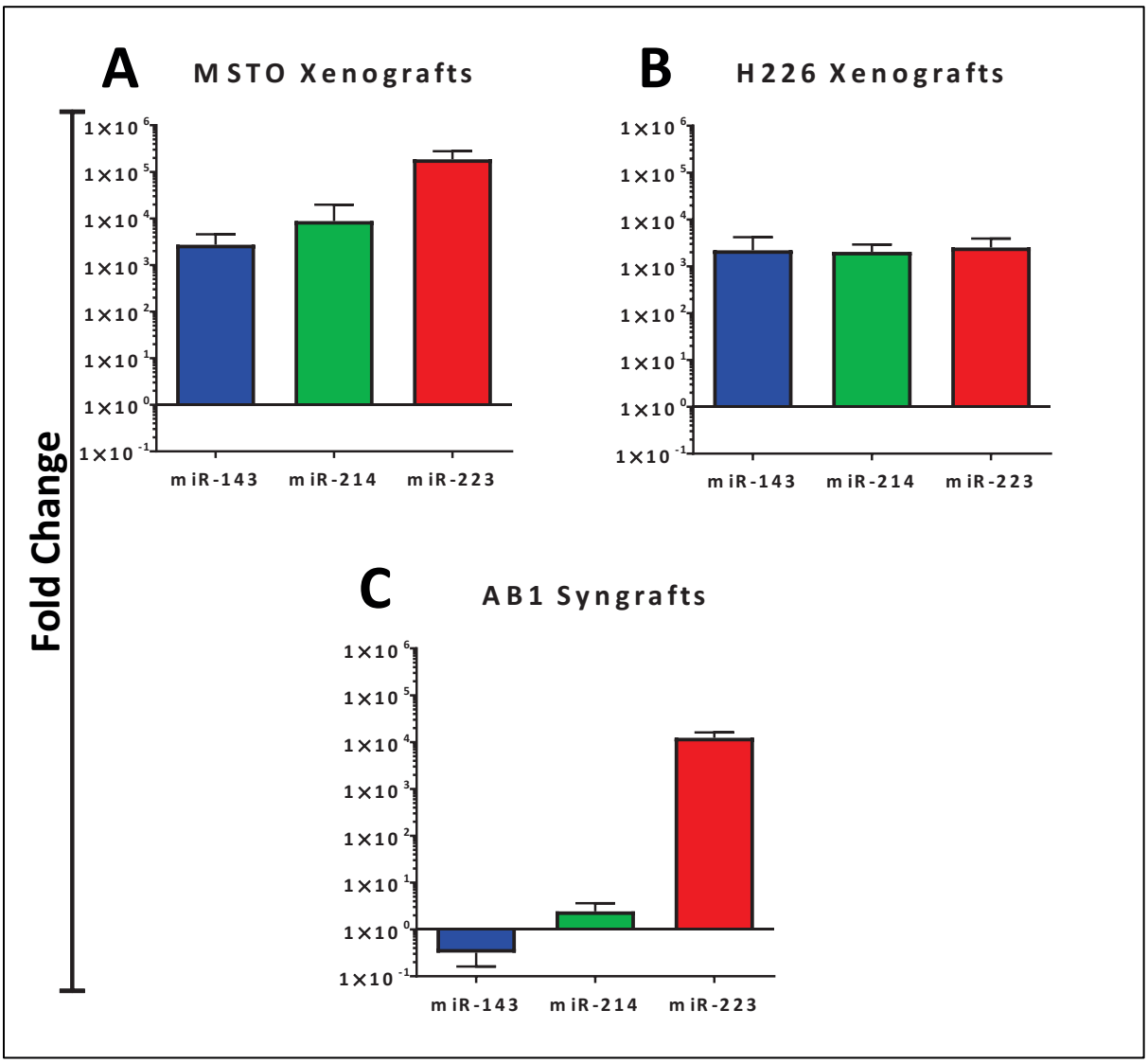

Figure 3.1: Expression of mir-143-3p, miR-214-3p and miR-223-3p in MSTO and H226 cell-line-derived xenografts compared against corresponding cultured cells. (A) Histogram of fold change expression of miR-143-3p (2728±757), miR-214-3p (8769±4494) and miR-223-3p (186062±37823) among MSTO xenografts (n =6) against cultured MSTO. (B) Histogram of fold change expression of miR-143-3p (2192±814), miR-214-3p (2038±362) and miR-223-3p (2512±572) among H226 xenografts (n =6) against cultured H226. (C) Histogram of fold change expression of miR-143-3p (0.320±0.079), miR-214-3p (2.438±0.602) and miR-223-3p (12397±1813) among AB1 syngrafts (n =4) against cultured AB1.

3.2 Determining the tumour and stromal cell source of miRNAs in MPM xenograft tumours.

The validation qPCR experiment confirmed that miR-143-3p, miR-214-3p and miR-223-3p are expressed substantially higher in MSTO and H226 cell line derived xenografts compared to their corresponding cultured cells. However, these findings only suggest strong mouse stromal cell contribution to the expression of the candidate miRNAs. The species difference between human tumour cells and mouse stromal cells in the xenograft tumours was used to determine the cell source of miRNAs. To achieve this, the species specific pri-miRNA sequence of xenograft tumours was quantified using ddPCR. As the mature sequence is identical between human and mouse species and the stem loop pre-miRNA sequence only has a few nucleotide differences, it is the initial pri-miRNA transcript that has long sequences which differ most between species. It is within these regions that TaqMan pri-miRNA Assay primers and probes are designed and able to distinguish between human and mouse species and thus tumour and stromal cell contribution to miRNA expression levels (Table 3.2).

To determine the tumour and stromal cell source of mature miRNAs in xenograft tumours the pri-miRNA transcripts were quantified to copies per 20 μL using the TaqMan pri-miRNA Assay and ddPCR method. The human and mouse pri-miRNAs of pri-miR-143, pri-miR-214, pri-miR-223 and pri-miR-15a were quantified for MSTO xenograft (n =4) and H226 xenograft (n =5) samples. The human and mouse pri-miR-15a was included as a reference as it is ubiquitously expressed among cell types with preliminary data (Table 1.2) showing only a 2-fold increase in MSTO and H226 xenografts compared to cultured cells with the same RNA input. Thus, pri-miR-15a can provide an indication of tumour to stromal cell composition of xenograft samples. Among the MSTO xenografts, pri-miR-214 and pri-miR-223 had higher mouse stromal expression (158.5±46.5 and 4239±1093 respectively) compared to human tumour expression (50.5±23.4 and 122.5±68.2 respectively) with only pri-miR-223 showing significance (P =0.0094). Also, pri-miR-143 was expressed lower in mouse stroma (94±38.4) than human tumour (156±58.5) cells but keeping in mind that reference pri-miR-15a was expressed significantly higher (P =0.0026) in human (507±78.5) than mouse (110±16.5) cells suggesting that there was much more tumour than stromal cells in the MSTO xenograft samples (Table 3.3A). On the other hand, for H226 xenografts, pri-miR-143, pri-miR-214 and pri-miR-223 all had higher mouse stromal expression (103.6±35, 155.2±35.5 and 2412±700.6 respectively) compared to human tumour expression (77.2±30.5, 44.7±13.3 and 33.6±14 respectively) with pri-miR-214 and pri-miR-223 showing significance (P =0.0194 and P =0.0094 respectively). Also, the reference pri-miR-15a was expressed at higher levels in human (422.8±198.7) than mouse (169.6±40.9) cells suggesting that there was also more tumour than stromal cells in the H226 xenograft samples (Table 3.3B).

As the reference pri-miR-15a is ubiquitously expressed among cell types its human and mouse variant expression levels in xenograft tumours also indicates the human tumour cell to mouse stromal cell ratio. Therefore, by normalising candidate pri-miRNAs to their corresponding human or mouse pri-miR-15a transcripts the difference in tumour to stromal cell composition of xenograft tumours is also corrected. Using the same quantitative data generated through ddPCR, the results for pri-miR-143, pri-miR-214 and pri-miR-223 are now expressed as fold change (normalised to pri-miR-15a) in MSTO (n =4) and H226 (n =5) xenograft samples. Among the MSTO xenografts, pri-miR-143, pri-miR-214 and pri-miR-223 all had higher expression in mouse stromal cells (8.26±2.57, 14.04±2.71 and 27.47±4.20 respectively) compared to human tumour cells (3.13±0.99, 0.94±0.37 and 2.38±0.48 respectively) with pri-miR-214 and pri-miR-223 showing statistical significance (P =0.0031 and P =0.0010 respectively; Table 3.4A). Additionally, for H226 xenografts, pri-miR-143, pri-miR-214 and pri-miR-223 also all had higher expression in mouse stromal cells (11.21±7.49, 14.75±7.39 and 14.70±2.71 respectively) compared to human tumour cells (2.32±0.82, 1.34±0.31 and 0.87±0.11 respectively) with only pri-miR-223 holding statistical significance (P =0.0088; Table 3.4B).

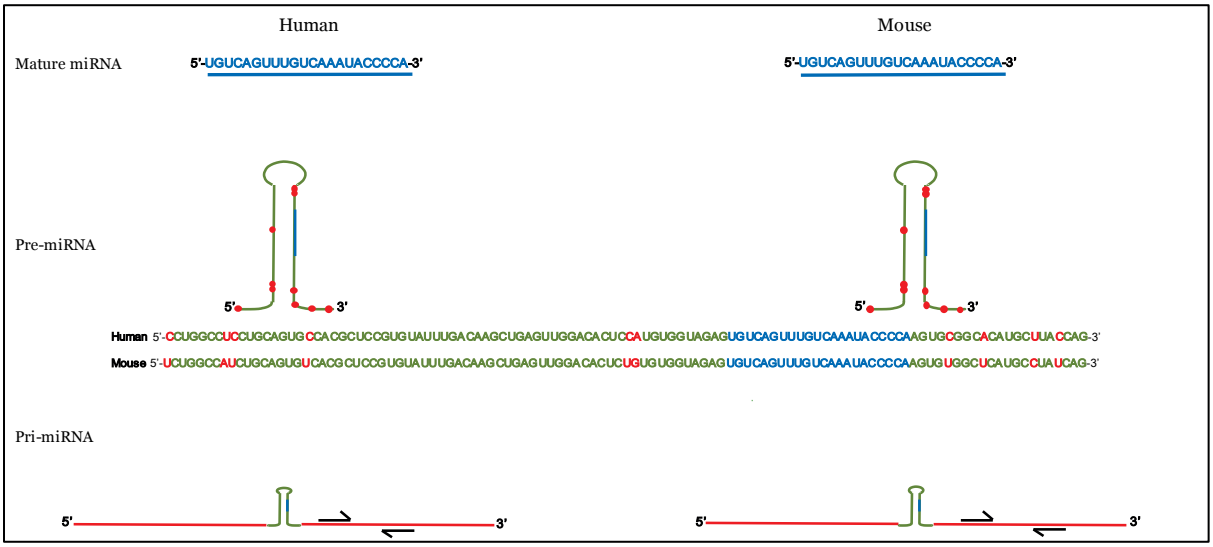

Figure 3.2: Schematic representation of mature miRNA, pre-miRNA, and pri-miRNA sequences between human and mouse species. The mature miRNA strand is identical in nucleotide sequence between species and the stem loop pre-miRNA sequence only has a few nucleotides difference highlighted in red. The initial pri-miRNA transcript below harbours long sequences differing between human and mouse species also highlighted in red. It is within these differing regions that primers and probes are designed to distinguish pri-miRNAs between species.

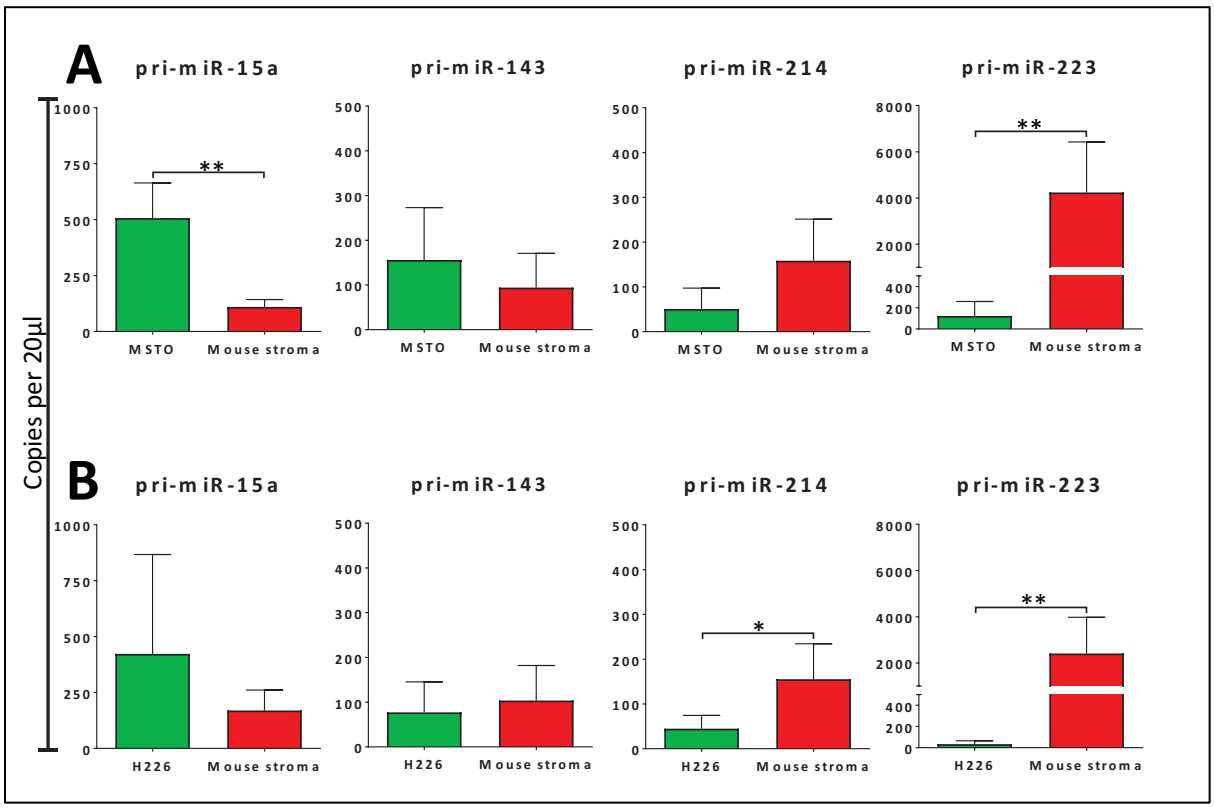

Figure 3.3: ddPCR quantitative expression of human and mouse pri-miRNA transcripts in MSTO and H226 xenograft tumours. Histograms quantifying human and mouse pri-miRNA variants, as copies per 20 µL, in MSTO (n =4) and H226 (n =5) xenograft tumours. (A) MSTO xenografts expressed higher mouse pri-miR-214 and pri-miR-223 copies than the human variants, with only pri-miR-223 being significant (P =0.0094). Pri-miR-143 expressed higher human than mouse variants with no significance. The reference pri-miR-15a expressed significantly higher human variant than the mouse variant (P =0.0026) indicating a substantially larger proportion of tumour than stromal cells in the MSTO xenografts. (B) H226 xenografts expressed higher mouse pri-miR-143, pri-miR-214 and pri-miR-223 copies than the human variants, with pri-miR-214 and pri-miR-223 being statistically significant (P =0.0194 and P =0.0094 respectively). The reference pri-miR-15a expressed higher human variant than the mouse variant representing a larger proportion of tumour than stromal cells in the H226 xenografts. * P value <0.05; ** P value <0.01

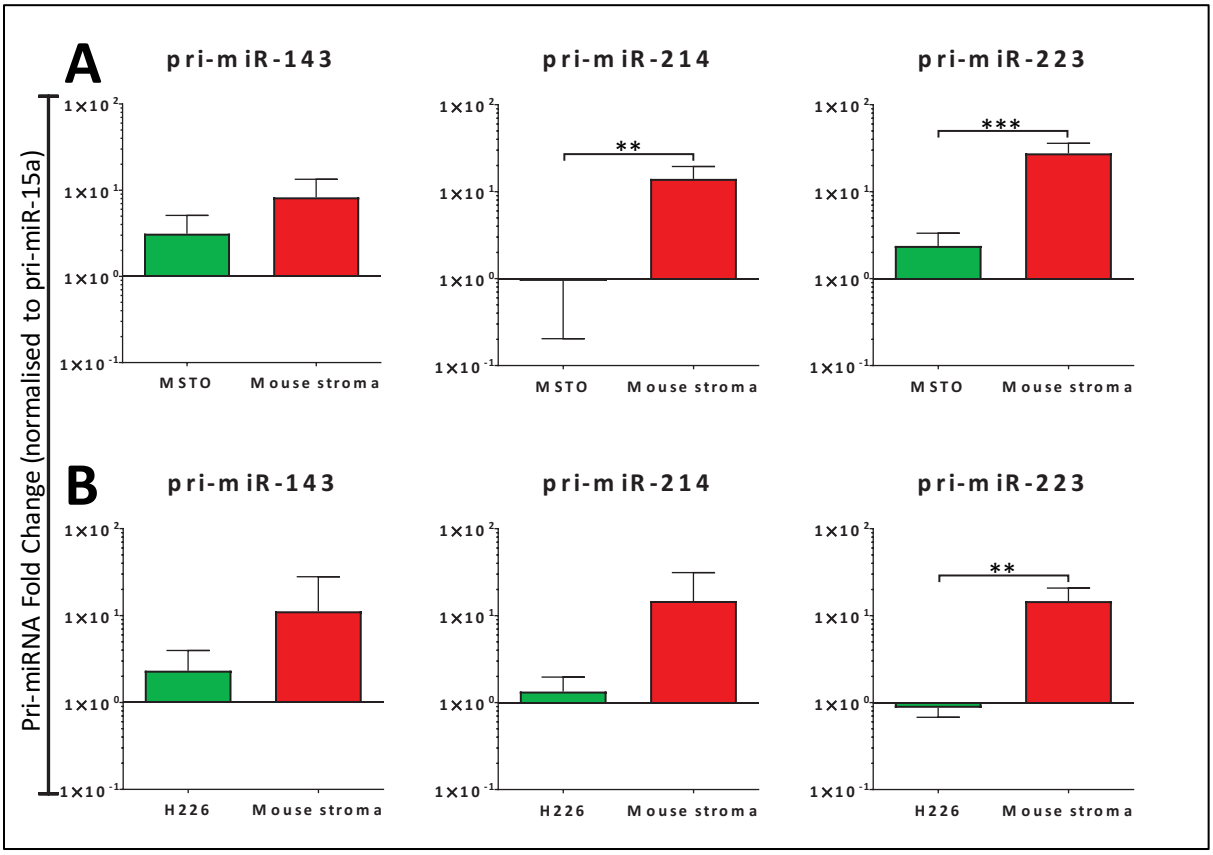

Figure 3.4: Fold change of normalised human and mouse pri-miRNA transcripts in MSTO and H226 xenograft tumours. Fold change histograms of pri-miR-143, pri-miR-214 and pri-miR-223 normalised to pri-miR-15a in MSTO (n =4) and H226 (n =5) xenograft tumours. (A) MSTO xenografts expressed a higher mouse pri-miR-143, pri-miR-214 and pri-miR-223-fold change than human variants, with pri-miR-214 and pri-miR-223 showing statistical significance (P =0.0031 and P =0.0010 respectively). (B) H226 xenografts also expressed a higher mouse pri-miR-143, pri-miR-214 and pri-miR-223-fold change than human variants, with only pri-miR-223 holding statistical significance (P =0.0088). ** P value <0.01; *** P value <0.001.

3.3 Identifying the stromal cell origin of miRNA expression in the tumour microenvironment

To identify the specific cells in the tumour microenvironment contributing to stromal microRNA expression, *in situ* hybridisation (ISH) was performed to localise miR-223-3p as it was most abundantly expressed by mouse stromal cells. ISH was performed on H226 and MSTO cell line derived xenograft tumour FFPE samples. Initially, ISH conditions recommended as a starting point by the manufacturer were followed. The xenograft samples were sectioned at a thickness of 4 μm and post fixing was conducted with 4 % PFA. The sections were also proteinase-K (10 μg/mL) treated for 15 min and hybridised with LNA probes U6 (20 nM), miR-223-3p (40 nM) and Scramble miR (20 nM). All xenograft samples were counterstained with Eosin (Figure 3.5). The conditions described above were progressively optimised after each ISH attempt.

The results obtained from the first ISH attempt were not as expected. The positive control U6 probe only produced light brown nuclear staining of some cells in a patchy pattern for both H226 (Figure 3.5A) and MSTO (Figure 3.5B) xenografts. There was no ISH staining of the miR-223-3p probe in H226 (Figure 3.5C) and MSTO (Figure 3.5D). As expected there was no staining of negative control Scramble miR probe in H226 (Figure 3.5E) and MSTO (Figure 3.5F) samples. There was also some false positive brown staining around the edges of H226 xenograft tumours (Figure 3.5A, C and E), likely due to over exposure to DAB treatment (Figure 3.5), which can be disregarded.

Although there are many steps to be optimised, post fixing with 4 % PFA was initially suspected as excess fixing of samples inhibits proteinase-K treatment leading to the inconsistent patchy DAB staining. Hence, the next ISH experiment tested the effects of post fixing with 4 % PFA in an MSTO xenograft. The U6 and Scramble miR probes were both run through ISH without PFA (Figure 3.6A and C respectively) and with PFA (Figure 3.6B and D respectively). Without PFA the positive control U6 probe presented light brown staining with improved consistency (Figure 3.6A) when compared to the result with PFA which had no staining (Figure 3.6B). The Scramble miR probe had no staining with or without PFA (Figure 3.6D and C respectively). The results of this experiment clearly identified that post fixing with 4 % PFA was interfering with ISH staining results and was therefore was completely excluded from the experiment (Figure 3.6).

The next ISH experiment focused on optimising the duration of proteinase-K treatment to enhance the faint brown staining previously achieved. Proteinase-K treatment concentration was kept constant at 10 μg/mL while a range of treatment durations (5, 15, 30 and 45 min) were tested. Results for the positive control U6 probe indicated that as proteinase-K treatment duration increased so did the intensity of DAB staining. At 5 min there was faint staining (Figure 3.7A) and at 15, 30 and 45 min there was strong staining with little increases (Figure 3.7C, E and G respectively). The negative control

Scramble miR probe presented no indication of DAB staining throughout the 5, 15, 30 and 45 min proteinase-K treatments (Figure 3.7B, D, F and H respectively). As there was not a significant difference in DAB staining intensity between 15 to 45 min the optimal proteinase-K treatment was set at 30 min at a concentration of 10 μg/mL (Figure 3.7).

Despite improvements, DAB staining was still considered to be weak and needed further optimisation. In order to increase the intensity of brown DAB staining 1 % $CuSO_4$ was incorporated to the protocol. Also, to enhance the contrast of the DAB staining both Eosin and Hematoxylin counterstains were compared. In regards to the U6 probe, the inclusion of 1 % $CuSO_4$ did not seem to have much of an effect on the intensity of brown DAB staining between eosin counterstained (Figure 3.8A and E) and hematoxylin counterstained (Figure 3.8C and G) sections. The negative control Scramble miR probe produced no DAB staining (Figure 3.8B, D, F and H). However, the $CuSO_4$ did improve Eosin counterstaining intensity (Figure 3.8E and F) compared to without $CuSO_4$ (Figure 3.8A and B). Overall, Hematoxylin counterstaining with 1 % $CuSO_4$ DAB enhancing treatment was considered as an improved method to visualise ISH (Figure 3.8G).

Once hematoxylin stain was selected as the counterstain of choice another series of optimisation tested the tissue section thickness and LNA probe concentration (Figure 3.9). The tissue thickness was considered to ensure there was enough depth of sectioned samples for sufficient staining to occur. Samples were sectioned at 4 and 7 μm thickness and hybridised with 20 and 40 nM of the U6 probe. Among the 20 nM of U6 probe only the 4 μm section (Figure 3.9A) produced a light DAB stain compared to the 7μm section (Figure 3.9B). When hybridised with 40 nM of the U6 probe both the 4 μm section (Figure5.5C) and 7 μm section (Figure5.5D) produced a stronger stain compared to the 4 μm section with 20nM probe concentration (Figure 3.9A). These results indicated that the thicker tissue does not improve DAB staining probably due to limited proteinase-K treatment penetration. However, increasing probe concentration did improve DAB staining intensity.

The proteinase-K treatment concentration was revised again with differing U6 probe concentrations to improve DAB staining intensity (Figure 3.10). With 20 nM of the U6 probe hybridisation the section with 10 μg/mL of proteinase-K treatment (Figure 3.10A) had less intense DAB staining compared to the 20 μg/mL proteinase-K treated sample (Figure 3.10B). The 40 nM U6 probe hybridised sample also had stronger staining for the 20 μg/mL proteinase-K treated sample (Figure 3.10D) than the 10 μg/mL proteinase-K treated sample (Figure 3.10C). Also, the higher U6 probe concentrations within the same proteinase-K concentrations again produced more intense DAB staining. Therefore, both higher proteinase-K and U6 probe concentrations significantly improved DAB staining intensity.

After determining that an increase in U6 probe concentration and proteinase-K treatment concentration improved DAB staining intensity. The U6 probe concentration was raised to 40 nM and proteinase-K treatment concentration was further exponentially increased to find optimal the concentration (Figure 3.11). The proteinase-K treatment range tested was 20, 40, 80 and 160 μg/mL and results depicted were of two regions of the xenograft sample. For the lowest proteinase-K concentration of 20 μg/mL the first and second region (Figure 3.11A and B respectively) show light DAB staining of tumour cells and no staining of mouse stromal cells. The next concentration of 40 μg/mL there was stronger staining in both regions (Figure 3.11C and D) of tumour cells and slight staining of some mouse stromal cells. As the proteinase-K concentration reached 80 μg/mL the DAB staining was even more intense for tumour cells and slightly increasing in mouse stromal cells of both regions (Figure 3.11E and F). The highest concentration of 160 μg/mL produced the most intense DAB staining amongst tumour cells and resulted in the most mouse stromal cell staining in both regions (Figure 3.11G and H). These results indicate that as the proteinase-K treatment concentration increased the DAB staining intensity increased among tumour cells and mouse stromal cells. However, a negative side effect of such a high proteinase-K treatment concentration was a loss of xenograft sample structure. Therefore, to visualise ISH DAB staining of tumour and mouse stromal cells, the proteinase-K treatment concentration needs to be no higher than 160 μg/mL to balance between mouse stromal cell inclusion and loss of xenograft sample structure.

The final ISH experiment integrated all of the optimised steps and consisted of xenograft tumour, syngraft tumour and murine spleen sectioned samples (Figure 3.12). The syngraft tumour was added to ensure a similar DAB staining pattern of mouse tumour and stromal cells was achieved compared to the xenograft tumour. The murine spleen sample was also added as a high concentration of myeloid cells suspected of expressing miR-223-3p are located in the spleen tissue. To summarise the optimised ISH protocol the samples were sectioned at 5 μm thickness, proteinase-K treated at 160 μg/mL for 30 min, hybridised with U6 (40 nM), Scramble miR (40 nM) and miR-223-3p (160 nM) probes. Also, the DAB staining was enhanced with 1% $CuSO_4$ and counterstained with hematoxylin. The positive control U6 probe hybridisation results produced an intense DAB stain consistently among xenograft tumour, syngraft tumour and murine spleen (Figure 3.12A, D and G respectively). Unfortunately, the miR-223-3p probe hybridisation did not result in any distinct DAB staining in any of the xenograft tumour, syngraft tumour and murine spleen samples (Figure 3.12B, E and H respectively). As expected, the negative control Scramble miR probe hybridisation did not depict any DAB staining in the xenograft tumour, syngraft tumour and murine spleen samples (Figure 3.12C, F and I respectively).

In conclusion, the *in situ* hybridisation experiments failed to localise miR-223-3p and hence was unsuccessful in identifying which specific stromal cells in the tumour microenvironment are expressing this miRNA. After many optimisation steps, the resulting positive control U6 probe hybridisation was producing intense DAB staining results confirming that the protocol was working well. However, hybridisation with the miR-223-3p probe still did not show any DAB staining. The negative control Scramble miR probe hybridisation showed no stain as expected.

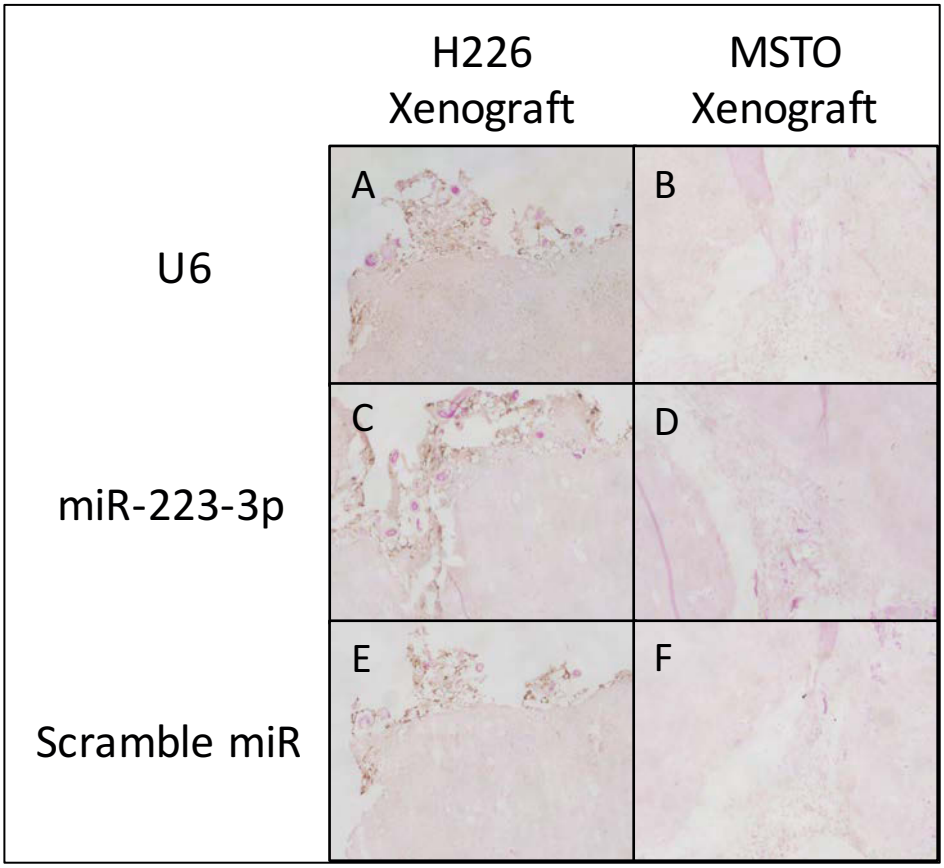

Figure 3.5: Initial *in situ* hybridisation of H226 and MSTO xenograft tumours using miRCURY LNA miRNA probes. ISH staining results of 4 μm thick xenograft tumour sections, PFA post fixed, proteinase-K treated (10 μg/mL) for 15 min, hybridised with U6 (20 nM), miR-223-3p (40 nM) and Scramble miR (20 nM) probes, counterstained with eosin and captured with a 10X objective. H226 xenograft #3 ISH with (A) U6, (C) miR-223-3p and (E) Scramble miR probes. MSTO xenograft #9 ISH with (B) U6, (D) miR-223-3p and (F) Scramble miR probes. Only ISH with positive control U6 probe produced light brown and patchy DAB staining.

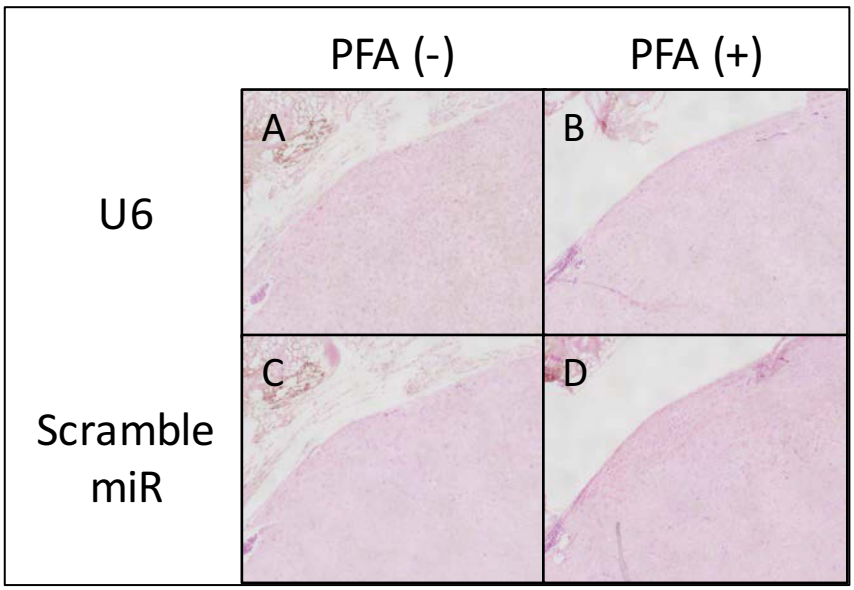

Figure 3.6: Testing the effects of paraformaldehyde post fixing on ISH of xenograft tumours. ISH staining results of 4 μm thick xenograft tumour sections, proteinase-K treated (10 μg/mL) for 15 min, hybridised with U6 (20 nM) and Scramble miR (20 nM) probes, counterstained with eosin and captured with a 10X objective. For the MSTO xenograft #1 samples (A and C) results were not post fixed and (B and D) results were post fixed with 4 % paraformaldehyde. ISH with positive control U6 probe showed improved DAB staining.

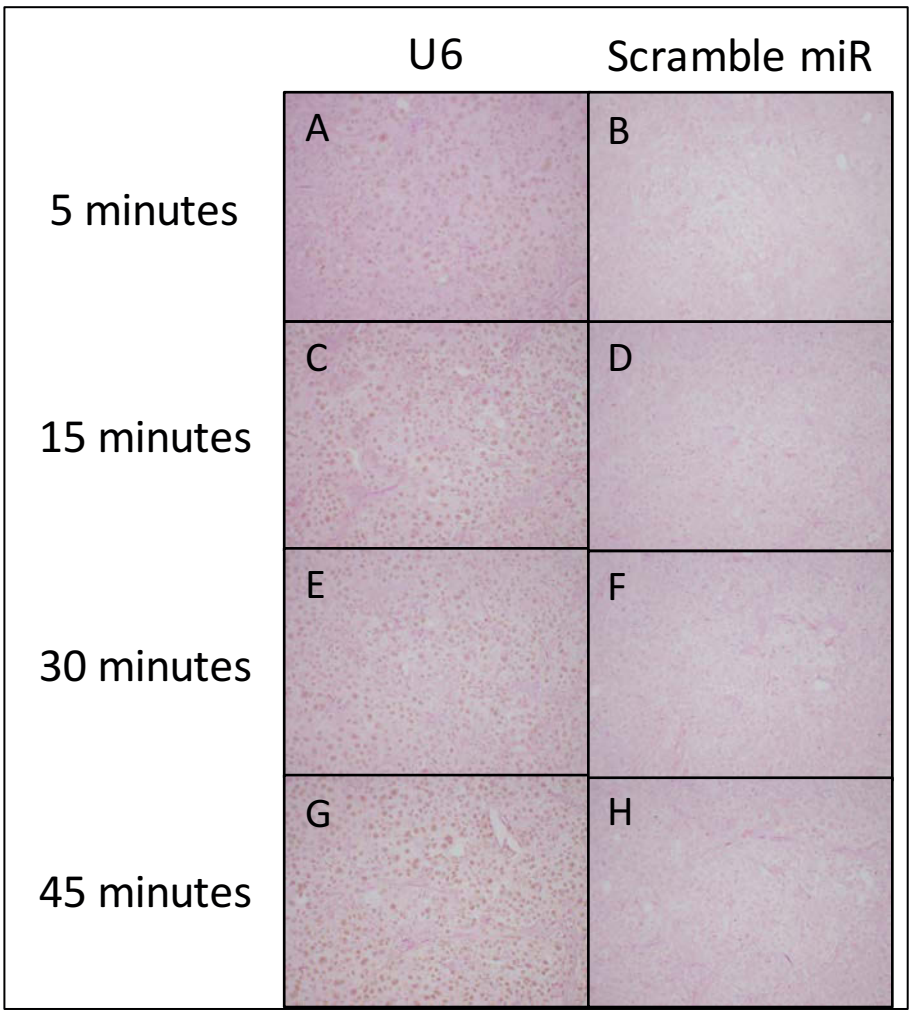

Figure 3.7: Optimizing incubation time of proteinase-K treatment for ISH of xenograft tumours. ISH staining results of 4 μm thick xenograft tumour sections, proteinase-K treated (10 μg/mL), hybridised with U6 (20 nM), and Scramble miR (20 nM) probes, counterstained with eosin and captured with a 20X objective. H226 xenograft #8 sample proteinase-K treated for (A and B) 5 minutes, (C and D) 15 min, (E and F) 30 min and (G and H) 45 min duration. ISH with positive control U6 probe showed increasing DAB staining intensity as proteinase-K treatment duration increased.

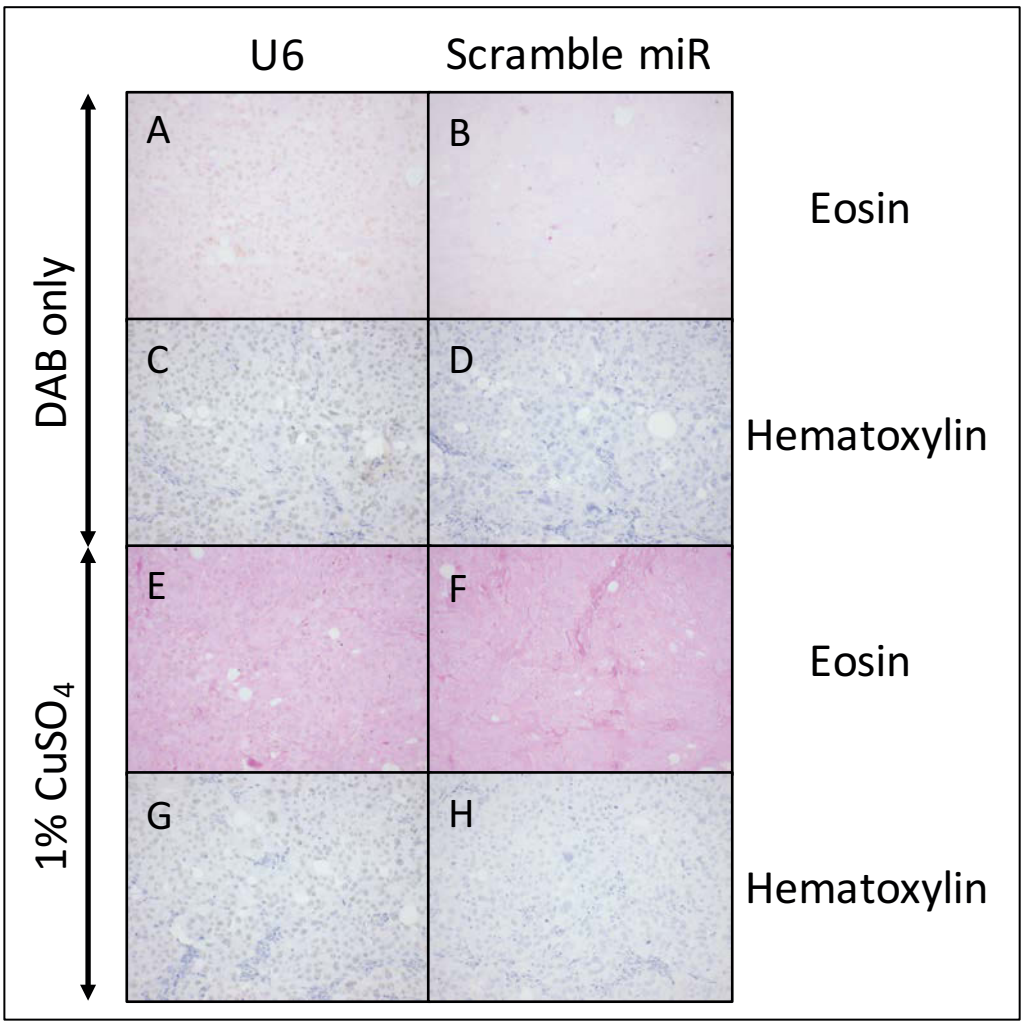

Figure 3.8: Testing DAB stain enhancement with $CuSO_4$ treatment and comparing improved DAB counterstaining with eosin and hematoxylin for ISH of xenograft tumours. ISH staining results of 4 μm thick xenograft tumour sections, proteinase-K treated (10 μg/mL) for 30 min, hybridised with U6 (20 nM), and Scramble miR (20nM) probes and captured with a 20X objective. H226 xenograft #10 samples were DAB stained and counterstained with (A and B) eosin and (C and D) hematoxylin. Samples treated with 1 % $CuSO_4$ for DAB stain enhancement were counterstained with (E and F) eosin and (G and H) hematoxylin. Hematoxylin counterstaining provided a better contrasting stain to DAB and the DAB enhancement did not noticeably improve DAB staining.

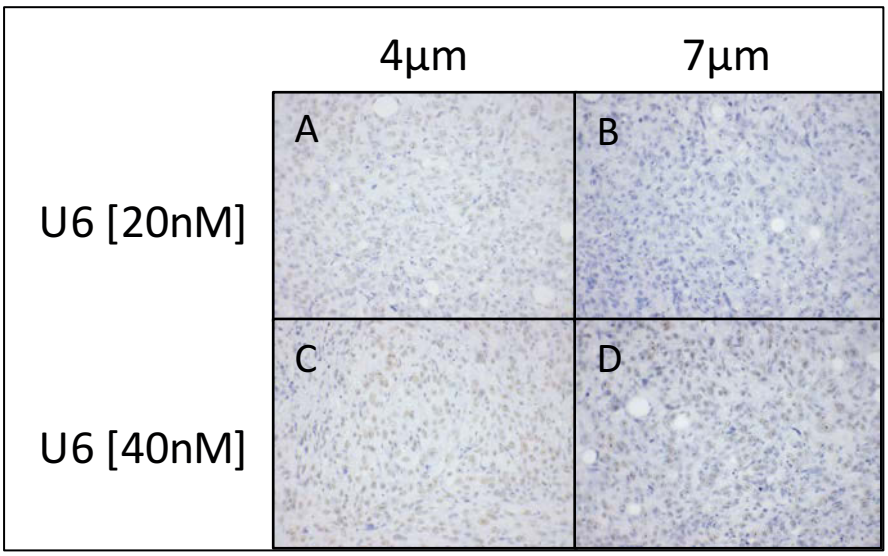

Figure 3.9: Optimising tissue thickness and LNA probe concentration for ISH of xenograft tumours. ISH staining results of xenograft tumour sections, proteinase-K treated (10 µg/mL) for 30 min, hybridised with U6 probe, hematoxylin counterstained and captured with a 20X objective. MSTO xenograft #8 samples were hybridised with U6 probe at a concentration of 20 nM and at a thickness of (A) 4 µm and (B) 7 µm. Samples were also hybridised with U6 probe at a concentration of 40 nM and at a thickness of (A) 4 µm and (B) 7 µm. The results indicate that the thicker sections do not stain well but increasing the U6 probe concentration significantly increases the DAB staining.

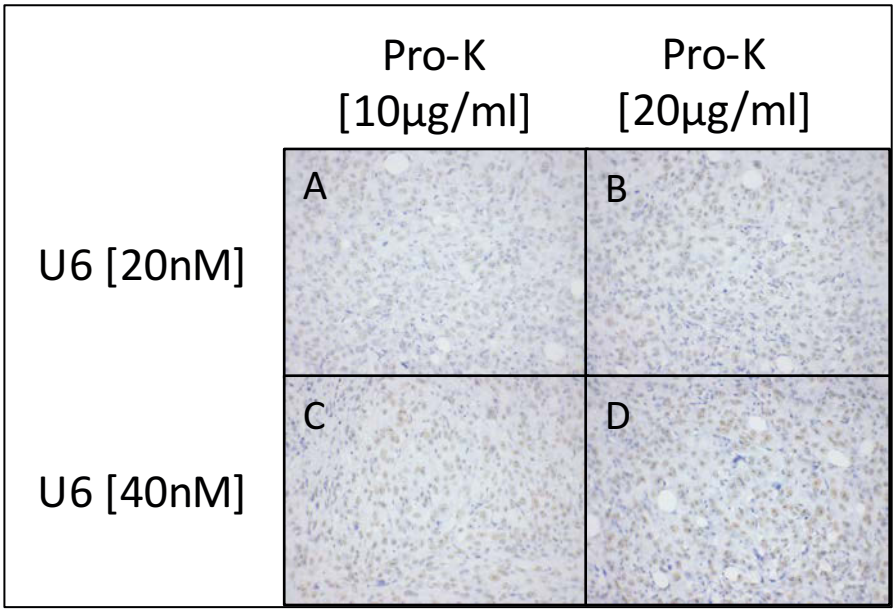

Figure 3.10: Optimising proteinase-K treatment concentration and LNA probe concentration for ISH of xenograft tumours. ISH staining results of 4 µm thick xenograft tumour sections, proteinase-K treated for 30 min, hybridised with U6 probe, hematoxylin counterstained and captured with a 20X objective. MSTO xenograft #8 samples were hybridised with U6 probe at a concentration of 20 nM and proteinase-K treated at (A) 10 µg/mL and (B) 20 µg/mL. Samples were also hybridised with U6 probe at a concentration of 40 nM and proteinase-K treated at (C) 10 µg/mL and (D) 20 µg/mL. Increasing the concentrations of both the proteinase-K treatment and the U6 probe independently improved DAB staining.

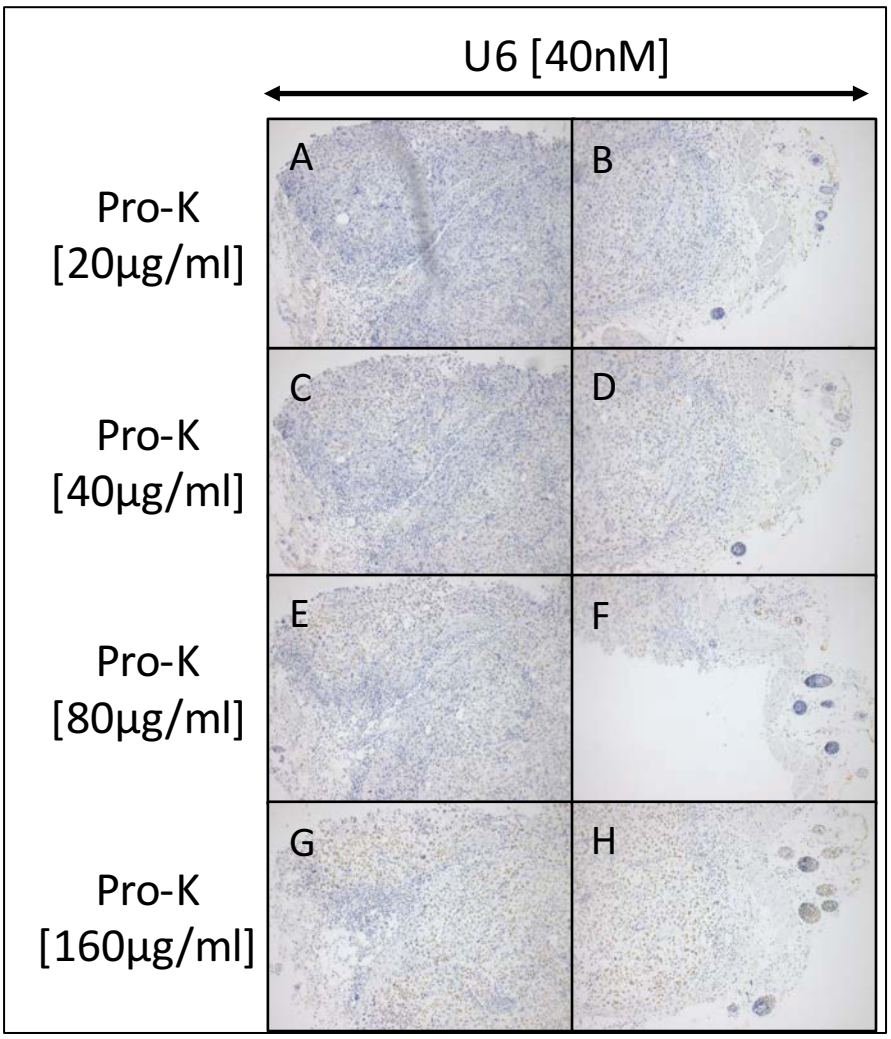

Figure 3.11: Further optimising proteinase-K treatment concentration for ISH of xenograft tumours. ISH staining results of 5 µm thick xenograft tumour sections, proteinase-K treated for 30 min, hybridised with U6 probe (40nM), hematoxylin counterstained and captured at two regions with a 10X objective. H226 xenograft #10 samples were proteinase-K treated with increasing concentrations of (A and B) 20 µg/mL, (C and D) 40 µg/mL, (E and F) 80 µg/mL and (G and H) 160 µg/mL. The intensity of DAB staining increased significantly as proteinase-K treatment concentration increased.

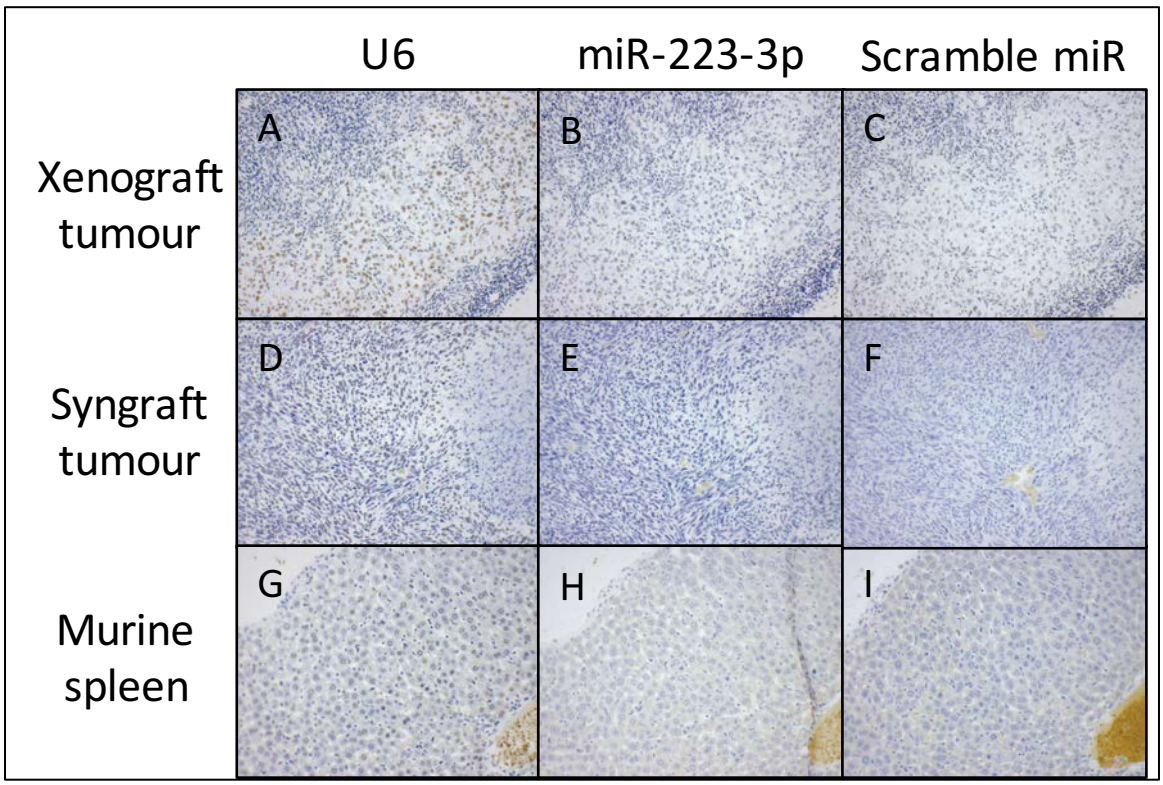

Figure 3.12: Final ISH experiment of xenograft tumour, syngraft tumour and murine spleen with the optimised protocol conditions. ISH staining results of 5 μm thick xenograft tumour, syngraft tumour and murine spleen sections, proteinase-K treated (160 μg/mL) for 30 min, hybridised with U6 (40 nM), miR-223-3p (160 nM) and Scramble miR (40 nM) probes, hematoxylin counterstained and captured with a 20X objective. ISH with positive control U6 probe produced intense DAB staining consistently among (A) xenograft tumour, (D) syngraft tumour and (G) murine spleen. ISH with the miR-223-3p probe depicted no DAB staining in (B) xenograft tumour, (E) syngraft tumour and (H) murine spleen. ISH with negative control Scramble miR probe showed no DAB staining in (C) xenograft tumour, (F) syngraft tumour and (I) murine spleen samples. Overall, the ISH protocol has been optimised well for the positive control U6 probe, however as there is no miR-223-3p probe staining, the experiment is inconclusive.

3.4 – Exploring the functional consequences of the dysregulated expression of these miRNAs in MPM cell lines.

As multiple microRNAs were overexpressed in tumours, the functional consequences miR-143-3p, miR-214-3p and miR-223-3p overexpression were investigated. A SYBR green based proliferation assay and crystal violet stained colony formation assay was performed to determine the effects on growth inhibition and colony formation respectively. Mesothelioma cell lines MSTO, H28, VMC23 and the immortalised mesothelial cell line MeT-5A were transfected with mimics to overexpress miR-143-3p, miR-214-3, miR-223-3p, along with mimic positive control miR-16-5p and also siRNAs C81 and RRM1-3 as negative and positive controls respectively.

3.4.1 SYBR green based proliferation assay

The SYBR green assay explored any growth inhibitory effects by measuring the fluorescence intensity of mesothelioma and immortalised mesothelial cell lines transfected with mimics and siRNA at 48, 72 and 96 h after transfection. The siRNA negative control C81 did not inhibit growth while the positive siRNA RRM1-3 inhibited growth in all of the cell lines as expected (Figure 3.13A, B, C and D respectively). Also the positive control mimic miR-16-5p inhibited growth among the mesothelioma cell lines MSTO, H28 and VMC23 (Figure 3.13A, B and C) and did not inhibit growth in the immortalised mesothelial cell line MeT-5A (Figure 3.13D) as previously shown [80]. The transfected candidate mimics were all tested for growth inhibitory significance against negative control siRNA C81. The miR-143-3p mimic did not show any growth inhibition and was not significantly different in any of the cell lines transfected except for a slight promotion of growth in H28 (Figure 3.13B) (adjusted P =0.0192). Mimic miR-223-3p also showed no growth inhibition in any of the cell lines transfected except for a significant promotion of growth in H28 (Figure 3.13B) (adjusted P =0.0037). More interestingly, transfection of mimic miR-214-3p significantly inhibited growth in all mesothelioma cell lines MSTO, H28 and VMC23 (Figure 3.13A, B and C respectively) (adjusted P =0.0001, 0.0055 and 0.0050 respectively). However, miR-214-3p also significantly inhibited growth in the immortalised mesothelial cell line MeT-5A (Figure 3.13D) (adjusted P =0.0193).

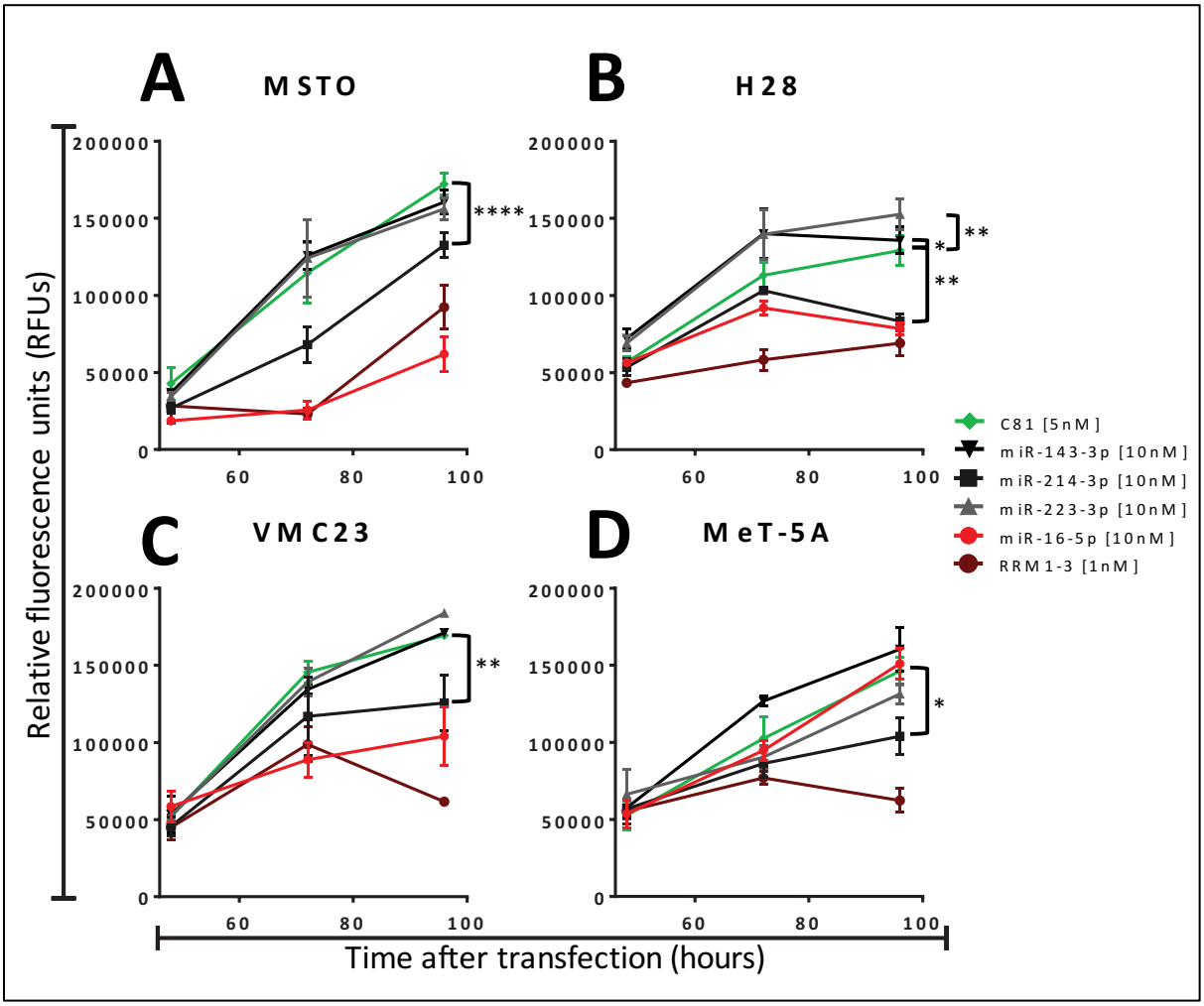

Figure 3.13: SYBR green based cell proliferation assays of mesothelioma and mesothelial cells transfected with miRNA mimics. Growth inhibitory effects of over expressing candidate miRNA mimics miR-143-3p, miR-214-3p and miR-223-3p in mesothelioma cell lines (A) MSTO, (B) H28, (C) VMC23 and immortalised mesothelial cell line (D) MeT-5A. One of three biological repeats was chosen for representation (n =3). The miR-143-3p mimic showed no growth inhibition in any of the cell lines except for a slight promotion of growth in (B) H28 (adjusted P =0.0192). Also, miR-223-3p had no growth inhibition among any of the cell lines except for a significant growth promotion in (B) H28 (adjusted P =0.0037). The miR-214-3p mimic showed significant growth inhibition in all the cell lines (A) MSTO, (B) H28, (C) VMC23 and (D) MeT-5A (adjusted P =0.0001, 0.0055, 0.0050 and 0.0193 respectively). * P value <0.05; ** P value <0.01, **** P value <0.0001

3.4.2 Colony formation assays

Colony formation assays explored the ability of mesothelioma cell lines MSTO, H28, VMC23 and immortalised mesothelial cell line MeT-5A to form colonies after transfection with miR-143-3p, miR-

214-3p and miR-223-3p mimics, along with positive control miR-16-5p at 10, 3.3 and 1.1 nM concentrations. The siRNA negative control C81 and positive control RRM1-3 were also included at 5 and 1 nM respectively. Untreated (UT) cells were also included to ensure Lipofectamine RNAiMAX and C81 did not affect colony formation. The siRNA negative (c81) and positive (RRM1-3) controls worked as expected. The positive mimic miR-16-5p inhibited colony formation in a dose dependant manner with 10 nM showing the most inhibition and 1.1 nM showing the least inhibition in 2 out of 3 mesothelioma cell lines MSTO and H28 (Figure 3.14A and B respectively) while VMC23 and MeT-5A did not exhibit inhibited colony formation (Figure 3.14C and D). Mimic miR-143-3p had no distinct effects on colony formation in MSTO, VMC23 and MeT-5A (Figure 3.14A, C and D respectively) and only showed a dose dependant colony formation inhibition in H28 (Figure 3.14B). The miR-214-3p mimic also showed no considerable effects on colony formation in MSTO and VMC23 (Figure 3.14A and C respectively) but showed pronounced inhibition in H28 (Figure 3.14B) and slight inhibition in MeT-5A (Figure 3.14D) dependant on miR-214-3p concentration. Lastly, mimic miR-223-3p did not inhibit colony formation in any cell line (Figure 3.14A, B, C and D).

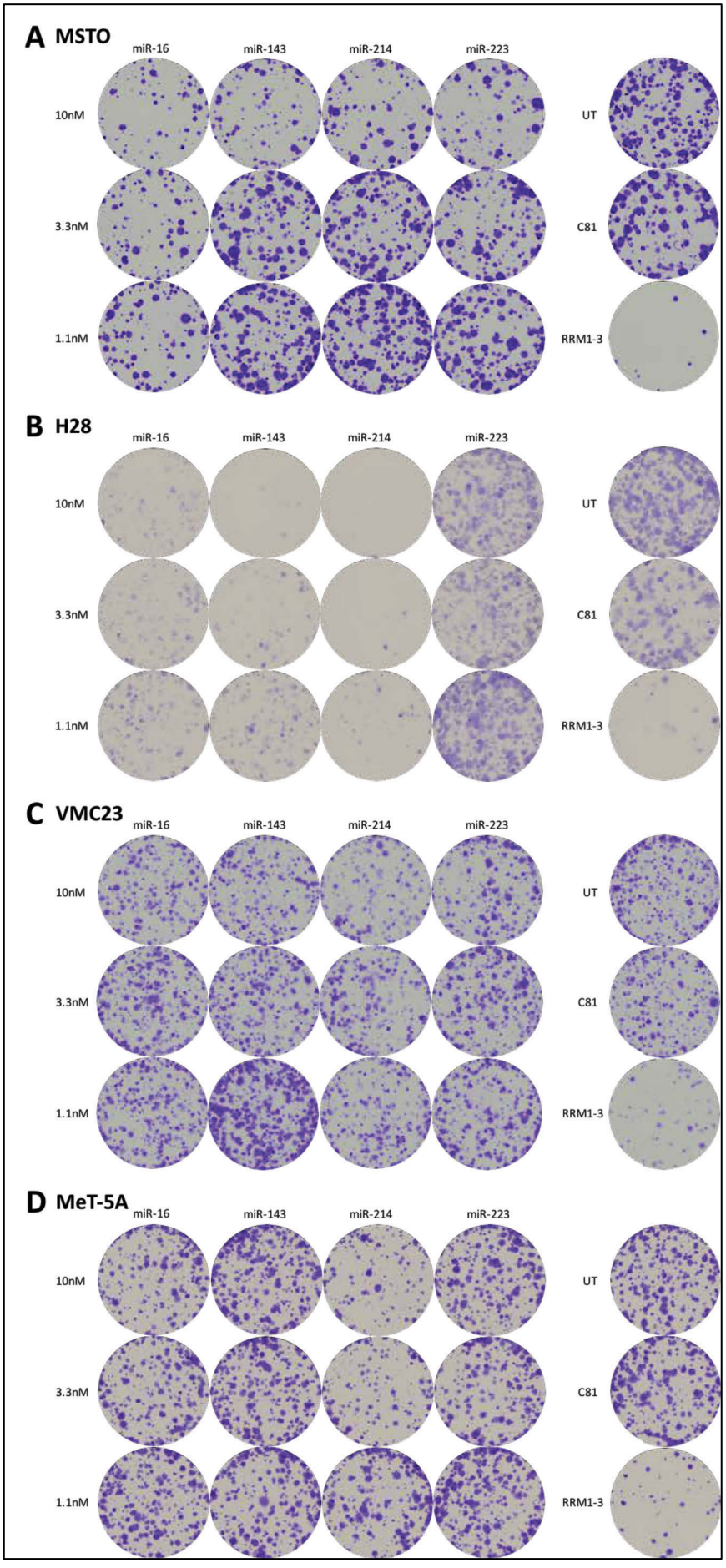
A MSTO
miR-16
miR-143
miR-214
miR-223
10nM
3.3nM
1.1nM
UT
C81
RRM1-3
B H28
miR-16
miR-143
miR-214
miR-223
10nM
3.3nM
1.1nM
UT
C81
RRM1-3
C VMC23
miR-16
miR-143
miR-214
miR-223
10nM
3.3nM
1.1nM
UT
C81
RRM1-3
D MeT-5A
miR-16
miR-143
miR-214
miR-223
10nM
3.3nM
1.1nM
UT
C81
RRM1-3

Figure 3.14: Crystal violet stained colony formation assays of mesothelioma and mesothelial cells transfected with miRNA mimics. Effects of overexpressing miR-143-3p, miR-214-3p and miR-223-3p on colony formation of mesothelioma cell lines (A) MSTO, (B) H28, (C) VMC23 and the immortalised mesothelial cell line (D) MeT-5A. One of three biological repeats was chosen for representation (n =3). Mimic miR-143-3p did not inhibit colony formation in all of the cell lines except (B) H28, which depicted a dose dependent response. The miR-214-3p mimic also did not inhibit colony formation in the majority of the cells lines except for a dose dependent response in (B) H28 showing dramatic inhibitory effects and (D) MeT-5A showing subtle inhibitory effects. Also, miR-223-3p mimic had no effects on colony formation in any of the cell lines.

Chapter 4 – Discussion

Despite extensive ongoing studies, MPM remains an aggressive cancer with very poor prognosis [1, 2] and few effective treatments [21, 56, 96]. MicroRNAs are the subject of a growing field of research as they are powerful gene regulators and frequently dysregulated in cancers [59] including MPM. Studies investigating dysregulated miRNAs in MPM have shown the potential of these miRNAs to serve as biomarkers and therapeutic targets. The majority of miRNAs dysregulated in MPM are downregulated and restoring expression of some of these miRNAs in functional studies has identified them as tumour suppressors and potential therapeutic targets [74].

4.1 Tumour miRNA expression profiles also contain stromal cell miRNA expression

A common method to screen for and identify dysregulated miRNAs in cancer involves the generation of miRNA profiles comparing tumour tissue and/or cells to their normal counterparts [70, 71]. MPM studies have also incorporated this method to identify tumour suppressor miRNAs such as miR-31, miR-16 and miR-126 [74]. The miRNA profiles generated from cultured tumour and normal cell lines are regarded as pure cell type samples. However, miRNA profiles generated from tumour and normal tissue samples also include cells from the microenvironment referred to as stromal cells. In tumours, stromal cells consist of tumour supporting cells such as fibroblasts, endothelial cells and immune cells [97]. These cells play an important role in the tumour development by supporting tumour cells with angiogenesis, growth, and invasion [98].

As stromal cells are present in tumour tissue, they also contribute to miRNA expression in tumours, hence contributing to the dysregulated miRNA expression. This was clearly demonstrated by a study of pancreatic cancer in which miRNA expression was profiled separately in matching tumour, stromal and normal tissues, leading to identification of a number of differentially expressed miRNAs between the sample types [99]. This revealed that miRNAs are also differentially expressed in the stromal cells usually present in solid tumour samples. Similarly, another study observed miRNAs differentially expressed among normal fibroblasts and cancer-associated fibroblasts with differing functional consequences when co-cultured with ovarian cancer cells [100]. Such dysregulated expression of stromal cell miRNAs can significantly influence the selection of dysregulated miRNAs in tumour miRNA profiling studies.

4.2 MPM xenograft tumour miRNA profiles contain significant stromal cell expression of miR-143-3p, miR-214-3p and miR-223-3p

To better understand the contribution of tumour cells and stroma to changes in miRNA expression in MPM, this study investigated the relative contribution of miRNAs from tumour and stromal cells in

MPM xenograft tumours. The preliminary miRNA expression profiles of MSTO and H226 cell line derived xenograft tumours were directly compared to corresponding cultured tumour cells and miRNAs with the most relevant increase in expression selected for validation.

The levels of miR-143-3p, miR-214-3p and miR-223-3p were significantly increased in both MSTO and H226 xenograft samples compared to corresponding cultured cells. This suggested strong expression of these miRNAs from stromal cells. To further emphasise stromal expression, these miRNAs have all been reported to be downregulated in MPM. A study investigating the diagnostic potential of miRNAs in MPM tissues reported several miRNAs including miR-143-3p to be downregulated [89]. Also another study exploring the dysregulation of miRNAs in MPM cell lines found miR-214 to be downregulated [73]. The loss of miR-223 in MPM tissue and cell lines has also been shown to elevate stathmin levels in MPM [85]. In addition, all these miRNAs have been indicated to be significantly downregulated in MPM through a miRNA array study comparing MPM cell lines to non-neoplastic pleural tissue [133].

Mesothelioma AB1 syngraft tumours were also included in the validation step to investigate if the candidate miRNAs were also expressed higher in the tumour model compared to corresponding cultured cells. This model was included with the hypothesis that candidate miRNAs would still hold notably higher expression levels amongst the syngraft tumours. Interestingly, only miR-223-3p expressed similarly high levels among the syngraft tumours. This data leads to doubt as to whether miR-143-3p and miR-214-3p are actually expressed substantially more among xenograft tumours due to stromal cell contribution. However, it should be kept in mind that the two mouse models and species differences may be the cause of such different levels of miRNA expression.

The immunodeficient mice used to generate xenograft tumours lack immune T and B lymphocytes hence their tumour infiltrate, whereas immunocompetent mice used to generate syngraft tumours would have an influx of these lymphocytes infiltrating the tumour region [134]. A study linking miRNA expression to specific blood cell types identifies miR-223-3p to be abundantly expressed by myeloid cells and lymphocytes while miR-143-3p and miR-214-3p are not detected by qPCR among flow sorted blood cell types [135]. Therefore, the presence of lymphocyte infiltrate in syngraft tumours may be diluting the expression of miR-143-3p and miR-214-3p by increasing the total miRNA contributed from stromal cells.

On the other hand, the consistently higher fold change expression of miR-223-3p among all xenograft and syngraft tumours strengthens our hypothesis that there is a significant amount of stromal cell contribution. To bring clarity to the contribution of tumour and stromal cells to the mature miRNA expression in MPM xenograft tumour samples, the species-specific pri-miRNA transcripts were analysed.

4.3 Species-specific pri-miRNA transcripts determine tumour and stromal cell source of miRNAs in MPM xenograft tumours

To determine the tumour and stromal cell contribution to miRNA expression in MPM xenograft tumours, the species-specific pri-miRNA transcripts were quantified using ddPCR. All candidates, pri-miR-143, pri-miR-214 and pir-miR-223 were mostly expressed by mouse stromal cells in MSTO and H226 xenograft samples with the exception of pri-miR-143 in MSTO xenografts. However, only pri-miR-223 expression was significantly higher in both MSTO and H226 xenograft samples compared with cultured cell lines. This is similar to a miRNA profiling study that reported miR-223-3p expression to be significantly higher in the stroma than tumour regions of pancreatic cancer [99].

Another point to consider when interpreting these results is the cellular composition of the xenograft tumour samples. An important colon cancer study demonstrated that miR-143-3p is exclusively expressed by surrounding mesenchymal cells, and together with the lack of mesenchymal cells and increase in malignant cells of epithelial origin in colon cancer samples, this has resulted in the misinterpretation that miR-143-3p expression is lost in colon cancer [111].

Thus, the cellular composition of the xenograft tumours also needed be considered when measuring the pri-miRNA transcripts as there will be a difference between tumour and stromal cell numbers. To account for this difference, pri-miR-15a was also quantified as it is ubiquitously expressed among cell types. After using pri-miR-15a to normalise the high tumour to stromal cell ratio of each xenograft sample, all candidate pri-miRNAs were shown to be predominantly expressed by mouse stromal cells. These results further emphasise that pri-miRNAs and subsequently mature miRNAs are primarily being expressed by stromal cells in these xenograft samples.

4.4 Identifying the cell-type specific expression of miRNAs in MPM xenograft tumours

As miRNAs are expressed at a cellular level, identifying the cell type specific expression of these miRNAs will give better understanding of how stromal cells can contribute to tumour miRNA profiling studies. Methods used to identify cell-type specific expression of miRNAs include *in situ* hybridization (ISH) to localise miRNA expression to specific cells and also fluorescence-activated cell sorting (FACS) to separate cell types before generating miRNA expression profiles.

Highlighting the importance of understanding cell-type specific miRNA expression is the expression of the miR-143/145 cluster. These two co-expressed miRNAs have been shown to be downregulated in a range of epithelial cell malignancies and linked to various tumour promoting targets, hence labelling them as tumour suppressors [112, 113]. However, revealing research has demonstrated that miR-143 and miR-145 are not expressed by intestinal epithelial cells. Instead, through ISH techniques, these

miRNAs are shown to be expressed exclusively by mesenchymal cells and RT-qPCR confirmed this with almost undetectable levels in FACS epithelial preparations [114]. In an independent evaluation small RNA RNA-seq was performed on flow-sorted $EPCAM^+$ epithelial cells, isolated red blood cells and cultured endothelial, fibroblast and smooth muscle cells (SMC). The results also demonstrated abundant mesenchymal expression of miR-143 in fibroblast and SMC [111].

In MPM, miR-145 has also been reported to be downregulated based on expression in MPM tissues without considering cell type specific expression. It has been deemed a tumour suppressor after overexpressing mimic miR-145 in MPM cell lines inhibited clonogenicity, cell migration and resistance to pemetrexed treatment [81]. As MPM is also an epithelial cell malignancy it would be interesting to identify if miR-145 is even expressed in mesothelial cells or is it also exclusively expressed by surrounding stromal mesenchymal cells in pleural tissue.

Cell type specific miRNA expression has only recently been gaining recognition in miRNA research thus there are limited publications available. However, online miRNA expression databases such as miRmine provide an in-silico platform to identify tissue and cell type specific expression levels of miRNAs of interest [136]. Although the range of tissue and, more importantly, cell type range is still quite limited the database provides a starting point for future studies. From this database miR-143-3p has been shown to be strongly expressed in an immortalized mesenchymal cell line iMSC, miR-214-3p most abundantly expressed in a bone marrow cell line SH-SY5Y and miR-223-3p highly expressed in monocyte cells THP1. These examples all identify specific stromal cell types that express the miRNA candidates of the study.

To identify cell-type specific expression of our candidate miRNAs ISH was performed on existing FFPE xenograft tumour samples as fresh samples for FACS were not available. ISH was performed on the miRNA most significantly expressed by mouse stromal cells. Unfortunately, after repeated attempts to optimise the protocol and extensive trouble shooting, the results were inconclusive. Only the positive control U6 probe stained nuclear cells well whereas there were no signs of staining with the miR-223-3p probe. Further efforts were not possible due to limited sample and time constraints.

Current studies that have successfully performed miRNA ISH in MPM have only visualised expression levels in mesothelial cells. One study reported that the activation of EphrinA1 lead to the induction of let-7a miRNA expression and subsequent repression of the proto-oncogene RAS. The expression of let-7a was determined by qPCR and ISH of cultured MPM cells [137]. Also an epithelial-mesenchymal transition study found miR-205 to be significantly downregulated from epithelioid to biphasic, to sarcomatoid subtypes in MPM samples using qPCR and ISH [138]. Although these miRNA ISH studies

do not explore cell type specific miRNA expression in MPM other studies have successfully identified cell type specific expression in various tissues.

The ISH candidate, miR-223-3p, has been successfully stained and localised in several studies. A chapter on the protocol of microRNA ISH has identified miR-223 to be expressed in granulocytes located in a blood vessel and in surrounding inflamed tissue [139]. More specifically, with the combination of ISH and fluorescent immunohistochemistry (IHC) staining, other studies have successfully identified the specific granulocyte cells expressing miR-223. This co-staining technique has identified myeloperoxidase and Gr-1 positive neutrophils [140, 141], CD68 positive macrophages, CD14 positive monocytes and CD4 positive T cells to be specifically expressing miR-223 [142].

In addition to the cell type specific expression of miR-223, a comprehensive study investigating the cell source of miRNAs in a range of cancers has identified several more miRNAs with cell type specific expression. A few examples include miR-126 expression in CD31 and CK20 positive endothelial cells, miR-155 expression in CK19 and CD45 positive leukocytes and miR-21 expression in smooth muscle actin expressing cancer-associated fibroblasts (CAF) [143]. The CAF specific expression of miR-21 was more prominent in colorectal [143], breast [143, 144] and oral squamous cell carcinoma [145]. Therefore, co-staining with ISH and fluorescent IHC provides an exceptional technique in identifying cell type specific miRNA expression for future MPM xenograft samples.

4.5 Potential functional roles of candidate miRNAs in MPM cell lines

Although there is strong evidence suggesting that miR-143-3p, miR-214-3p and miR-223-3p are predominantly being expressed by stromal cells in MPM xenograft tumours, these miRNAs have all been reported to be downregulated in MPM [133]. Downregulated miRNAs are usually further investigated for their gene targets and functional roles. In MPM, reintroducing the expression of downregulated miRNAs in past functional studies has successfully identified tumour suppressor miRNAs with therapeutic potential [74].

Thus, this study explored the functional consequences of the dysregulated expression of these miRNAs in MPM cell lines. Mimics of miR-143-3p, miR-214-3p and miR-223-3p were overexpressed in MPM cell lines MSTO, H28, VMC23 and immortalized mesothelial cell line MeT-5A. The functional consequences assessed were growth inhibition and colony formation.

4.6 Overexpression of miR-143-3p has no effect on cell proliferative functions in MPM cells

The expression of miR-143 has repeatedly been reported to be downregulated in MPM [89, 133]. However, to date no studies have published functional data on overexpressing miR-143-3p in MPM cells. This study aimed to investigate if there were any functional consequences of restoring miR-143-

3p in MPM cells. The functional roles investigated were effects on growth inhibition and colony formation. Overexpression of miR-143-3p in MPM and mesothelial cell lines did not show any growth inhibition effects excepts for a slight promotion in growth in H28. Also, there was no effect on colony formation except for a dose dependent inhibition in H28. Overall, there were no overt significant functional consequences of overexpressing the downregulated miR-143-3p in MPM.

In previous studies, miR-143-3p has been shown to be downregulated in a range of other epithelial cell malignancies and linked to various tumour promoting targets, hence labelling miR-143-3p as a tumour suppressor [112, 113]. However, growing awareness of cell-type specific expression of miRNAs has revealed that miR-143-3p is not expressed by epithelial cells but instead exclusively expressed by mesenchymal [114] and endothelial [115] cells. A study exploring the tumour suppressive role of miR-143-3p in a mouse model of lung adenocarcinoma initially found that the loss of miR-143-3p did not promote tumour development and forced expression did not significantly reduce tumour burden. After identifying miR-143-3p expression to be lacking in epithelial cells and predominant in endothelial cells, further investigation demonstrated the loss of miR-143-3p inhibited endothelial cell growth [115]. In summary, as miR-143-3p lacks expression in epithelial cells (including MPMs) and is abundantly expressed in mesenchymal and endothelial cells, future functional studies should focus on altering expression in these tumour-supporting stromal cells.

4.7 Overexpression of miR-214-3p inhibits cell growth in MPM and immortalised mesothelial cells

Two independent studies have found miR-214-3p to be downregulated in MPM [73, 133], with the second demonstrating that transfection of mesothelioma cells with mimic miR-214-3p led to the inhibition of cell growth, invasion and migration [133]. Work in this thesis also aimed to investigate the functional consequences on cell growth and colony formation by overexpressing miR-214-3p in MPM and mesothelial cells. The overexpression of miR-214-3p showed significant growth inhibitory effects in all the MPM cell lines MSTO, H28, VMC23 including mesothelial cells MeT-5A. Also, there were no effects on colony formation in MPM cells except for a dose dependent inhibition in H28 showing great inhibitory effects and MeT-5A showing subtle inhibitory effects. Overall, overexpressing miR-214-3p in MPM cell lines significantly inhibited cell growth similar to previous published findings. However, growth of immortalized mesothelial cells was also significantly inhibited, raising concerns as to whether miR-214-3p targets are MPM specific.

Several other studies of epithelial cell malignancies have reported miR-214-3p to be downregulated and these include hepatocellular, cervical, adrenocortical, bladder and colorectal carcinomas [146]. Overexpressing miR-214-3p in malignancies where this miRNA has been shown to be downregulated, such as in hepatocellular carcinoma cells, showed an inhibition of cell growth [147]. Dysregulated miR-

214-3p expression has also been reported in stromal fibroblast cells. An ovarian cancer study comparing miRNA expression levels between cancer-associated fibroblasts (CAFs) with normal fibroblasts found miR-214-3p to be significantly downregulated in CAFs. Overexpressing miR-214-3p in CAFs inhibited migration and cancer cell invasiveness to similar levels of normal fibroblasts. Also inhibiting miR-214-3p expression in normal fibroblasts increased migration and cancer cell invasiveness to similar levels of CAFs [100].

These studies have investigated the functional consequences of overexpressing miR-214-3p in both tumour and stromal cells reporting anti-tumour effects. Therefore, this miRNA may have an important role in tumorigenesis by targeting both tumour cells and supporting stromal cells in the tumour microenvironment. This could be further investigated by co-culturing tumour cells with matching stromal cells like CAFs and altering miR-214-3p expression for functional studies.

4.8 Cell specific functions of miR-223-3p overexpression

The expression of miR-223-3p has been shown to be downregulated in MPM cell lines and tissues [85, 133], and although overexpressing miR-223-3p in MPM cells did not inhibit cell growth or colony formation, it significantly inhibited cell motility at 24 h [83]. My work also investigated the functional consequences of overexpressing miR-223-3p by assessing growth inhibition and colony formation. Overexpressing miR-223 showed no growth inhibition in MPM cell lines MSTO and VMC23, including mesothelial cells MeT-5A, except for a significant growth promotion in H28. Also, miR-223-3p had no distinct effects on colony formation in any of the MPM and mesothelial cells.

Studies in other malignancies of epithelial origin have also reported downregulation of miR-223-3p and investigated the functional consequence of restoring expression [125]. One study found miR-223-3p to be downregulated in gastric cancer cells and overexpressing miR-223-3p did not alter cell proliferation and apoptosis but significantly induced cell motility [148]. Another example is the re-expression of miR-223-3p in hepatocellular carcinoma cells, which revealed a consistent inhibitory effect on cell viability [86].

Interestingly, miR-223-3p is known to be specifically expressed in the myeloid cell lineage [123, 124]. The first important role of miR-223-3p was discovered in the field of haematology as it was shown to modulate the differentiation of haematopoietic cell lineages. In the bone marrow, miR-223-3p is primarily expressed in myeloid cells and is induced during the lineage differentiation of myeloid progenitor cells [124]. Expression of miR-223 is also known to fine-tune the differentiation of myeloid progenitor cells as miR-223 expression is repressed during monocyte differentiation and highly expressed during granulocyte differentiation [125].

Given the role of miR-223 in differentiating myeloid progenitor cells, it is no surprise that it is found to be downregulated in leukaemia and lymphomas. The most common fusion protein, AML1/ETO, in acute myeloid leukaemia (AML), reduces miR-223 expression through chromatin remodelling. Ectopic re-expression of miR-223, targeting AML1/ETO, or demethylating treatments, have been shown to restore cell differentiation of myeloid cancer cells by enhancing miR-223 levels [127].

Overall, miR-223-3p expression is well known to be specific to the myeloid cell lineage and has been shown to play an important role in myeloid cell differentiation and in malignancies. Thus, miR-223-3p expression in tumour samples could be from the myeloid cell lineage and altering expression in these myeloid derived stromal cells may have a more functional role in tumorigenesis.

4.9 Future directions

This project has demonstrated the contribution of stromal cells to miRNA expression in tumour and normal tissue samples and has also shown the cell type specificity of miRNA expression [111]. Future studies aiming to generate miRNA expression profiles of tumour and normal tissue could first use FACS to separate the different cell populations [111] or use microdissection techniques to concentrate particular cell populations [99]. miRNA profiles produced in this way would be less likely to be influenced by stromal cell specific expression.

Another future direction would be to successfully identify the type of stromal cells specifically expressing miR-143-3p, miR-214-3p and miR-223-3p in MPM xenograft tumours by revisiting *in situ* hybridisation (ISH) in combination with fluorescent IHC to localise these miRNAs to specific cells [143]. This could also be achieved using FACS on fresh homogenised xenograft tumours to separate cell populations and compare expression profiles.

The identification of stromal cells specifically expressing miR-143-3p, miR-214-3p and miR-223-3p in MPM xenograft tumours will allow for future miRNA functional studies to be performed in these cells. These miRNA-altering functional studies may initially be performed on pure cultured stromal cells and may also be investigated in co-cultures with MPM cell lines. Altering the miRNA expression of tumour supporting stromal cells using mimics or miRNA inhibitors may provide another perspective on potential treatment options for MPM.

4.10 Conclusion

A convenient and popular method for identifying dysregulated miRNAs in most cancers, including MPM, is by generating and comparing miRNA expression profiles of tumour and normal tissue. However, these samples also contain stromal cells that can contribute to the totality of miRNA expression at varying levels. This will ultimately influence the miRNAs identified as dysregulated in

MPM and can have an impact on their potential function and tumour gene targets. Therefore, it remains important to understand the cell source of miRNAs and the cell type composition of tissue samples. Subsequent functional studies on dysregulated miRNAs that have cell-type specific expression should be carried out in the appropriate cell lines. This will lead to a better understanding of the contribution of miRNAs to the roles of tumour and stromal cells in MPM.

Chapter 5 – References:

1. Zucali, P.A., et al., *Advances in the biology of malignant pleural mesothelioma.* Cancer Treat Rev, 2011. **37**(7): p. 543-58.
2. Milano, M.T. and H. Zhang, *Malignant pleural mesothelioma: a population-based study of survival.* Journal of Thoracic Oncology, 2010. **5**(11): p. 1841-1848.
3. Yap, T.A., et al., *Novel insights into mesothelioma biology and implications for therapy.* Nature Reviews Cancer, 2017. **17**(8): p. 475.
4. Carbone, M., R.A. Kratzke, and J.R. Testa. *The pathogenesis of mesothelioma*. in *Seminars in oncology*. 2002. Elsevier.
5. Rudd, R., *Malignant mesothelioma.* British medical bulletin, 2010. **93**(1).
6. Construction, A.A. *Asbestos Abatement & Removal*. 2013 [cited 2017 12/10/2017]; Pleural Mesothleioma]. Available from: http://www.atlanticabate.com/wp-content/uploads/2013/12/Asbestos-2_l.jpg.
7. Pass, H.I., et al., *Malignant pleural mesothelioma.* Current problems in cancer, 2004. **28**(3): p. 93-174.
8. Tsao, A.S., et al., *Malignant pleural mesothelioma.* Journal of clinical oncology, 2009. **27**(12): p. 2081-2090.
9. LaDou, J., *The Asbestos Cancer Epidemic.* Environmental Health Perspectives, 2003. **112**(3): p. 285-290.
10. Hodgson, J.T. and A. Darnton, *The quantitative risks of mesothelioma and lung cancer in relation to asbestos exposure.* Annals of Occupational Hygiene, 2000. **44**(8): p. 565-601.
11. Røe, O.D. and G.M. Stella, *Malignant Pleural Mesothelioma: History, Controversy, and Future of a Man-Made Epidemic*, in *Asbestos and Mesothelioma*. 2017, Springer. p. 73-101.
12. Organization, W.H., *Elimination of asbestos-related diseases.* 2006.
13. Delgermaa, V., et al., *Global mesothelioma deaths reported to the World Health Organization between 1994 and 2008.* Bulletin of the World Health Organization, 2011. **89**(10): p. 716-724.
14. Marinaccio, A., et al., *Analysis of latency time and its determinants in asbestos related malignant mesothelioma cases of the Italian register.* Eur J Cancer, 2007. **43**(18): p. 2722-8.
15. Robinson, B.W., A.W. Musk, and R.A. Lake, *Malignant mesothelioma.* The Lancet, 2005. **366**(9483): p. 397-408.
16. Hyland, R.A., et al., *Incidence trends and gender differences in malignant mesothelioma in New South Wales, Australia.* Scand J Work Environ Health, 2007. **33**(4): p. 286-92.
17. Leigh, J., et al., *Malignant mesothelioma in Australia, 1945-2000.* Am J Ind Med, 2002. **41**(3): p. 188-201.
18. Robinson, B.M., *Malignant pleural mesothelioma: an epidemiological perspective.* Ann Cardiothorac Surg, 2012. **1**(4): p. 491-6.
19. Welfare, A.I.o.H.a., *Mesothelioma in Australia 2017*. 2018, Australian Government: Online. p. 8.

20. Olsen, N.J., et al., *Increasing incidence of malignant mesothelioma after exposure to asbestos during home maintenance and renovation.* Med J Aust, 2011. **195**(5): p. 271-4.

21. Kondola, S., D. Manners, and A.K. Nowak, *Malignant pleural mesothelioma: an update on diagnosis and treatment options.* Therapeutic advances in respiratory disease, 2016: p. 1753465816628800.

22. Scherpereel, A., et al., *Guidelines of the European Respiratory Society and the European Society of Thoracic Surgeons for the management of malignant pleural mesothelioma.* European Respiratory Journal, 2010. **35**(3): p. 479-495.

23. Byrne, M. and A. Nowak, *Modified RECIST criteria for assessment of response in malignant pleural mesothelioma.* Annals of Oncology, 2004. **15**(2): p. 257-260.

24. Leung, A.N., N. Müller, and R.R. Miller, *CT in differential diagnosis of diffuse pleural disease.* AJR. American journal of roentgenology, 1990. **154**(3): p. 487-492.

25. Segal, A., et al., *A diagnosis of malignant pleural mesothelioma can be made by effusion cytology: results of a 20 year audit.* Pathology, 2013. **45**(1): p. 44-48.

26. Fasola, G., et al., *Low-dose computed tomography screening for lung cancer and pleural mesothelioma in an asbestos-exposed population: baseline results of a prospective, nonrandomized feasibility trial—an Alpe-adria Thoracic Oncology Multidisciplinary Group Study (ATOM 002).* The oncologist, 2007. **12**(10): p. 1215-1224.

27. Wai, P.Y. and P.C. Kuo, *The role of osteopontin in tumor metastasis.* Journal of Surgical Research, 2004. **121**(2): p. 228-241.

28. Pass, H.I., et al., *Asbestos exposure, pleural mesothelioma, and serum osteopontin levels.* New England Journal of Medicine, 2005. **353**(15): p. 1564-1573.

29. Sandhu, H., et al., *mRNA expression patterns in different stages of asbestos-induced carcinogenesis in rats.* Carcinogenesis, 2000. **21**(5): p. 1023-1029.

30. Creaney, J., et al., *Comparison of osteopontin, megakaryocyte potentiating factor, and mesothelin proteins as markers in the serum of patients with malignant mesothelioma.* Journal of Thoracic Oncology, 2008. **3**(8): p. 851-857.

31. Yamaguchi, N., et al., *A novel cytokine exhibiting megakaryocyte potentiating activity from a human pancreatic tumor cell line HPC-Y5.* Journal of Biological Chemistry, 1994. **269**(2): p. 805-808.

32. Hellstrom, I., et al., *Mesothelin variant 1 is released from tumor cells as a diagnostic marker.* Cancer Epidemiology and Prevention Biomarkers, 2006. **15**(5): p. 1014-1020.

33. Scholler, N., et al., *Soluble member (s) of the mesothelin/megakaryocyte potentiating factor family are detectable in sera from patients with ovarian carcinoma.* Proceedings of the National Academy of Sciences, 1999. **96**(20): p. 11531-11536.

34. Zhou, Y.-H., *EFEMP1 (EGF containing fibulin-like extracellular matrix protein 1).* 2013.

35. Pass, H.I., et al., *Fibulin-3 as a blood and effusion biomarker for pleural mesothelioma.* New England Journal of Medicine, 2012. **367**(15): p. 1417-1427.

36. Creaney, J., et al., *Comparison of fibulin-3 and mesothelin as markers in malignant mesothelioma.* Thorax, 2014. **69**(10): p. 895-902.

37. Kirschner, M.B., et al., *Fibulin-3 levels in malignant pleural mesothelioma are associated with prognosis but not diagnosis.* British journal of cancer, 2015. **113**(6): p. 963.

38. Kao, S.H., et al., *Patterns of care for malignant pleural mesothelioma patients compensated by the Dust Diseases Board in New South Wales, Australia.* Internal medicine journal, 2013. **43**(4): p. 402-410.

39. Vogelzang, N.J., et al., *Phase III study of pemetrexed in combination with cisplatin versus cisplatin alone in patients with malignant pleural mesothelioma.* Journal of clinical oncology, 2003. **21**(14): p. 2636-2644.

40. Zalcman, G., et al., *Bevacizumab for newly diagnosed pleural mesothelioma in the Mesothelioma Avastin Cisplatin Pemetrexed Study (MAPS): a randomised, controlled, open-label, phase 3 trial.* The Lancet, 2016. **387**(10026): p. 1405-1414.

41. Flores, R.M., et al., *Extrapleural pneumonectomy versus pleurectomy/decortication in the surgical management of malignant pleural mesothelioma: results in 663 patients.* The Journal of thoracic and cardiovascular surgery, 2008. **135**(3): p. 620-626. e3.

42. Jenkins, P., R. Milliner, and C. Salmon, *Re-evaluating the role of palliative radiotherapy in malignant pleural mesothelioma.* European journal of cancer, 2011. **47**(14): p. 2143-2149.

43. Ung, Y.C., et al., *The role of radiation therapy in malignant pleural mesothelioma: a systematic review.* Radiotherapy and oncology, 2006. **80**(1): p. 13-18.

44. Maasilta, P., et al., *Radiographic chest assessment of lung injury following hemithorax irradiation for pleural mesothelioma.* European Respiratory Journal, 1991. **4**(1): p. 76-83.

45. Rice, D.C., et al., *Outcomes after extrapleural pneumonectomy and intensity-modulated radiation therapy for malignant pleural mesothelioma.* The Annals of thoracic surgery, 2007. **84**(5): p. 1685-1693.

46. Van Schil, P., et al., *Trimodality therapy for malignant pleural mesothelioma: results from an EORTC phase II multicentre trial.* European Respiratory Journal, 2010. **36**(6): p. 1362-1369.

47. Ribas, A., *Releasing the brakes on cancer immunotherapy.* New England Journal of Medicine, 2015. **373**(16): p. 1490-1492.

48. Calabrò, L., et al., *Tremelimumab for patients with chemotherapy-resistant advanced malignant mesothelioma: an open-label, single-arm, phase 2 trial.* The Lancet Oncology, 2013. **14**(11): p. 1104-1111.

49. Calabrò, L., et al., *Efficacy and safety of an intensified schedule of tremelimumab for chemotherapy-resistant malignant mesothelioma: an open-label, single-arm, phase 2 study.* The Lancet Respiratory Medicine, 2015. **3**(4): p. 301-309.

50. *AstraZeneca reports top-line result of trememlimumab monotherpay trial in mesothelioma*. 2016 Feb 29 [cited 2018 15/05/2018]; Available from: https://www.astrazeneca.com/media-centre/press-releases/2016/astrazeneca-reports-top-line-result-of-tremelimumab-monotherapy-trial-in-mesothelioma-29022016.html.

51. Alley, E.W., et al., *Clinical safety and activity of pembrolizumab in patients with malignant pleural mesothelioma (KEYNOTE-028): preliminary results from a non-randomised, open-label, phase 1b trial.* The Lancet Oncology, 2017. **18**(5): p. 623-630.

52. Hassan, R., et al., *Avelumab (MSB0010718C; anti-PD-L1) in patients with advanced unresectable mesothelioma from the JAVELIN solid tumor phase Ib trial: Safety, clinical activity, and PD-L1 expression*. 2016, American Society of Clinical Oncology.

53. Nowak, A.K., et al., *DREAM: A phase II study of durvalumab with first line chemotherapy in mesothelioma—First results*. 2018, American Society of Clinical Oncology.

54. Antonia, S., et al., *Safety and antitumour activity of durvalumab plus tremelimumab in non-small cell lung cancer: a multicentre, phase 1b study.* The lancet oncology, 2016. **17**(3): p. 299-308.

55. Larkin, J., et al., *Combined nivolumab and ipilimumab or monotherapy in untreated melanoma.* New England Journal of Medicine, 2015. **373**(1): p. 23-34.

56. Ceresoli, G.L., M. Bonomi, and M.G. Sauta, *Immune checkpoint inhibitors in malignant pleural mesothelioma: promises and challenges.* Expert Review of Anticancer Therapy, 2016(just-accepted).

57. Bueno, R., et al., *Second generation sequencing of the mesothelioma tumor genome.* PloS one, 2010. **5**(5): p. e10612.

58. Bartel, D.P., *MicroRNAs: genomics, biogenesis, mechanism, and function.* cell, 2004. **116**(2): p. 281-297.

59. Di Leva, G., M. Garofalo, and C.M. Croce, *MicroRNAs in cancer.* Annual review of pathology, 2014. **9**: p. 287.

60. Lee, Y., et al., *MicroRNA maturation: stepwise processing and subcellular localization.* The EMBO journal, 2002. **21**(17): p. 4663-4670.

61. Lee, Y., et al., *MicroRNA genes are transcribed by RNA polymerase II.* The EMBO journal, 2004. **23**(20): p. 4051-4060.

62. Han, J., et al., *The Drosha-DGCR8 complex in primary microRNA processing.* Genes & development, 2004. **18**(24): p. 3016-3027.

63. Kim, V.N., *MicroRNA precursors in motion: exportin-5 mediates their nuclear export.* Trends in cell biology, 2004. **14**(4): p. 156-159.

64. Ketting, R.F., et al., *Dicer functions in RNA interference and in synthesis of small RNA involved in developmental timing in C. elegans.* Genes & development, 2001. **15**(20): p. 2654-2659.

65. Chendrimada, T.P., et al., *TRBP recruits the Dicer complex to Ago2 for microRNA processing and gene silencing.* Nature, 2005. **436**(7051): p. 740-744.

66. Lee, Y., et al., *The role of PACT in the RNA silencing pathway.* The EMBO journal, 2006. **25**(3): p. 522-532.

67. Schwarz, D.S., et al., *Asymmetry in the assembly of the RNAi enzyme complex.* Cell, 2003. **115**(2): p. 199-208.

68. Bartel, D.P., *MicroRNAs: target recognition and regulatory functions.* Cell, 2009. **136**(2): p. 215-233.

69. Winter, J., et al., *Many roads to maturity: microRNA biogenesis pathways and their regulation.* Nature cell biology, 2009. **11**(3): p. 228-234.

70. Lu, J., et al., *MicroRNA expression profiles classify human cancers.* nature, 2005. **435**(7043): p. 834-838.

71. Calin, G.A. and C.M. Croce, *MicroRNA signatures in human cancers.* Nature Reviews Cancer, 2006. **6**(11): p. 857-866.

72. Yanaihara, N., et al., *Unique microRNA molecular profiles in lung cancer diagnosis and prognosis.* Cancer cell, 2006. **9**(3): p. 189-198.

73. Balatti, V., et al., *MicroRNAs dysregulation in human malignant pleural mesothelioma.* J Thorac Oncol, 2011. **6**(5): p. 844-51.

74. Reid, G., *MicroRNAs in mesothelioma: from tumour suppressors and biomarkers to therapeutic targets.* Journal of thoracic disease, 2015. **7**(6): p. 1031.

75. Pass, H.I., et al., *hsa-miR-29c* is linked to the prognosis of malignant pleural mesothelioma.* Cancer research, 2010. **70**(5): p. 1916-1924.

76. Ivanov, S.V., et al., *Pro-tumorigenic effects of miR-31 loss in mesothelioma.* Journal of Biological Chemistry, 2010. **285**(30): p. 22809-22817.

77. Kubo, T., et al., *Epigenetic silencing of microRNA-34b/c plays an important role in the pathogenesis of malignant pleural mesothelioma.* Clinical Cancer Research, 2011. **17**(15): p. 4965-4974.

78. Tanaka, N., et al., *Downregulation of microRNA-34 induces cell proliferation and invasion of human mesothelial cells.* Oncology reports, 2013. **29**(6): p. 2169-2174.

79. Aqeilan, R., G. Calin, and C. Croce, *miR-15a and miR-16-1 in cancer: discovery, function and future perspectives.* Cell Death & Differentiation, 2010. **17**(2): p. 215-220.

80. Reid, G., et al., *Restoring expression of miR-16: a novel approach to therapy for malignant pleural mesothelioma.* Annals of oncology, 2013. **24**(12): p. 3128-3135.

81. Cioce, M., et al., *Protumorigenic effects of mir-145 loss in malignant pleural mesothelioma.* Oncogene, 2014. **33**(46): p. 5319-5331.

82. Canino, C., et al., *SASP mediates chemoresistance and tumor-initiating-activity of mesothelioma cells.* Oncogene, 2012. **31**(26): p. 3148-3163.

83. Tomasetti, M., et al., *MicroRNA-126 suppresses mesothelioma malignancy by targeting IRS1 and interfering with the mitochondrial function.* Antioxidants & redox signaling, 2014. **21**(15): p. 2109-2125.

84. Tomasetti, M., et al., *MicroRNA-126 induces autophagy by altering cell metabolism in malignant mesothelioma.* Oncotarget, 2016. **7**(24): p. 36338.

85. Birnie, K.A., et al., *Loss of miR-223 and JNK Signaling Contribute to Elevated Stathmin in Malignant Pleural Mesothelioma.* Mol Cancer Res, 2015. **13**(7): p. 1106-18.

86. Wong, Q.W.L., et al., *MicroRNA-223 is commonly repressed in hepatocellular carcinoma and potentiates expression of Stathmin1.* Gastroenterology, 2008. **135**(1): p. 257-269.

87. Gee, G.V., et al., *Downregulated microRNAs in the differential diagnosis of malignant pleural mesothelioma.* International journal of cancer, 2010. **127**(12): p. 2859-2869.

88. Benjamin, H., et al., *A diagnostic assay based on microRNA expression accurately identifies malignant pleural mesothelioma.* The Journal of Molecular Diagnostics, 2010. **12**(6): p. 771-779.

89. Andersen, M., et al., *Diagnostic potential of miR-126, miR-143, miR-145, and miR-652 in malignant pleural mesothelioma.* J Mol Diagn, 2014. **16**(4): p. 418-30.

90. Matsumoto, S., et al., *Upregulation of microRNA-31 associates with a poor prognosis of malignant pleural mesothelioma with sarcomatoid component.* Medical Oncology, 2014. **31**(12): p. 1-7.

91. Weber, D.G., et al., *Identification of miRNA-103 in the cellular fraction of human peripheral blood as a potential biomarker for malignant mesothelioma–a pilot study.* PLoS One, 2012. **7**(1): p. e30221.

92. Santarelli, L., et al., *Association of MiR-126 with soluble mesothelin-related peptides, a marker for malignant mesothelioma.* PloS one, 2011. **6**(4): p. e18232.

93. Tomasetti, M., et al., *Clinical significance of circulating miR-126 quantification in malignant mesothelioma patients.* Clinical biochemistry, 2012. **45**(7): p. 575-581.

94. Kirschner, M.B., et al., *Increased circulating miR-625-3p: a potential biomarker for patients with malignant pleural mesothelioma.* Journal of Thoracic Oncology, 2012. **7**(7): p. 1184-1191.

95. Kurai, J., et al., *Therapeutic antitumor efficacy of anti-epidermal growth factor receptor antibody, cetuximab, against malignant pleural mesothelioma.* International journal of oncology, 2012. **41**(5): p. 1610-1618.

96. van Zandwijk, N., et al., *Safety and activity of microRNA-loaded minicells in patients with recurrent malignant pleural mesothelioma: a first-in-man, phase 1, open-label, dose-escalation study.* The Lancet Oncology, 2017. **18**(10): p. 1386-1396.

97. Hanahan, D. and L.M. Coussens, *Accessories to the crime: functions of cells recruited to the tumor microenvironment.* Cancer cell, 2012. **21**(3): p. 309-322.

98. Chou, J. and Z. Werb, *MicroRNAs play a big role in regulating ovarian cancer-associated fibroblasts and the tumor microenvironment.* Cancer Discov, 2012. **2**(12): p. 1078-80.

99. Sandhu, V., et al., *Differential expression of miRNAs in pancreatobiliary type of periampullary adenocarcinoma and its associated stroma.* Mol Oncol, 2016. **10**(2): p. 303-16.

100. Mitra, A.K., et al., *MicroRNAs reprogram normal fibroblasts into cancer-associated fibroblasts in ovarian cancer.* Cancer Discov, 2012. **2**(12): p. 1100-8.

101. Liu, B., et al., *MiR-126 restoration down-regulate VEGF and inhibit the growth of lung cancer cell lines in vitro and in vivo.* Lung cancer, 2009. **66**(2): p. 169-175.

102. Ebrahimi, F., et al., *miR-126 in human cancers: clinical roles and current perspectives.* Experimental and molecular pathology, 2014. **96**(1): p. 98-107.

103. Coussens, L.M. and Z. Werb, *Inflammation and cancer.* Nature, 2002. **420**(6917): p. 860-867.

104. Chou, J., P. Shahi, and Z. Werb, *microRNA-mediated regulation of the tumor microenvironment.* Cell Cycle, 2013. **12**(20): p. 3262-3271.

105. Joyce, J.A. and J.W. Pollard, *Microenvironmental regulation of metastasis.* Nature Reviews Cancer, 2009. **9**(4): p. 239-252.

106. Mantovani, A., et al., *Role of tumor-associated macrophages in tumor progression and invasion.* Cancer and Metastasis Reviews, 2006. **25**(3): p. 315-322.

107. O'Connell, R.M., et al., *MicroRNA-155 is induced during the macrophage inflammatory response.* Proceedings of the National Academy of Sciences, 2007. **104**(5): p. 1604-1609.

108. Martinez-Nunez, R.T., F. Louafi, and T. Sanchez-Elsner, *The interleukin 13 (IL-13) pathway in human macrophages is modulated by microRNA-155 via direct targeting of interleukin 13 receptor α1 (IL13Rα1).* Journal of Biological Chemistry, 2011. **286**(3): p. 1786-1794.

109. Nazari-Jahantigh, M., et al., *MicroRNA-155 promotes atherosclerosis by repressing Bcl6 in macrophages.* The Journal of clinical investigation, 2012. **122**(11): p. 4190-4202.

110. Yang, M., et al., *Microvesicles secreted by macrophages shuttle invasion-potentiating microRNAs into breast cancer cells.* Molecular cancer, 2011. **10**(1): p. 1.

111. Kent, O.A., et al., *Lessons from miR-143/145: the importance of cell-type localization of miRNAs.* Nucleic Acids Res, 2014. **42**(12): p. 7528-38.

112. Akao, Y., Y. Nakagawa, and T. Naoe, *MicroRNAs 143 and 145 are possible common onco-microRNAs in human cancers.* Oncology reports, 2006. **16**(4): p. 845-850.

113. Zhang, J., et al., *Loss of microRNA-143/145 disturbs cellular growth and apoptosis of human epithelial cancers by impairing the MDM2-p53 feedback loop.* Oncogene, 2013. **32**(1): p. 61-69.

114. Chivukula, R.R., et al., *An essential mesenchymal function for miR-143/145 in intestinal epithelial regeneration.* Cell, 2014. **157**(5): p. 1104-16.

115. Dimitrova, N., et al., *Stromal expression of miR-143/145 promotes neoangiogenesis in lung cancer development.* Cancer discovery, 2016. **6**(2): p. 188-201.

116. Voellenkle, C., et al., *Deep-sequencing of endothelial cells exposed to hypoxia reveals the complexity of known and novel microRNAs.* Rna, 2012. **18**(3): p. 472-484.

117. Wang, S., et al., *The endothelial-specific microRNA miR-126 governs vascular integrity and angiogenesis.* Developmental cell, 2008. **15**(2): p. 261-271.

118. Png, K.J., et al., *A microRNA regulon that mediates endothelial recruitment and metastasis by cancer cells.* Nature, 2012. **481**(7380): p. 190-194.

119. Li, Z., et al., *Expression of miR-126 suppresses migration and invasion of colon cancer cells by targeting CXCR4.* Molecular and cellular biochemistry, 2013. **381**(1-2): p. 233-242.

120. Feng, R., et al., *miR-126 functions as a tumour suppressor in human gastric cancer.* Cancer letters, 2010. **298**(1): p. 50-63.

121. Musiyenko, A., V. Bitko, and S. Barik, *Ectopic expression of miR-126*, an intronic product of the vascular endothelial EGF-like 7 gene, regulates prostein translation and invasiveness of prostate cancer LNCaP cells.* Journal of molecular medicine, 2008. **86**(3): p. 313-322.

122. Zhang, J., et al., *The cell growth suppressor, mir-126, targets IRS-1.* Biochemical and biophysical research communications, 2008. **377**(1): p. 136-140.

123. Pritchard, C.C., et al., *Blood cell origin of circulating microRNAs: a cautionary note for cancer biomarker studies.* Cancer prevention research, 2012. **5**(3): p. 492-497.

124. Chen, C.-Z., et al., *MicroRNAs modulate hematopoietic lineage differentiation.* science, 2004. **303**(5654): p. 83-86.

125. Haneklaus, M., et al., *miR-223: infection, inflammation and cancer.* J Intern Med, 2013. **274**(3): p. 215-26.

126. Johnnidis, J.B., et al., *Regulation of progenitor cell proliferation and granulocyte function by microRNA-223.* Nature, 2008. **451**(7182): p. 1125-1129.

127. Fazi, F., et al., *Epigenetic silencing of the myelopoiesis regulator microRNA-223 by the AML1/ETO oncoprotein.* Cancer cell, 2007. **12**(5): p. 457-466.

128. Jia, C.Y., et al., *MiR-223 suppresses cell proliferation by targeting IGF-1R.* PLoS One, 2011. **6**(11): p. e27008.

129. Valadi, H., et al., *Exosome-mediated transfer of mRNAs and microRNAs is a novel mechanism of genetic exchange between cells.* Nature cell biology, 2007. **9**(6): p. 654-659.

130. Ismail, N., et al., *Macrophage microvesicles induce macrophage differentiation and miR-223 transfer.* Blood, 2013. **121**(6): p. 984-995.

131. Liang, H., et al., *MicroRNA-223 delivered by platelet-derived microvesicles promotes lung cancer cell invasion via targeting tumor suppressor EPB41L3.* Molecular cancer, 2015. **14**(1): p. 1.

132. Pfaffl, M.W., *A new mathematical model for relative quantification in real-time RT–PCR.* Nucleic acids research, 2001. **29**(9): p. e45-e45.

133. Amatya, V.J., et al., *Differential microRNA expression profiling of mesothelioma and expression analysis of miR-1 and miR-214 in mesothelioma.* International journal of oncology, 2016. **48**(4): p. 1599-1607.

134. Belizário, J.E., *Immunodeficient mouse models: an overview.* The Open Immunology Journal, 2009. **2**(1).

135. Pritchard, C.C., et al., *Blood cell origin of circulating microRNAs: a cautionary note for cancer biomarker studies.* Cancer prevention research, 2011: p. canprevres. 0370.2011.

136. Panwar, B., G.S. Omenn, and Y. Guan, *miRmine: a database of human miRNA expression profiles.* Bioinformatics, 2017. **33**(10): p. 1554-1560.

137. Khodayari, N., et al., *EphrinA1 inhibits malignant mesothelioma tumor growth via let-7 microRNA-mediated repression of the RAS oncogene.* Cancer gene therapy, 2011. **18**(11): p. 806.

138. Fassina, A., et al., *Epithelial–mesenchymal transition in malignant mesothelioma.* Modern Pathology, 2012. **25**(1): p. 86.

139. Nielsen, B.S., *MicroRNA in situ hybridization*, in *Next-Generation MicroRNA Expression Profiling Technology*. 2012, Springer. p. 67-84.

140. Hand, N.J., et al., *The microRNA-30 family is required for vertebrate hepatobiliary development.* Gastroenterology, 2009. **136**(3): p. 1081-1090.

141. Izumi, B., et al., *MicroRNA-223 expression in neutrophils in the early phase of secondary damage after spinal cord injury.* Neuroscience letters, 2011. **492**(2): p. 114-118.

142. Shibuya, H., et al., *Overexpression of microRNA-223 in rheumatoid arthritis synovium controls osteoclast differentiation.* Modern rheumatology, 2013. **23**(4): p. 674-685.

143. Sempere, L.F., et al., *Fluorescence-based codetection with protein markers reveals distinct cellular compartments for altered MicroRNA expression in solid tumors.* Clinical cancer research, 2010: p. 1078-0432. CCR-10-1152.

144. Nielsen, B.S. and K. Holmstrøm, *Combined microRNA in situ hybridization and immunohistochemical detection of protein markers*, in *Target identification and validation in drug discovery*. 2013, Springer. p. 353-365.

145. Hedbäck, N., et al., *MiR-21 expression in the tumor stroma of oral squamous cell carcinoma: an independent biomarker of disease free survival.* PloS one, 2014. **9**(4): p. e95193.

146. Penna, E., F. Orso, and D. Taverna, *miR-214 as a key hub that controls cancer networks: small player, multiple functions.* Journal of Investigative Dermatology, 2015. **135**(4): p. 960-969.

147. Wang, X., et al., *MiR-214 inhibits cell growth in hepatocellular carcinoma through suppression of β-catenin.* Biochemical and biophysical research communications, 2012. **428**(4): p. 525-531.

148. Kang, W., et al., *Stathmin1 plays oncogenic role and is a target of microRNA-223 in gastric cancer.* Plos one, 2012. **7**(3): p. e33919.